INVESTIGATING THE DEVELOPMENTAL, GENETIC, AND EVOLUTIONARY UNDERPINNINGS OF POSTZYGOTIC BARRIERS IN *MIMULUS*

by

GABRIELLE D. SANDSTEDT

(Under the direction of Andrea L. Sweigart)

ABSTRACT

Despite their importance in speciation, major questions involving postzygotic barriers still remain, such as why they evolve and how much they contribute to species divergence. Here, we investigate the genetic mechanisms and evolutionary drivers of postzygotic isolation among a group of closely related taxa in the genus *Mimulus*. In the *M. tilingii* complex, the three species are largely allopatric and grow only at high elevations. In Chapter II, we determined that these three species are morphologically and genetically distinct, and diverged ~400kya. Additionally, each species pair in the *M. tilingii* complex is nearly completely reproductively isolated by many postzygotic barriers, including F1 hybrid seed inviability, F1 hybrid necrosis, and F1 male and female hybrid sterility. In Chapter III, we investigated the developmental, genetic, and evolutionary processes that contribute to the first-acting postzygotic barrier: F1 hybrid seed

inviability. We performed a detailed developmental assessment of hybrid seed inviability between species in the *M. tilingii* complex, and a more distant relative, *M. guttatus*. We determined that between any species pair, hybrid seed development was disrupted in regions of the seed that potentially control nutrient acquisition. This finding provides empirical evidence for the classic theory that parental conflict over resource allocation targets nutrient acquiring tissues within the seed. Finally, in Chapter IV, we investigated the genetic basis of severe F1 hybrid sterility between species in the *M. tilingii* complex and discovered that this postzygotic barrier is largely explained by underdominant chromosomal rearrangements. This finding might suggest a role for genetic drift in fixing such underdominant rearrangements. Alternatively, if maladaptive gene flow has occurred between these species, these costly rearrangements might have evolved via strong selection for suppressed recombination among locally adapted loci. Together, our findings provide context for how strong postzygotic barriers may evolve and contribute to speciation.

INDEX WORDS: speciation, postzygotic barriers, intrinsic, allopatric, *Mimulus*

INVESTIGATING THE DEVELOPMENTAL, GENETIC, AND EVOLUTIONARY UNDERPINNINGS OF POSTZYGOTIC BARRIERS IN *MIMULUS*

by

GABRIELLE D. SANDSTEDT

BS, Arizona State University – West, 2016

A Dissertation Submitted to Graduate Faculty of The University of Georgia in Partial Fulfillment of the Requirements for the Degree

DOCTOR OF PHILOSOPHY

ATHENS, GEORGIA

2022

INVESTIGATING THE DEVELOPMENTAL, GENETIC, AND EVOLUTIONARY UNDERPINNINGS OF POSTZYGOTIC BARRIERS IN *MIMULUS*

by

GABRIELLE D. SANDSTEDT

Major Professor:	Andrea L. Sweigart
Committee:	Jill T. Anderson
	Robert G. Franks
	Wolfgang Lukowitz
	Robert J. Schmitz

Electronic Version Approved:

Ron Walcott
Vice Provost for Graduate Educations and Dean of the Graduate School
The University of Georgia
August 2022

ACKNOWLEDGEMENTS

I have so many people that I would love to acknowledge in helping me complete this dissertation. I cannot put into words how grateful I am to have been surrounded by such an amazing and supportive group throughout all these years. This would not be possible without you all.

To my advisor, Andrea Sweigart: I am incredibly grateful for the compassion and patience you have given me since the beginning of this process. You are a brilliant scientist, writer, mentor, advocate, and more! It has been such a pleasure to learn from you. Thank you for everything.

I am also very thankful for my committee, Jill Anderson, Bob Schmitz, Wolfgang Lukowitz, and Bob Franks: Thank you for motivating me to make my research better and my experiments stronger. Thank you for investing your time in me.

To the current and former members in the Sweigart lab, Sam Mantel, Makenzie Whitener, Alex Sotola, Matt Farnitano, Rachel Kerwin, Matt Zuellig, and Taylor Harrel: Thank you for being such amazing lab mates and great friends. This process is not always (if ever) easy. However, knowing that I get to come to lab each day and work alongside amazing people really helps. I am lucky to have shared this experience with this group.

To the greenhouse staff: Thank you for keeping my plants alive, and always troubleshooting any problems that we have!

To the amazing undergraduate researchers, Mason Lin, Sydney Dilworth, Tylanna Baker, Jenna Mathwig, Jasmine Hawkins, and Jaylin Knight: Thank you for helping me collect and

analyze data. Thank you for helping me think through difficult projects. Without your help, this dissertation would not be possible. It has been such an honor to know you and do science with you all. You make me want to be a better mentor every day. Thank you.

To the *Mimulus* community: I had no idea that when I signed up to work with *Mimulus* that I also signed up to have the greatest and biggest support system I could have ever imagined. This group is so special in that everyone wants others to succeed in life and in science. To John Willis, Jay Sobel, Bob Franks, Elen Oneal, Miguel Flores-Vergara, Jenn Coughlan, and the rest of our HSI group – thank you for being such an amazing group of collaborators and always so helpful!

To Shivangi Nath: Thank you for being a wonderful friend, always checking in, and always making me laugh, especially with memes.

To Thomas: My best friend, my love, my everything! Thank you for your kindness, your calmness, and balancing me out always. Thank you for being you.

To my family, Adam, Megan, Grandma, and Mom: Thank you for getting me through this process. I love you so much. Mom, I cannot put into words how much your support has helped me get here. You are everything. Thank you.

TABLE OF CONTENTS

Page

LIST OF TABLES

LIST OF FIGURES

CHAPTER I

INTRODUCTION

A fundamental goal in evolutionary biology is to understand how and why new species evolve. In the classic, allopatric model of speciation, incipient species begin to diverge when a population occupies a new geographical area (*i.e.*, dispersal) or when a physical barrier (*i.e.*, vicariance) emerges. While physically separated, incipient species accumulate ecological and genetic differences, and as a byproduct of this divergence, reproductive isolation evolves. There are two major categories of barriers that contribute to reproductive isolation: prezygotic barriers that prevent fertilization (*e.g.*, differences in habitat, reproductive timing, or behavior) and postzygotic barriers that cause low fitness in hybrids (*e.g.*, sterility and inviability; Coyne and Orr 2004). Given that species are often described by their ability to reproduce (*i.e.*, Biological Species Concept; Mayr 1942), speciation research seeks to define which barriers between closely related taxa greatly limit gene flow. While species typically require multiple barriers, often both pre- and postzygotic, to effectively reduce genetic exchange upon secondary contact (Schluter 2001, Rieseberg and Willis 2007), there is some argument as to which barriers are most important for species divergence (Coyne and Orr 2004).

The importance of reproductive barriers in speciation can depend on several factors, including: the absolute strength of a barrier (*i.e.*, how strong the barrier is when acting alone), the relative contribution of a barrier to overall reproductive isolation (*i.e.*, the sequential order in which the barrier acts), and timing when a barrier arises during species divergence (*i.e.*, before or

after reproductive isolation is complete; Coyne and Orr 2004). To reveal general patterns in plant reproductive isolating barriers, some studies have quantified the strength of barriers across the life-history of recently diverged species (Ramsey et al. 2003, Martin and Willis 2007; Husband and Sabara 2004; Christie and Strauss 2019). In general, such studies find that prezygotic barriers are often individually stronger in reducing gene flow between species than postzygotic barriers (Lowry et. al., 2008; Widmer et. al., 2009). Even if prezygotic and postzygotic barriers have similar absolute strengths, the sequential nature of reproductive isolating mechanisms allows early-acting prezygotic barriers to contribute more to total isolation (Schemske 2000; Ramsey et. al., 2003). However, intrinsic postzygotic barriers can be quite strong in reducing gene flow and important for speciation (Coughlan and Matute 2020). They might also contribute to reinforcement, a situation in which selection against unfit hybrids promotes the evolution of additional earlier-acting barriers (Dobzhansky 1951, Butlin 1989). Indeed, it is important to note that current estimates of the relative contribution of reproductive barriers do not always reflect their historical role in species divergence – barriers that arise later in speciation can mask the contributions of initially-evolving barriers (Nosil et. al., 2005). Therefore, to develop a more comprehensive understanding of the importance of reproductive barriers in plant speciation, it is necessary to perform comparative approaches that consider taxa at different stages in divergence.

Because most speciation events begin in allopatry, it is likely that barriers involved in adaptation to different environments are the first to arise (Sobel et al. 2010). Extrinsic barriers (both pre- and postzygotic) typically involve ecological and/or behavioral differences between species. For example, when divergent selection drives genetically-based habitat preferences between two species, their ability to geographically overlap might be severely inhibited (*i.e.*,

habitat isolation), thereby preventing interspecific mating. If interspecific mating does occur, hybrid offspring may be maladapted to either parental habitat and suffer a fitness cost (Coyne and Orr 2004). Although extrinsic barriers are certainly important, they are vulnerable to shifts in the environment and can often be leaky (Sobel et al. 2010). Because even small amounts of gene flow may prolong or reverse the speciation process (Hendry et al. 2009; Nosil et al. 2009), intrinsic post-mating barriers are thought to be critical for preventing the breakdown of species boundaries (Clausen 1951; reviewed in Lowry 2012).

Although Darwin (1859) initially proposed that natural selection can drive the origin of a species, the production of inviable and sterile hybrids posed a challenge to his theory. Because selection cannot favor the formation of unfit progeny, how do intrinsic postzygotic barriers evolve? In light of Mendelian genetics and neutral evolutionary processes, biologists in the early twentieth century outlined how hybrid dysfunction might arise. In plants, intrinsic postzygotic barriers are now commonly explained by three genetic mechanisms: ploidy-level differences, structural karyotypic differences, and epistatic interactions among loci (Dobzhansky 1937, Coyne and Orr 2004).

Polyploidy, or when individuals carry three or more sets of chromosomes, is often viewed as an instantaneous speciation event because polyploids arise in sympatry and are reproductively isolated from their co-occurring progenitors (Winge 1917). When a new tetraploid (4n) individual and its diploid ancestor (2n) attempt to intercross, triploid (3n) offspring are produced. In 3n individuals, which have an odd number of chromosome sets, meiosis is disrupted during chromosome pairing and segregation, which results in the production of aneuploid, sterile gametes. While ploidy-level differences that cause sterility are very common

among plant taxa, flowering plants (angiosperms) can also suffer from seed inviability when individuals with divergent ploidies cross. In flowering plants, interploidy crosses may disrupt dosage in the endosperm, which is a specialized tissue that transfers maternal nutrients to the developing embryo and is thought to play a critical role in regulating seed viability (Brink and Cooper 1947; Woodell and Valentine 1961). The embryo and endosperm undergo a process unique to flowering plants, known as double fertilization—one sperm fuses with the egg to develop a zygote that forms a diploid embryo, while the second sperm fuses with two polar nuclei to achieve a relative contribution of two maternal to one paternal genome (2m:1p) and forms a dosage sensitive triploid endosperm tissue. Therefore, in interploidy crosses (*e.g.*, 4*n* central cell from a tetraploid + 1*n* sperm cell from a diploid or 2*n* central cell from a diploid + 2*n* sperm cell from a tetraploid), an imbalance of parental dosage in the endosperm can form a 'triploid block', which is a term used to describe the process preventing the formation of viable triploid seeds (Marks 1966). However, because interspecific crosses of the same ploidy can result in similar endosperm developmental defects as interploidy crosses (Cooper and Brink 1942; Stephens 1949; Nishiyama and Yabuno 1978), theory predicts that proper seed development depends on the balanced dosage of a discrete number of gene products in the endosperm, rather than on ploidy level (*i.e.*, endosperm balance number; Johnston et al. 1980).

While changes in ploidy can impact the entire genome, structural changes within and between chromosomes (*e.g.*, inversions, translocations, fusions, and fissions) can also establish strong reproductive barriers. Crosses between species with divergent karyotypes can directly disrupt pairing during meiosis in hybrids and yield aneuploid gametes, thereby reducing fertility (White 1948). Because individuals heterozygous for underdominant rearrangements would suffer

fertility loss, it is theoretically difficult to explain how they might rise in frequency within a population. Theory suggests that strong underdominant chromosomal rearrangements might spread locally when genetic drift overwhelms selection in small populations (Lande 1979; Lande 1985). However, this explanation does not reconcile how species like sunflowers that have large effective population sizes (Sambatti et al. 2012) can accumulate extensive karyotypic changes (Ostevik et al. 2020), with hybrid sterility primarily mapping to structural divergent regions between species (Lai et al. 2005). To address these theoretical difficulties, Kirkpatrick and Barton (2006) proposed a model for the spread of chromosomal rearrangements that does not rely solely on genetic drift. Given that chromosomal rearrangements can effectively suppress recombination (either by mechanical pairing problems or the loss of unbalanced gametes; reviewed in Faria and Navarro 2006), this model suggests that underdominant chromosomal rearrangements may be favored by natural selection if they suppress recombination between locally adapted alleles and prevent maladaptive gene flow (Kirkpatrick and Barton 2006). Under this more recent theory, it might be easier to imagine how underdominant chromosomal rearrangements can overcome the difficulty initially spreading within a population; however, it is still not well understood how often these rearrangements are involved in sterility.

Alternatively, genetic incompatibilities can evolve without populations needing to pass through a low-fitness transitional state. Dobzhansky (1937) and Muller (1942) independently formulated a model for the evolution of intrinsic hybrid incompatibilities demonstrating that the breakdown of hybrid fitness can be caused by mutational differences that might be adaptive or neutral in a native background of one species but not the other because of epistatic interactions with the genetic background. For example, if we consider a scenario where some species with an

"*aa*" genotype at one locus and "*bb*" at another, unlinked locus diverges in allopatry, an "*A*" mutation arises in one incipient species and a "*B*" mutation in the other. Through adaptive or neutral processes, the mutations fix and result in one species with the genotype "*AAbb*" and the other species with the genotype "*aaBB*". In their own native genetic backgrounds, these mutations are compatible. However, if these two species hybridize upon secondary contact, these mutations are "tested" against a new foreign background, and if the "*A*" allele interacts negatively with the "*B*" allele of the other species, offspring might suffer a loss in fitness. Since Dobzhansky-Muller incompatibilities commonly result in hybrid fitness breakdown in both plants and animals (Fishman and Sweigart 2018; Blackman 2016), they are thought to be the most important genetic cause of intrinsic postzygotic isolation between species of the same ploidy (Coyne and Orr 2004).

The extent of geographical overlap over the course of species divergence may play a role in whether certain genetic factors contribute to maintaining species boundaries. For instance, in addition to polyploid speciation that occurs in sympatry, underdominant chromosomal rearrangements may also evolve in the presence of gene flow when selection for suppressed recombination between adaptive alleles outweighs their deleterious effects on fertility (Kirkpatrick and Barton 2006). However, other evolutionary processes that can explain the evolution of underdominant rearrangements, such as genetic drift and meiotic drive, do not rely on the presence of gene flow (White 1978; King 1993; Feder et al. 2011). Alternatively, genetic incompatibilities may evolve to high frequencies during periods of allopatry. With even small amounts of gene flow, the negative effects of genetic incompatibilities are exposed, and incompatible alleles are expected to be purged unless there is selection for them within parental

species (Gavrilets 1997; Bank et. al. 2012). Although there are some cases where genetic incompatibilities are under strong selection (Presgraves et al. 2003; Brideu et. al. 2006; Sweigart and Flagel 2015), others are likely neutral (Bikard et al. 2009; Mizuta et al. 2010; Yamagata et al. 2010; Zuellig and Sweigart 2018) – only when isolation is complete will neutral alleles be maintained upon secondary contact (Bank et al. 2012). Given that each of the three genetic mechanisms can invoke very different evolutionary histories, understanding the genetic basis of a given barrier can provide insight into how species diverge.

Here, we investigate the evolutionary, developmental, and genetic mechanisms of intrinsic postzygotic reproductive barriers in the monkeyflower genus, *Mimulus*, to assess the role of these barriers in the speciation process. We note that while we refer to this genus as *Mimulus*, there is ongoing debate over the taxonomic designations of species within this genus (Lowry et al. 2019; Nesom et al. 2019). As a whole, the genus *Mimulus* is comprised of >150 species, containing different sections and complexes of closely related species. Within and across complexes, species are rich with ecological, morphological, and genetic variation, and they vary in their extent of geographical overlap (Wu et al. 2007). Therefore, *Mimulus* is a premier system to study the genetics and evolution of reproductive isolation among species at different stages in the speciation process.

The bulk of our work focuses on the *M. tilingii* species complex, which is a group of yellow mountain monkeyflowers that are mat-forming perennials, growing exclusively at high elevations (>1500m; Grant 1924; Pennell 1951). In the field, this complex was subdivided into three distinct species based on morphology and geography: *M. caespitosa*, *M. minor*, and *M. tilingii* (Nesom 2012). Members in this species complex are thought to be mostly allopatric,

growing west of the Rocky Mountains – *M. caespitosa* grows exclusively in Washington state, *M. minor* grows in Colorado, and *M. tilingii* occupies many alpine regions across western North America (Nesom 2012; Nesom 2014). Furthermore, some of our work also includes *M. guttatus*, which is a member of its own species complex and occupies a more diverse range in western North America, sometimes overlapping with high-alpine populations in the *M. tilingii* complex. *Mimulus guttatus* and species in the *M. tilingii* complex share many characteristics: populations are self-compatible, though they are thought to be mainly outcrossing, with large, bee-pollinated flowers. Despite their morphological similarities and occasional geographic overlapping, *M. guttatus* and *M. tilingii* are strongly reproductively isolated due to nearly complete F1 hybrid seed inviability (Vickery, 1978; Garner et al. 2016).

By leveraging largely allopatric, closely related species in the *M. tilingii* complex and, in some cases, their more distant relative that sometimes grows sympatrically, *M. guttatus*, we explore the strength of intrinsic reproductive isolation at different stages of species divergence. In Chapter II, we determined patterns of morphological and genetic variation and reproductive isolation within the *M. tilingii* species complex in a common garden and show that many intrinsic postzygotic barriers have evolved (hybrid seed inviability, F1 hybrid necrosis, and F1 hybrid male and female sterility) among species in this complex despite being genetically closely related. In Chapters III and IV, we further detail the evolutionary, developmental, and genetic mechanisms of hybrid seed inviability and hybrid sterility, respectively. Finally, Chapter V discusses additional approaches that may be useful in investigating how these reproductive barriers have evolved. As a whole, this dissertation illustrates the importance of detailed

investigations into the developmental and genetic mechanisms of reproductive isolation for understanding the evolutionary origins of species.

REFERENCES

Bank, C., Hermisson, J., & Kirkpatrick, M. 2012. Can reinforcement complete speciation? *Evolution: International Journal of Organic Evolution*, *66*(1), 229-239.

Bikard, D., Patel, D., Le Metté, C., Giorgi, V., Camilleri, C., Bennett, M.J., & Loudet, O. 2009. Divergent evolution of duplicate genes leads to genetic incompatibilities within *A. thaliana. Science*, *323*(5914), 623-626.

Blackman, B.K. 2016. Speciation genes. *Encyclopedia of Evolutionary Biology*, *4*, 66-175.

Brideau, N.J., Flores, H.A., Wang, J., Maheshwari, S., Wang, X.U., & Barbash, D.A. 2006. Two Dobzhansky-Muller genes interact to cause hybrid lethality in *Drosophila. Science*, *314*(5803), 1292-1295.

Brink, R. A., & Cooper, D. C. 1947. The endosperm in seed development. *The Botanical Review*, *13*(9), 479-541.

Butlin, R. 1989. Reinforcement of premating isolation. *Speciation and its consequences.*,158-179.

Christie, K., & Strauss, S. Y. 2019. Reproductive isolation and the maintenance of species boundaries in two serpentine endemic Jewelflowers. *Evolution*, *73*(7), 1375-1391.

Clausen, J. 1951. Stages in the evolution of plant species. Ithaca, NY: Cornell University Press.

Cooper, D.C., & Brink, R.A., 1942. The endosperm as a barrier to interspecific hybridization in flowering plants. *Science*, *95*(2455), 75-76.

Coughlan, J.M., & Willis, J.H., 2019. Dissecting the role of a large chromosomal inversion in life history divergence throughout the Mimulus guttatus species complex. *Molecular ecology*, *28*(6), 1343-1357.

Coyne, J.A., & H. A. Orr. 2004. Speciation. Sinauer Associates, Sunderland, MA.

Darwin, C. R. 1859. The Origin of species. 6th ed. John Murray, London.

Dobzhansky, T. 1937. Genetic nature of species differences. *The American Naturalist*, *71*(735), 404-420.

Dobzhansky, T. 1951. Genetics and the origin of species. 3rd ed. Columbia Univ. Press, New York

Fang, Z., Pyhäjärvi, T., Weber, A.L., Dawe, R.K., Glaubitz, J.C., González, J.D.J.S., Ross-Ibarra, C., Doebley, J., Morrell, P.L., & Ross-Ibarra, J., 2012. Megabase-scale inversion polymorphism in the wild ancestor of maize. *Genetics*, *191*(3), 883-894.

Faria, R. and Navarro, A. 2010. Chromosomal speciation revisited: rearranging theory with pieces of evidence. *Trends in ecology & evolution*, *25*(11), 660-669.

Feder, J.L., Gejji, R., Powell, T.H. & Nosil, P. 2011. Adaptive chromosomal divergence driven by mixed geographic mode of evolution. *Evolution: International Journal of Organic Evolution*, *65*(8), 2157-2170.

Garner, A. G., Kenney, A. M., Fishman, L., & Sweigart, A. L. 2016. Genetic loci with parent of-origin effects cause hybrid seed lethality in crosses between *Mimulus* species. *New Phytologist*, *211*(1), 319-331.

Gavrilets, S. 1997. Hybrid zones with Dobzhansky-type epistatic selection. *Evolution*, *51*(4), 1027-1035.

Grant, A.L. 1924. A monograph of the genus *Mimulus*. Ann. Missouri Bot. Gard. 11:99-389

Hendry, A.P., Bolnick, D.I., Berner, D. & Peichel, C.L. 2009. Along the speciation continuum in sticklebacks. *Journal of fish biology*, *75*(8), 2000-2036.

Husband, B.C., & Sabara, H.A. 2004. Reproductive isolation between autotetraploids and their diploid progenitors in fireweed, *Chamerion angustifolium* (Onagraceae). *New Phytologist*, *161*(3), 703-713.

Johnston S.A., den Nijs T.P.M, Peloquin S.J., & Hanneman R.E. 1980. The Significance of Genic Balance to Endosperm Development in Interspecific Crosses. *Theoretical and applied genetics* 57: 5–9

King, M. 1987. Chromosomal rearrangements, speciation and the theoretical approach. *Heredity*, *59*(1), 1-6.

King, M. 1993. *Species Evolution. The Role of Chromosome Change*. Cambridge University Press, Cambridge.

Kirkpatrick, M., & Barton, N. 2006. Chromosome inversions, local adaptation and speciation. *Genetics*, *173*(1), 419-434.

Lai, Z., Nakazato, T., Salmaso, M., Burke, J. M., Tang, S., Knapp, S. J., & Rieseberg, L. H. 2005. Extensive chromosomal repatterning and the evolution of sterility barriers in hybrid sunflower species. *Genetics*, *171*(1), 291-303.

Lande, R. 1979. Effective deme sizes during long-term evolution estimated from rates of chromosomal rearrangement. *Evolution*, 234-251.

Lande, R. 1985. The fixation of chromosomal rearrangements in a subdivided population with local extinction and colonization. *Heredity*, *54*(3), 323-332.

Lowry, D. B., Modliszewski, J. L., Wright, K. M., Wu, C. A., & Willis, J. H. 2008. The strength and genetic basis of reproductive isolating barriers in flowering plants. *Philosophical Transactions of the Royal Society B: Biological Sciences*, *363*(1506), 3009-3021.

Lowry, D.B., Sobel, J.M., Angert, A.L., Ashman, T.L., Baker, R.L., Blackman, B.K., Brandvain, Y., Byers, K.J., Cooley, A.M., Coughlan, J.M., & Dudash, M.R. 2019. The case for the continued use of the genus name *Mimulus* for all monkeyflowers. *Taxon*, *68*(4), 617-623.

Lowry, D.B. 2012. Ecotypes and the controversy over stages in the formation of new species. *Biological Journal of the Linnean Society*, *106*(2), 241-257.

Marks, G.E., 1966. The origin and significance of intraspecific polyploidy: experimental evidence from Solanum chacoense. *Evolution*, 552-557

Martin, N.H., & Willis, J.H. 2007. Ecological divergence associated with mating system causes nearly complete reproductive isolation between sympatric Mimulus species. *Evolution*, *61*(1), 68-82.

Mayr, E. 1942. Systematics and the origin of species. Columbia Univ. Press, New York.

Mizuta, Y., Harushima, Y., & Kurata, N. 2010. Rice pollen hybrid incompatibility caused by reciprocal gene loss of duplicated genes. *Proceedings of the National Academy of Sciences*, *107*(47), 20417-20422.

Muller H. J. 1942. Isolating mechanisms, evolution, and temperature. Biological Symposium 6: 71–125.

Nesom, G. L. 2012. Taxonomy of *Erythranthe* sect. Simiola (Phrymaceae) in the USA and Mexico. *Phytoneuron*, *40*, 1-123.

Nesom, G.L. 2014. Updated classification and hypothetical phylogeny of *Erythranthe* sect. Simiola (Phrymaceae). *Phytoneuron*, *2014*, 1-6.

Nesom, G.L. 2019. Taxonomic status of *Erythranthe minor* (Phrymaceae). *Phytoneuron 2019*, 32: 1-7.

Nishiyama I., & Yabuno T. 1978. Causal Relationships between the Polar Nuclei in Double Fertilization and Interspecific Cross-incompatibility in Avena. *Cytologia*, 43: 453–466.

Nosil, P., Vines, T.H., & Funk, D.J. 2005. Reproductive isolation caused by natural selection against immigrants from divergent habitats. *Evolution*, *59*(4), pp.705-719.

Oneal, E., Lowry, D.B., Wright, K.M., Zhu, Z., & Willis, J.H., 2014. Divergent population structure and climate associations of a chromosomal inversion polymorphism across the *Mimulus guttatus* species complex. *Molecular ecology*, *23*(11), pp.2844-2860.

Ostevik, K.L., Samuk, K., & Rieseberg, L.H. 2020. Ancestral reconstruction of karyotypes reveals an exceptional rate of nonrandom chromosomal evolution in sunflower. *Genetics*, *214*(4), 1031-1045.

Pennell, F. W. 1951. *Mimulus*. *Illustrated flora of the Pacific states*, *3*, 688-731.

Presgraves, D.C., Balagopalan, L., Abmayr, S.M., & Orr, H.A. 2003. Adaptive evolution drives divergence of a hybrid inviability gene between two species of Drosophila. *Nature*, *423*(6941), 715-719.

Ramsey, J., Bradshaw Jr, H. D., & Schemske, D. W. 2003. Components of reproductive isolation between the monkeyflowers *Mimulus lewisii* and *M. cardinalis* (Phrymaceae). *Evolution*, *57*(7), 1520-1534.

Rieseberg, L. H., & Willis, J. H. 2007. Plant speciation. *Science*, *317*(5840), 910-914.

Sambatti, J.B., Strasburg, J.L., Ortiz-Barrientos, D., Baack, E.J. and Rieseberg, L.H. 2012. Reconciling extremely strong barriers with high levels of gene exchange in annual sunflowers. *Evolution: International Journal of Organic Evolution*, *66*(5), 1459-1473.

Schemske, D.W. 2000. Understanding the origin of species.

Schluter, D. 2001. Ecology and the origin of species. *Trends in ecology & evolution*, *16*(7), 372-380.

Scopece, G., Musacchio, A., Widmer, A. & Cozzolino, S. 2007. Patterns of reproductive isolation in Mediterranean deceptive orchids. *Evolution: International Journal of Organic Evolution*, *61*(11), 2623-2642.

Sobel, J. M., Chen, G. F., Watt, L. R., & Schemske, D. W. 2010. The biology of speciation. *Evolution: International Journal of organic evolution*, *64*(2), 295-315.

Stebbins, G.L. 1958. The inviability, weakness and sterility of interspecific hybrids. *Advances in Genetics*, *9*, 147-215.

Stephens S.G. 1949. The cytogenetics of speciation in Gossypium. I. Selective elimination of the donor parent genotype in interspecific backcrosses. *Genetics* 34: 627.

Sweigart, A.L., & Flagel, L.E. 2015. Evidence of natural selection acting on a polymorphic hybrid incompatibility locus in Mimulus. *Genetics*, *199*, 543-554.

Vickery, R.K., Jr. 1978. Case studies in the evolution of species complexes in *Mimulus. Evolutionary Biology.***11**: 405– 507.

White, M.J.D., 1948. *Animal cytology & evolution*. Cambridge university press.

White, M.J.D. 1978. Chain processes in chromosomal speciation. *Systematic zoology*, *27*(3), 285-298.

Widmer, A., Lexer, C., & Cozzolino, S. 2009. Evolution of reproductive isolation in plants. *Heredity*, *102*(1), 31-38.

Winge, O. 1917. The chromosomes, their number and general importance. *Compt Rend Trav Lab Carlsberg* 13: 131–275.

Woodell, S.R., & Valentine, D.H., 1961. Studies in British Primulas IX. Seed incompatibility in diploid-autotetraploid crosses. *New Phytologist*, 282-294.

Wu, C.A., Lowry, D.B., Cooley, A.M., Wright, K.M., Lee, Y.W. and Willis, J.H. 2008. Mimulus is an emerging model system for the integration of ecological and genomic studies. *Heredity*, *100*(2), 220-230.

Yamagata, Y., Yamamoto, E., Aya, K., Win, K.T., Doi, K., Sobrizal, Ito, T., Kanamori, H., Wu, J., Matsumoto, T., & Matsuoka, M. 2010. Mitochondrial gene in the nuclear genome induces reproductive barrier in rice. *Proceedings of the National Academy of Sciences*, *107*(4), 1494-1499.

Zuellig, M.P. & Sweigart, A.L. 2018. Gene duplicates cause hybrid lethality between sympatric species of *Mimulus. PLoS genetics*, *14*(4), e1007130.

CHAPTER II

EVOLUTION OF MULTIPLE POSTZYGOTIC BARRIERS BETWEEN SPECIES OF THE *MIMULUS TILINGII* COMPLEX[1]

[1]Sandstedt, G.D., Wu, C.A. & Sweigart, A.L. 2021. Evolution of multiple postzygotic barriers between species of the Mimulus tilingii complex. *Evolution*, *75*(3), 600-613. Reprinted here with permission of publisher.

ABSTRACT

Species are often defined by their ability to interbreed (i.e., Biological Species Concept), but determining how and why reproductive isolation arises between new species can be challenging. In the *Mimulus tilingii* species complex, three species (*M. caespitosa*, *M. minor*, and *M. tilingii*) are largely allopatric and grow exclusively at high elevations (>2000m). The extent to which geographic separation has shaped patterns of divergence among the species is not well understood. In this study, we determined that the three species are morphologically and genetically distinct, yet recently diverged. Additionally, we performed reciprocal crosses within and between the species and identified several strong postzygotic reproductive barriers, including hybrid seed inviability, F1 hybrid necrosis, and F1 hybrid male and female sterility. In this study, such postzygotic barriers are so strong that a cross between any species pair in the *M. tilingii* complex would cause nearly complete reproductive isolation. We consider how geographical and topographical patterns may have facilitated the evolution of several postzygotic barriers and contributed to speciation of closely related members within the *M. tilingii* species complex.

Keywords: Speciation, Allopatric, Reproductive Isolation, *Mimulus*

INTRODUCTION

Since Darwin initially proposed that natural selection commonly drives the origin of species (Darwin 1859), evolutionary biologists have investigated fundamental questions of how and why new species evolve. Theory suggests that most speciation events begin in allopatry, where geographical barriers prevent gene flow and allow populations to diverge ecologically and

genetically (Coyne and Orr 2004). As a byproduct of this divergence, reproductive isolation arises between incipient, sexually reproducing species due to prezygotic barriers that prevent fertilization (e.g., differences in mating system, reproductive timing, or behavior) or postzygotic barriers that cause low fitness in hybrids (e.g., inviability and sterility). Following secondary contact, multiple barriers often act in concert to limit genetic exchange between species (Schluter 2001, Rieseberg and Willis 2007), and selection against hybrids can give rise to additional barriers that further enhance reproductive isolation (i.e., reinforcement; Dobzhansky 1951, Butlin 1989). Because species are often defined by their potential to interbreed (Biological Species Concept, Mayr 1942), a major goal of speciation research is to determine which reproductive barriers evolve during the initial stages of divergence.

One common approach to this problem has been to quantify the relative contributions of pre- and postzygotic barriers to total reproductive isolation (e.g., Ramsey et al. 2003). In plants, such studies often find that prezygotic isolation is stronger than postzygotic isolation (Lowry et al. 2008, Baack et al. 2015), and because reproductive isolating mechanisms act sequentially, it has been argued that the role of later-acting postzygotic barriers is diminished even further (Ramsey et al. 2003, Sobel et al. 2010). Nevertheless, it is important to note that current estimates of reproductive isolating barriers might not reflect their historical roles in species divergence (Widmer et al. 2009), and early-acting barriers can mask later-acting ones, regardless of the order in which they evolved. It is also clear that plant lineages show tremendous variation in patterns of reproductive isolation (Baack et al. 2015) and, in some cases, postzygotic barriers can be quite strong (e.g., Lowry et al. 2008, Ishizaki et al. 2013, Suni and Hopkins 2018, Ostevik et al. 2016, Christie and Strauss 2019).

The extent of geographic overlap between diverging species might also influence the relative importance of pre- versus postzygotic isolation in a given species pair. The potential for increased prezygotic isolation in sympatry due to reinforcement is well established (Coyne and Orr 1989, Noor 1999, Hopkins 2013), but the effect of geography on postzygotic isolation has received less attention. Although intrinsic postzygotic isolation between plant species can be due to chromosomal rearrangements (specifically, hybrid sterility: Stebbins 1958, Rieseberg 2001), in most cases, it is caused by genic incompatibilities (Fishman and Sweigart 2018). When species occur in complete allopatry, these incompatible alleles can evolve to high frequency – either by natural selection or genetic drift – because their negative effects are never exposed in hybrid genomes (Dobzhansky 1937, Muller 1942). In contrast, for species with ongoing gene flow, the build-up of postzygotic isolation requires that local adaptive benefits outweigh the costs of producing sterile or inviable hybrids (Bank et al. 2012). Thus, neutral or weakly selected incompatibility alleles that might evolve readily in allopatry are expected to be purged from species with extensive geographic overlap and hybridization. Given that many closely related plant species are connected by at least moderate levels of gene flow (Morjan and Rieseberg 2004), this geographic discrepancy might help explain the somewhat lower prevalence of intrinsic postzygotic isolation in plants.

In this study, we investigate reproductive isolation in the *Mimulus tilingii* species complex, a group of yellow mountain monkeyflowers restricted to high elevations (>2000m) along alpine and subalpine streams in western North America (Grant 1924, Pennell 1951). Recently, the *M. tilingii* complex was subdivided into three morphological species – *M. tilingii*, *M. caespitosa*, and *M. minor* – that appear to be largely allopatric (Nesom 2012, 2014). First, we

evaluate whether these putative species remain morphologically distinct when grown in a common environment and whether they show evidence of genetic differentiation. Next, we quantify several potential post-pollination barriers by performing reciprocal crosses within and between the three putative species. Surprisingly, we find multiple strong postzygotic isolating barriers between these *M. tilingii* complex species. We argue that strict allopatry might have facilitated the evolution of hybrid incompatibilities in this system, resulting in exceptionally strong postzygotic isolation.

MATERIALS AND METHODS

Study System

Members of the *Mimulus tilingii* complex are mat-forming perennials restricted to high elevations west of the Rocky Mountains (Grant 1924, Pennell 1951). They are self-compatible but thought to be predominantly outcrossing, with large, bee-pollinated flowers. We note that some taxonomists have recently reclassified several *Mimulus* species as *Erythranthe* (including the Tilingii group in Nesom 2012, 2014), but because there is still much debate on the status of these taxa (Lowry et al. 2019, Nesom et al. 2019), we continue to refer to them here as *Mimulus*.

The taxonomic status of species in the *M. tilingii* complex has changed over the years, as taxonomists have attempted to grapple with the rich morphological and ecological diversity of the yellow monkeyflowers. In 1974, Vickery informally identified four distinct entities of *M. tilingii*: *M. tilingii* var. *tilingii* (Regel), *M. tilingii* var. *corallinus* (Greene), *M. implexus* (Greene), and *M. caespitosus*. Through crossing studies, he discovered multiple strong reproductive isolating barriers between *M. t.* var. *tilingii* and *M. t.* var. *corallinus* (including low seed

production, low seed germination, and strong F1 sterility; Vickery 1974), but these barriers were largely attributed to differences in chromosome number (n = 14 in *M. t.* var. *tilingii* and n = 24-28 in *M. t.* var. *corallinus*: Mukherjee and Vickery 1959, 1960, and 1962). In the last decade, Nesom (2012, 2013, 2014, 2019) has suggested several species revisions of the *M. tilingii* complex on the basis of differences in morphology (measured in the field and herbaria) and geographic location. Although his species designations vary somewhat among treatments, most include *M. tilingii*, *M. caespitosa*, and *M. minor* with the first two analogous to Vickery's designations. Of the three putative species, *M. tilingii* is the most widespread, growing throughout much of western North America, whereas *M. caespitosa* grows only in Washington state and southwest Canada, and *M. minor* is restricted to Colorado (Nesom 2012).

Plant material and care

When we began this study, we tentatively classified plants from 12 populations (17 maternal families) within the *M. tilingii* species complex into three putative species: *M. caespitosa*, *M. minor*, and *M. tilingii*. These 12 populations are distributed across the geographic range of the *M. tilingii* complex (Figure 1; Table S1) and putative species assignments were based on population location (Nesom 2012).

All maternal families were self-fertilized for one to eight generations (excluding A25; Table S1). To generate experimental plants, seeds were sown onto wet paper towels in petri dishes, sealed with parafilm, and cold-stratified at 4°C for seven days to disrupt seed dormancy. After cold-stratification, petri dishes were transferred to a growth chamber that provided constant supplemental light at 26°C. After germination, seedlings were transplanted to 3.5" pots with

moist Fafard 4P growing mix (Sun Gro Horticulture, Agawam, Massachusetts, USA) and transferred to a growth chamber with 16h days at 23°C and 8h nights at 16°C. For assessments of hybrid plant viability and fertility, seedlings were allowed to establish in the growth chamber then moved to a 16h, 23°C/8h, 16°C greenhouse.

Measuring morphological variation

To characterize genetically-based morphological differences among species within the *M. tilingii* complex, we grew 66 plants from 11 populations (16 maternal families) together in a growth chamber (Table S1). We measured a suite of 16 floral and vegetative traits (Figure S1, Table S2). First, we measured four leaf traits: when the third leaf pair was fully expanded, we used one leaf from the second leaf pair to measure leaf length and width, petiole length, and number of trichomes that exerted past the edge of the leaf (then standardized by leaf length). Next, we measured ten flower traits from one flower on the second flowering pair: corolla height and width, corolla tube length and width, stamen length, pistil length, pedicel length, capsule length, calyx length, and degree of flower nodding. When performing floral measurements, we also measured two stolon traits: number of stolons and stolon length. All traits were measured using calipers, except for the degree of flower nodding, which was measured on photographs using imageJ (Rasband 1997).

We assessed morphological differentiation among species in the *M. tilingii* complex by performing a linear discriminant analysis (LDA), which maximizes variance between predetermined classes (in our analyses, these corresponded to the three putative species) and projects those differences onto a two-dimensional subset. When needed, we transformed

morphological trait values to meet LDA assumptions (i.e., that values are normally distributed and means are centered and scaled to zero, Table S2). We assigned each of the 66 plants to *M. caespitosa*, *M. minor*, or *M. tilingii.* To model the LDA, we used the lda function in the R package 'MASS'. For samples with missing values (traits that were missing or not measured), we used the R package 'mice' to impute missing data using a predictive mean matching (PMM) method with 50 iterations. We produced 95% confidence intervals with the R package 'ellipse'. Finally, we used the R package 'caret' and predict function to determine the probability that proposed species in the *M. tilingii* complex correspond to classes predicted by the LDA model.

Determining genetic diversity and divergence

We generated whole genome sequence (WGS) data for 14 individuals used in the morphology assessments of the previous section (seven *M. caespitosa,* three *M. minor,* four *M. tilingii*). These 14 individuals were from distinct maternal families collected from nine populations (Table S1). We extracted DNA from bud and leaf tissue using a standard CTAB-chloroform protocol (Doyle and Doyle 1987). We submitted the 14 DNA samples to the Duke Center for Genomic and Computational Biology (GCB), which prepared standard 500-bp DNA-seq libraries and sequenced them on the Illumina HiSeq 4000 platform to produce 150-bp paired-end reads. In addition to these newly generated WGS data, we used existing data from two *M. tilingii* samples (A25 and LVR; Garner et al. 2016, Table S1). For population genomic comparisons, we also used existing WGS data for four *M. guttatus*, two *M. nasutus*, and one *M. dentilobus* individuals (Table S3; Brandvain et al. 2014).

To process sequence data, we first trimmed adapters and low-quality bases using Trimmomatic (Bolger et al. 2014) and confirmed removal using FastQC (Andrews 2010). Next,

we aligned trimmed paired-end reads to the *M. guttatus* v2.0 unmasked reference genome (http://www.phytozome.net) using BWA-MEM (Li 2013, Li and Durbin 2009). To filter the initial alignment, we used the view command in SAMtools to remove reads with an alignment quality below Q29 (Li et al. 2009). We processed the alignments using Picard tools (http://broadinstitute.github.io/picard); we added read groups with AddorReplaceReadGroups and removed potential PCR and optical duplicates with MarkDuplicates. To confirm paired-end reads mapped together, we used SAMtools fixmate and view commands. To produce a set of high-quality invariant and variant sites for all lines, we used Genome Analysis Toolkit's (GATK) HaplotypeCaller and performed joint genotyping using GenotypeGVCFs (McKenna et al. 2010). Subsequent filtering and analyses were performed using reference scaffolds 1-14 that correspond to the 14 chromosomes in the *Mimulus* genome. To obtain high-quality genotypes, we used GATK's VariantFiltration tool to apply hard filtering to sites with mapping quality (MQ) below 40, mapping quality rank sum (MQRankSum) below -12.5, fisher strand (FS) above 60, quality depth (QD) below 2, and read position rank sum (ReadPosRankSum) below -8. We further filtered all sites by removing indels using GATK's SelectVariants. For each sample, we set a minimum depth of at least ten reads per site and a maximum depth of two standard deviations above the mean read depth, which was calculated after the initial alignment using Qualimap2 (Okonechnikov et al. 2015). We restricted all polymorphic sites to biallelic and, for heterozygous sites, randomly assigned one of the two alleles. Note that because most samples were naturally or artificially inbred, individual heterozygosity was generally low (0.63% - 2%; Table S1). Finally, we identified fourfold degenerate sites from each sample (using a script courtesy of Tim

Sackton: https://github.com/tsackton/linked-selection/tree/master/misc_scripts), merged fourfold degenerate sites that are shared across all samples, and extracted these sites from our VCF.

To examine patterns of genomic variation in the *M. tilingii* complex, we used a VCF that contained polymorphic (SNP), fourfold degenerate synonymous sites. We selected sites with more than one copy of the minor allele and genotypes for at least 17 of the 21 samples. Note that sample A25 was excluded from these analyses because it had much lower sequence coverage than all other samples with < 20% coverage at these sites. We down-sampled this polymorphic VCF by randomly selecting 1000 SNPs per chromosome, totaling 14,000 sites. We characterized genetic differentiation among individuals in the *M. tilingii* complex using a neighbor-joining (nj) tree. To produce a nj tree, we first converted our SNP genotype file to a pairwise distance matrix. Then, we used the nj function in the R package 'ape' to construct a nj tree rooted by the outgroup *M. dentilobus* and rate-smoothed using the function chronopl, where $\lambda = 1$ (Paradis et al. 2004). We produced a list of 1000 bootstrapped trees using the package 'phangorn' and plotted the distribution of trees using Densitree (Schliep 2010, Bouckaert 2010). We also explored genetic relatedness among species in the *M. tilingii* complex using a principal component analysis (PCA). To perform this PCA, we used the function pca in the R package 'SNPRelate' and plotted the first two principal components using the R command plot to visualize genetic clusters (Zheng 2013).

In addition to these analyses to visualize genomic structure, we used a VCF containing monomorphic and polymorphic genotype calls at fourfold degenerate sites to calculate pairwise sequence diversity (π_s) and divergence (d_s). To perform these calculations, we used a python script (Notes S1 in Garner et al. 2016) and included only one maternal family per population. For

populations with two maternal families, we arbitrarily selected one maternal family, i.e., GAB1, UTC1, NOR511, and SAB1. Moreover, we tested for the possibility of gene flow between *M. tilingii* and *M. caespitosa*/*M. minor* lineages using an ABBA-BABA test. To estimate the D-statistic for multiple samples of each species, we calculated genome-wide allele frequencies and computed ABBA and BABA proportions at each site, where we assigned *M. caespitosa* and *M. minor* samples to Population 1 and Population 2, respectively, and *M. tilingii* samples to Population 3. We determined significance of D-statistics with a block jackknife approach using a z-score (>3) and p-value (<0.05) threshold. We computed and evaluated all ABBA-BABA statistics using scripts courtesy of Simon Martin : https://github.com/simonhmartin/genomics_general.

Testing reproductive isolating barriers

To investigate postmating reproductive isolating barriers among species in the *M. tilingii* complex, we performed a crossing experiment using plants from 13 maternal families across 10 populations (maternal families: *M. caespitosa* = 7, *M. minor* = 2, *M. tilingii* = 4; Table S1). For this experiment, we used some of the same individuals as in the morphological and genetic analyses above but supplemented them with full siblings from each maternal family. Intraspecific crosses (CxC, MxM, and TxT, where C = *M. caespitosa,* M = *M. minor*, and T = *M. tilingii*) included two types: 1) crosses within maternal families (i.e., between full sibs), and 2) crosses between maternal families within species. Although we detected some significant differences in postmating isolation between these intraspecific cross types (Table S4), they were likely due to inbreeding depression, as crosses between maternal families usually did better than crosses within maternal families. Therefore, we grouped the two intraspecific cross types for all

analyses. Three days prior to each cross, we emasculated maternal parents to avoid contamination from self-pollination. For intraspecific crosses, we generated 62 unique maternal-family cross combinations and 160 total crosses (CxC = 44, MxM = 4, TxT = 14; 1-6 fruits per cross combination). For interspecific crosses, we performed 86 unique and 210 total interspecific crosses (CxM =10, MxC =12, MxT = 8, TxM = 7, TxC = 25, CxT = 24; 1-8 fruits per cross combination; Table S5). We used these crosses to assess the following sequentially-acting postmating reproductive isolating barriers: 1) postmating, prezygotic reproductive isolation, 2) hybrid seed inviability, 3) later-acting hybrid inviability, and 4) hybrid male and female sterility.

Postmating, prezygotic isolation

To assess postmating, prezygotic reproductive isolation, we measured seed production per fruit from crosses within and between species. We note that this measure of postmating, prezygotic isolation is likely to be conservative because it reflects only pollen-pistil incompatibilities and not conspecific pollen precedence, which would require mixed pollinations. We modeled the effect of cross type (i.e., CxC, CxM, MxC, MxM, MxT, TxM, TxT, TxC, CxT) on seed production by fitting a generalized linear model (GLM) with a Gamma distribution using the glm function in the 'lme4' package implemented in R (Bates et al. 2007). In this model, the response variable was the number of seeds produced per fruit and the fixed factors were maternal species, paternal species, and their interaction. To determine whether fixed factors and interactions significantly affected the variance of seed production, we computed an ANOVA test using the anova function in the 'car' package in R with type III sums of squares, which corrects

for unbalanced sample sizes and implements likelihood-ratio chi-square tests for GLMs (Fox et al. 2012). We calculated least-squares means (lsmeans) using the emmeans function in the 'emmeans' package in R and performed pairwise comparisons between all cross types (Lenth and Lenth 2018). We used a post-hoc Tukey method adjustment to determine which of the nine cross types differed significantly in the total number of seeds produced.

Seed viability

We used two different methods as a proxy for measuring seed viability. First, we performed a visual seed assessment. Recent studies in *Mimulus* have shown that inviable hybrid seeds are often darkened and/or shriveled (Garner et al. 2016, Oneal et al. 2016, Coughlan et al. 2020). Following these studies, we scored round, plump seeds as fully developed and seeds with irregular phenotypes (darkened, shriveled, or wrinkled) as underdeveloped. Second, for a subset of crosses, we also assessed seed viability by scoring seed germination (Table S5). For intraspecific crosses, we measured seed germination rates for 48 unique and 76 total crosses (CxC = 36, MxM = 3, TxT = 9; 1-3 fruits per cross combination). For interspecific crosses, we scored germination for 72 unique and 133 total crosses (CxM = 8, MxC = 7, MxT = 7, TxM = 7, TxC = 20, CxT = 23; 1-4 fruits per cross combination). To determine germination rates, we sowed all seeds from each fruit onto wet paper towels in petri dishes (≤100 seeds per petri dish to avoid overcrowding). Petri dishes were sealed with parafilm, cold-stratified at 4°C for seven days, and then transferred to a growth chamber that provided constant light at 26°C. Ten days later, we scored germination rate as the number of seedlings that had germinated per total number of seeds planted per fruit.

To model the effects of cross type on seed viability, we used generalized linear mixed models (GLMMs). We ran GLMMs for both measures of seed viability (visual assessment and seed germination) with a binomial distribution using the glmer command in the 'lme4' package. In this model, we combined the number of viable seeds and the number of inviable seeds into a single response variable using the R function cbind. We set the maternal species, paternal species, and their interaction as fixed factors with their corresponding maternal families set as random factors. Using the anova function with type III sums of squares in R, which applies Wald chi-square tests for mixed models, we computed an ANOVA and determined which fixed factor(s) and interactions significantly contributed to variance of seed viability. We estimated the lsmeans of viable seeds per fruit, performed pairwise comparisons of lsmeans between all cross types, and determined which cross types significantly differed in the number of viable seeds using a post-hoc Tukey method.

F1 viability

To investigate later-acting (post-seed) hybrid inviability, we tracked survival to flowering in a subset of the seedlings from the germination tests described in the previous section. We transplanted seedlings from petri dishes into flats with 6-cm cells and transferred them to a 16h, 23°C/8h, 16°C greenhouse. We transplanted 5-16 offspring from each of 27 unique intraspecific crosses (CxC = 17, MxM = 2, TxT = 8; total intraspecific offspring = 315) and 1-23 F1 hybrids from each of 29 unique interspecific crosses (F1s: CxM = 5, MxC = 4, TxM = 4, TxC = 9, CxT = 7; total interspecific offspring = 334). All interspecific cross combinations were represented in these analyses except for MxT, which did not produce viable offspring due to the severe seed

inviability phenotype. For each individual, we scored the number of days to flowering as a proxy for viability. For individuals that successfully flowered, we modeled the effect of cross type on days to flower using a GLMM with a Poisson distribution (log link). In this model, we set the response variable as the number of days to flower and the fixed factors as maternal species, paternal species, and their interaction with maternal families treated as random factors. We computed an ANOVA and determined which fixed factor(s) and interactions contributed significantly to variation in days to flowering. We calculated and performed pairwise comparisons of lsmeans and used a post-hoc Tukey test to determine which crosses differed in days to flower. We also visually inspected individuals for signs of necrosis, a plant phenotype that is normally associated with environmental stresses (e.g., pathogen attack) but that can manifest in the absence of pathogens due to hybrid incompatibilities (Bomblies and Weigel 2007).

F1 sterility

Finally, using a subset of the intraspecific and hybrid offspring grown to flowering, we investigated both male and female fertility. We assessed male fertility in 4-14 offspring from each of 27 unique intraspecific crosses (CxC = 17, MxM = 2, TxT = 8; total intraspecific offspring = 206) and 4-13 F1 hybrids from each of 28 interspecific crosses (F1s: CxM = 5, MxC = 4, TxM = 4, TxC = 9, CxT = 6; total interspecific offspring = 193). For each individual, we collected anthers from 1-3 of the first four flowers and suspended the pollen in a lacto-phenol aniline blue stain, which stains viable pollen a dark blue color. To estimate pollen viability for each individual, we determined the proportion of viable pollen grains from a haphazard sample of about 100 pollen grains per flower. In a few cases, flowers did not produce functional anthers

or pollen (Table S6); these flowers were excluded from further analyses. We modeled whether cross type had a significant effect on pollen viability using a GLMM with a binomial distribution. We combined the number of viable pollen grains and inviable pollen grains into a single variable using the R function cbind and used this as our response variable. Similar to our previous models, we assigned the fixed factors as maternal species, paternal species, and their interaction, with the corresponding maternal families set as random factors. We determined which fixed factors and interactions contributed significantly to variation in pollen viability with ANOVA and estimated pollen viability lsmeans for each cross type. We performed pairwise comparisons of pollen viability lsmeans and determined which cross types differed significantly using a post-hoc Tukey test.

To investigate female fertility, we performed supplemental hand-pollinations on intraspecific and hybrid offspring using one or both of their fertile parents as pollen donors. For each of these hand-pollinations, we counted the number of seeds produced per fruit. We used this approach to assess female fertility in 2-9 offspring from each of 27 unique intraspecific crosses (CxC = 17, MxM = 2, TxT = 8; total intraspecific offspring = 119, 1-3 fruits per individual) and 1-7 F1 hybrids from each of 27 interspecific crosses (F1s: CxM = 5, MxC = 4, TxM = 4, TxC = 9, CxT = 5; total interspecific offspring = 112, 1-4 fruits per individual). To model whether cross type affects F1 seed set, we used a GLMM with a Poisson error distribution (log link). In this model, we first averaged the number of seeds per fruit for each individual, rounded the values to the nearest whole number, and set this as our response variable. The fixed factors of this model were the maternal and paternal species and their interaction, with the maternal families as random factors. We determined the fixed factor(s) and interactions that contributed significantly

to F1 seed set variance with ANOVA. Then, we calculated the lsmeans, performed pairwise comparisons of lsmeans, and determined which cross types differed in seed set using a post-hoc Tukey method.

RESULTS

Species in the *M. tilingii* complex are morphologically and genetically divergent

To characterize morphological variation within the *M. tilingii* species complex, we grew plants from 16 maternal families together in a common garden. The three putative species within the *M. tilingii* complex showed clear morphological differences in a suite of floral and vegetative traits (Table S2), with a linear discriminant analysis (LDA) separating *M. caespitosa*, *M. minor,* and *M. tilingii* into three non-overlapping clusters (Figure 2, Table S7). Indeed, the three proposed species assignments were identical to the classes predicted by the LDA model (100% of the plants were classified correctly, Table S8).

In addition to these phenotypic differences, patterns of genome-wide variation provide strong support for the existence of three genetically distinct species within the *M. tilingii* complex. A neighbor-joining tree shows the *M. tilingii* complex forms a monophyletic group, which is further separated into three clades corresponding to *M. caespitosa*, *M. minor,* and *M. tilingii* (Figure 3A). Additionally, a principal component analysis reveals genetic structure among species within the *M. tilingii* complex: PC1 (24.30%) splits *M. caespitosa* from *M. minor* and *M. tilingii*, while PC2 (21.89%) separates all three species (Figure 3B). To support these qualitative inferences of genetic structure, we calculated pairwise sequence divergence at fourfold degenerate synonymous sites among *Mimulus* species (Figure 3C, Table S9).

Interspecific divergence between *M. caespitosa* and *M. minor* (d_s = 3.76% [3.64%—3.88%]) well exceeds diversity within either species (*M. caespitosa*: π_s = 1.16% [1.11%—1.21%]; *M. minor:* π_s = 1.04%). Although nucleotide diversity within *M. tilingii* (π_s = 3.19% [3.06%—3.32%]) was much higher; interspecific divergence involving this species and *M. caespitosa* (d_s = 4.4% [4.39%—4.41%]) or *M. minor* (d_s = 4.27% [4.25%—4.29%]) was greater still. Using these values and assuming that current levels of diversity within *M. tilingii* approximate levels in the ancestral population, we estimate the species split time (T_S) between *M. tilingii* and the other two species to be 382 kya [337ky-430ky] (i.e., following Brandvain et al. 2014: [$T_S = d_{s\ \text{tilxcaes,minor}} - \pi_{s\ \text{til}}]/2\mu$, where $\mu = 1.5\text{x}10^{-8}$). In addition, an ABBA-BABA test suggests no evidence of gene flow between *M. tilingii* and *M. caespitosa*/*M. minor* lineages (D = -0.014, z = 1.545, p-value = 0.122). Finally, using a similar approach, we estimate 674 kya as the split time between the *M. tilingii* and *M. guttatus* species complexes (approximating ancestral diversity by the average of current diversity in the two complexes; i.e., [$d_{s\ \text{tilxgutt}} - \frac{1}{2}\ \pi_s]/2\mu$).

***M. tilingii* species show strong postmating reproductive isolation**

To determine the extent of postmating reproductive isolation among the three putative species within the *M. tilingii* complex, we performed a crossing experiment using plants from 10 populations (13 maternal families; *M. caespitosa* = 7, *M. minor* = 2, *M. tilingii* = 4; Table S1). We assessed several sequentially-acting postmating reproductive isolating barriers: 1) postmating, prezygotic reproductive isolation, 2) hybrid seed inviability, 3) later-acting hybrid inviability, and 4) hybrid male and female sterility; results for each are presented below.

Our crosses showed no evidence of postmating, prezygotic reproductive isolation among the three *M. tilingii* species. Indeed, the number of seeds produced by interspecific crosses was

just as high as the number produced by intraspecific crosses (Figure 4, Table S10), suggesting that interspecific pollen-pistil incompatibilities do not prevent fertilization among these species. Instead, variation in seed production was driven largely by species of the maternal parent: crosses with *M. minor* as the maternal parent produced 38% more seeds per fruit than crosses with *M. caespitosa* as the maternal parent and 30% more than crosses with *M. tilingii* as the maternal parent (Figure 4, Table S10, Figure S2).

In contrast to postmating, prezygotic isolation, we discovered very strong hybrid seed inviability in certain crosses within the *M. tilingii* complex using both seed viability measures (visual assessment and germination). In our visual assessment of seed viability, when *M. tilingii* acted as the paternal parent, interspecific crosses produced few to no fully developed seeds per fruit (F1 seed viability: CxT = 20%, MxT = 1%; Figure 5A, Table S11). When the same crosses were performed in the reciprocal direction, the proportion of fully developed hybrid seed was much higher (F1 seed viability: TxC = 91%, TxM = 76%). Hybrid seeds were also mostly fully developed in both reciprocal crosses of *M. caespitosa* and *M. minor* (F1 seed viability: CxM= 96%, MxC = 84%; Figure 5A). Variation in germination rates among cross types largely mirrored patterns of visually assessed seeds (i.e., the rank order among cross types did not change; Figure 5B, Table S12). In sum, hybrid seed inviability is a strong reproductive isolating barrier in one crossing direction between *M. tilingii* and *M. caespitosa* or *M. minor*.

Next, we assessed the viability of hybrids that survived to the seedling stage. Once established as seedlings, all progeny of intraspecific crosses, and most hybrid progeny of interspecific crosses, survived to flowering (Table S6). We detected no evidence of F1 hybrid inviability between *M. caespitosa* and *M. minor*: 100% of CxM and MxC F1 hybrids produced

flowers (*N* = 57 and 56, respectively). In fact, CxM F1 hybrids flower much earlier (~13 days) than progeny of *M. caespitosa* crosses (days to flowering: CxM = 36, CxC = 49; Table S13). Similarly, 100% of F1 hybrids between *M. tilingii* and *M. minor* flowered and showed no delay in flowering time relative to progeny of intraspecific crosses (*N* = 54 for TxM; severe hybrid seed inviability precluded generating F1 hybrids in the reciprocal direction, Table S13). However, one class of F1 hybrids – those produced from crosses between *M. caespitosa* and *M. tilingii* – did show evidence of inviability: 18% of CxT and TxC F1 hybrids did not survive to flowering because they were severely necrotic (*N* = 60 and 107, respectively, Figure S2; Table S6). It is important to note that this F1 hybrid necrosis phenotype was not segregating in all *M. caespitosa-M. tilingii* crosses. Instead, the 18% frequency is due to a high proportion of necrotic F1 hybrids between particular maternal families of *M. caespitosa* and *M. tilingii* (i.e., 25-100% F1 necrosis in crosses between *M. caespitosa* GAB1 or UTC1 and *M. tilingii* ICE10; Table S6). Thus, although hybrid inviability is not fixed between species of the *M. tilingii* complex, it can be a strong postzygotic isolating barrier in certain interspecific crosses.

Finally, for hybrids and intraspecific progeny that survived to flowering, we examined both male and female fertility. Strikingly, we discovered strong male sterility in both of the reciprocal F1 hybrids from all three interspecific crosses: pollen viability was much lower in all F1 hybrids than in the progeny of intraspecific crosses (Figure 6A, Table S14). Male sterility was particularly severe in F1 hybrids with *M. minor* as a parent (CxM, MxC, and TxM), which showed a 96% reduction in pollen viability compared to intraspecific crosses. Female sterility was also remarkably strong in all tested F1 hybrids (Figure 6B; Table S15). Reciprocal F1 hybrids between *M. caespitosa* and *M. tilingii* produced 81% fewer seeds per fruit than parental

intraspecific crosses (TxT and CxC). As with male sterility, F1 hybrids with *M. minor* as a parent showed particularly severe female sterility, with a 99% reduction in F1 seed set compared to intraspecific crosses. Taken together, these results indicate that F1 sterility – through both male and female functions – is an extremely strong postzygotic isolating barrier between species in the *M. tilingii* complex.

DISCUSSION

A fundamental goal in evolutionary biology is understanding how new species evolve. In this study, we determined that three species in the *M. tilingii* complex (*M. caespitosa*, *M. minor*, and *M. tilingii*) are morphologically and genetically different. Additionally, we discovered that a cross between any species pair within the *M. tilingii* complex results in near complete reproductive isolation by several postzygotic barriers, including hybrid seed inviability, hybrid necrosis, and hybrid male and female sterility (*i.e.*, following Sobel and Chen 2014, cumulative postmating reproductive isolation ranges from 0.86 to 0.99). Below, we discuss the possibility that strict allopatry among these montane species within the *M. tilingii* complex might have facilitated the evolution of this strikingly high number of hybrid incompatibilities.

In this study, the first severe postzygotic barrier we found between certain species within the *M. tilingii* complex was hybrid seed inviability. In flowering plants, hybrid seed inviability is a common feature of interploidy and interspecific crosses (Scott et al. 1998, Rebernig et al. 2015, Roth et al. 2018) and, in fact, has evolved multiple times across the *Mimulus* genus (Vickery 1978, Garner et al. 2016, Oneal et al. 2016, Coughlan et al. 2020). Often, hybrid seed inviability is caused by a defective endosperm—a tissue critical for transferring maternal nutrients to the

developing embryo (Köhler et al. 2010, Lafon-Placette and Köhler 2016, Brink and Cooper 1947). The endosperm also serves as the primary tissue of genomic imprinting, which is parent-of-origin dependent gene expression due to differential epigenetic modifications established during male and female gametogenesis (Köhler et al. 2012). Classic theory suggests that the evolution of imprinted genes might be driven by parental conflict over maternal investment in the endosperm (Haig and Westoby 1989). In principle, misregulation of imprinted genes provides a mechanistic explanation for the common observation that the seeds of reciprocal interspecific crosses often show phenotypic differences (Haig and Westoby 1991). In like manner, we show parent-of-origin effects on hybrid seed inviability among species in the *M. tilingii* complex; notably, seeds are mostly inviable when *M. tilingii* acts as the pollen donor in any interspecific cross. Reciprocal differences in seed viability are a hallmark of endosperm defects (Haig and Westoby 1991), and although we do not show a defective endosperm as a mechanistic cause, patterns of seed viability among *M. tilingii* species (Figure 5) and preliminary developmental work suggest the endosperm is involved.

Crosses between species with divergent mating systems (i.e., self-fertilizers and outcrossers) can result in reciprocal seed phenotypes, which might be driven by differences in strength of conflict (weak inbreeder/strong outbreeder [WISO] hypothesis; Brandvain and Haig 2005). In the case of the *M. tilingii* species complex, a shift towards selfing in *M. minor* and *M. caespitosa* could explain reciprocal differences in seed viability in hybrid crosses with *M. tilingii*. Apart from mating system differences, the strength of parental conflict may depend on other factors that influence genetic variation, including demographic history or vegetative propagation (i.e., stolons) that can lead to clonal reproduction. Moreover, the genetic and

evolutionary basis of hybrid seed inviability among *M. tilingii* species might be much more complex. We note that although hybrid seed inviability appears to be mostly species-wide, one *M. caespitosa* maternal line (GAB1) consistently produced viable seeds when crossed reciprocally with *M. tilingii*, suggesting that causal genetic loci may be polymorphic within species.

In addition to early-acting hybrid seed inviability between species within the *M. tilingii* complex, we found later-acting inviability in the form of hybrid necrosis. This plant syndrome is associated with a suite of phenotypes including cell death, wilting, yellowing, chlorosis, reduced growth rates, and often lethality (Bomblies and Weigel 2007). In crosses between *M. tilingii* and *M. caespitosa*, we discovered severe F1 hybrid necrosis: plants produced unusually small buds that failed to develop into flowers, followed by plant senescence (observed; Figure S3). Hybrid lethality can readily evolve in many plant systems and has been reported several times in *Mimulus* (Macnair and Christie 1983, Lowry et al. 2008, Wright et al. 2013, Zuellig and Sweigart 2018). As in other plant taxa (Sicard et al. 2015, Zuellig and Sweigart 2018, Macnair and Christie 1983), we observed variation in the genetic basis of hybrid lethality within *M. tilingii* species— only specific maternal lines in combination give rise to hybrid lethal offspring (i.e., UTC1 and GAB1 in combination with ICE10). Often, hybrid necrosis is caused when incompatible disease resistance genes (i.e., R genes) against bacterial or fungal pathogens facilitate an autoimmune response (Chae et al. 2016). Disease resistance genes are thought to evolve rapidly in response to pathogen pressure; they exhibit exceptional variation in nucleotide sequence, high copy number, and gene expression (Jacob et al. 2013). Additionally, in natural plant populations, disease resistance genes often show signatures of balancing selection and

diversifying selection (Karasov et al. 2014), which might explain why causal genetic loci are polymorphic within *M. tilingii* and *M. caespitosa* species. Future experiments are needed to determine the molecular genetic basis of hybrid necrosis in the *M. tilingii* complex and whether divergence of disease resistance genes underlies this barrier.

Lastly, we show that viable F1 hybrids generated from crosses among species within the *M. tilingii* complex are severely male and female sterile, especially when *M. minor* is involved. Hybrid sterility is a common reproductive barrier across plants and animals and its genetic basis can vary from simple to complex (Kubo et al. 2008, Sweigart et al. 2006, Lai et al. 2005). Many factors have been implicated as causes underlying hybrid male sterility, including cytonuclear incompatibilities, chromosomal rearrangements, interactions among nuclear genes, or a combination of these factors (Bomblies 2010). For example, in closely related sunflower species, severe hybrid sterility was genetically mapped to karyotypic differences between species as well as genic interactions in non-rearranged regions (Lai et al. 2005). Because both male and female hybrid sterility are strong among species within the *M. tilingii* complex, we speculate that chromosomal rearrangements and/or multiple independent Dobzhansky-Muller incompatibilities may underlie these barriers. Although we cannot completely rule out slight variation in chromosome number as a potential cause for hybrid incompatibilities among species within the *M. tilingii* complex, preliminary chromosome squashes suggest no differences in ploidy (n=14; data not shown).

What factors might explain the evolution of multiple strong reproductive barriers among these closely related members of the *M. tilingii* species complex? During and following Pleistocene glaciation, it is possible that gene flow was severely limited among species in the *M.*

tilingii complex that were confined to distinct mountain ranges, facilitating the accumulation of hybrid incompatibilities and other genetic differences. Indeed, an ABBA-BABA test reveals no evidence of introgression between *M. tilingii* and *M. caespitosa*/*M. minor* lineages following species divergence. Although the *M. tilingii* complex is as genetically variable as the closely related and well-studied *M. guttatus* species complex (Brandvain et al. 2014), it shows much stronger F1 postzygotic isolation. Many hybrid incompatibilities have been identified within and between members of the *M. guttatus* complex, including several that affect F2 hybrids or backcross hybrids (hybrid lethality in Zuellig and Sweigart 2018, hybrid sterility in Sweigart et al. 2006, Fishman and Willis 2006) though some species pairs give rise to F1 hybrid seed inviability and various levels of hybrid lethality (Gardner and Macnair 2000, Macnair and Christie 1983, Wright et al. 2013). In addition, species in the *M. guttatus* complex have overlapping distributions throughout most of Western North America, and there is evidence for substantial introgression in regions of sympatry (Brandvain et al. 2014, Kenney and Sweigart 2016, Zuellig and Sweigart 2018). When interspecific gene flow is present, theory suggests that neutrally evolving hybrid incompatibility alleles may be purged from species because their deleterious effects become exposed in hybrids (Gavrilets 1997, Kondrashov 2003, Bank et al. 2012, Muir and Hahn 2015). Perhaps, then, extensive gene flow between species in the *M. guttatus* complex explains its lower prevalence of F1 postzygotic barriers, and strict allopatry in the *M. tilingii* complex might explain why much stronger postzygotic isolation has evolved among its species. In plants, closely related species often show extensive range overlap (Baack et al. 2015), yet it is unclear how such overlap will impact the strength of intrinsic postzygotic

isolation. More studies are needed to explicitly test the effect of interspecific gene flow on the relative strength of prezygotic versus postzygotic barriers in young species pairs.

Along with these strong intrinsic F1 postzygotic barriers, it is entirely possible that prezygotic and extrinsic postzygotic barriers might also have evolved among allopatric species within the *M. tilingii* complex. For example, even though we did not find evidence of postmating, prezygotic isolation in our study, we did not test for conspecific pollen precedence, which has been shown to partially isolate other closely related *Mimulus* species (Diaz and Macnair 1999; Ramsey et al. 2003, Fishman et al. 2008). Additionally, we find that patterns of morphological and genetic variation among *M. tilingii* species might be driven, at least in part, by mating system divergence. Shifts in mating system are common across the *Mimulus* genus and other flowering plants and can act as a strong premating barrier (Rieseberg & Willis 2007). Although members of the *M. tilingii* species complex appear to be predominantly outcrossing, the rate of selfing within and between species varies and can be as high as 30% (Ritland 1989; Ritland and Ritland 1989). Compared to *M. tilingii*, individuals from both *M. minor* and *M. caespitosa* show a relative decrease in anther-stigma distance and corolla width (Table S2), two traits that can promote selfing via contact between the stigma and anthers. Consistent with a transition toward increased selfing in these species, nucleotide diversity between populations of *M. caespitosa* and *M. minor* was only a third that of *M. tilingii* (Figure 3C). Additionally, nucleotide diversity within the NOR population of *M. minor* was 0.2% ($N = 2$), which represents a 50-fold reduction in intrapopulation variation compared to *M. caespitosa* and *M. tilingii* (Table S9). Although these results might suggest an increased propensity for selfing in *M. minor*, we note that one maternal line belonging to *M. minor* had the highest individual heterozygosity

compared to all other sequenced lines in this study (UNP12; Table S1). Further, some patterns may be explained by the fact that we have only two *M.* minor populations and a narrower sampling distribution for both *M. caespitosa* and *M. minor*.

Although it is tempting to speculate that speciation in the *M. tilingii* species complex has been driven in large part by postzygotic reproductive isolation, more work will be needed to understand the evolutionary causes and consequences of F1 postzygotic barriers in nature. The exact geographical distributions of members in the *M. tilingii* species complex are not well defined and we do not yet know whether these species occasionally come into secondary contact. Additionally, although we know species within the *M. tilingii* complex are restricted to high elevations, more investigation is needed to determine whether these montane environments are ecologically distinct and whether species within the *M. tilingii* complex have evolved premating barriers associated with divergent adaptation. In conclusion, species in the *M. tilingii* complex are closely related, yet genetically and morphologically distinct. Notably, this system is rich with possibilities to investigate the genetics and evolution of reproductive isolation in montane, allopatric species early in divergence.

REFERENCES

Andrews S. 2010. *FastQC: a quality control tool for high throughput sequence data. Available online at*: http://www.bioinformatics.babraham.ac.uk/projects/fastqc

Baack, E., Melo, M. C., Rieseberg, L. H., & Ortiz-Barrientos, D. 2015. The origins of reproductive isolation in plants. *New Phytologist*, *207*(4), 968-984.

Bank, C., Hermisson, J., & Kirkpatrick, M. 2012. Can reinforcement complete speciation? *Evolution: International Journal of Organic Evolution*, *66*(1), 229-239.

Bates, D., Sarkar, D., Bates, M. D., & Matrix, L. 2007. The lme4 package. *R package version*, *2*(1), 74.

Bolger, A. M., Lohse, M., & Usadel, B. 2014. Trimmomatic: a flexible trimmer for Illumina sequence data. *Bioinformatics*, *30*(15), 2114-2120.

Bomblies, K. 2010. Doomed lovers: mechanisms of isolation and incompatibility in plants. *Annual review of plant biology*, *61*, 109-124.

Bomblies, K., & Weigel, D. 2007. Hybrid necrosis: autoimmunity as a potential gene-flow barrier in plant species. *Nature Reviews Genetics*, *8*(5), 382-393.

Bouckaert, R. R. 2010. DensiTree: making sense of sets of phylogenetic trees. *Bioinformatics, 26*(10), 1372-1373.

Brandvain, Y., & Haig, D. 2005. Divergent mating systems and parental conflict as a barrier to hybridization in flowering plants. *The American Naturalist*, *166*(3), 330-338.

Brandvain, Y., Kenney, A. M., Flagel, L., Coop, G., & Sweigart, A. L. 2014. Speciation and introgression between *Mimulus* nasutus and *Mimulus guttatus*. *PLoS genetics*, *10*(6), e1004410.

Brink, R. A., & Cooper, D. C. 1947. The endosperm in seed development. *The Botanical Review*, *13*(9), 479-541.

Butlin, R. 1989. Reinforcement of premating isolation. Pp. 158–179 in Otte, D. and J. A. Endler (eds) Speciation and its consequences. Sinauer Associates, Inc., Sunderland, MA.

Chae, E., Tran, D. T., & Weigel, D. 2016. Cooperation and conflict in the plant immune system. *PLoS pathogens*, *12*(3).

Christie, K., & Strauss, S. Y. 2019. Reproductive isolation and the maintenance of species boundaries in two serpentine endemic Jewelflowers. *Evolution*, *73*(7), 1375-1391.

Coughlan, J. M., Brown, M. W., & Willis, J. H. 2020. Patterns of Hybrid Seed Inviability in the *Mimulus guttatus* sp. Complex Reveal a Potential Role of Parental Conflict in Reproductive Isolation. *Current Biology*, *30*(1), 83-93.

Coyne, J. A., and H. A. Orr. 1989. Patterns of speciation in *Drosophila*. Evolution 43:362–381.

Coyne, J.A., and H. A. Orr. 2004. Speciation. Sinauer Associates, Sunderland, MA.

Darwin, C. R. 1859. The Origin of species. 6th ed. John Murray, London.

Diaz, A., & Macnair, M. R. 1999. Pollen tube competition as a mechanism of prezygotic reproductive isolation between *Mimulus* nasutus and its presumed progenitor *M. guttatus*. *The New Phytologist*, *144*(3), 471-478.

Dobzhansky, T. 1937. Genetic nature of species differences. *The American Naturalist*, *71*(735), 404-420.

Dobzhansky, T. 1951. Genetics and the origin of species. 3rd ed. Columbia Univ. Press, New York

Doyle, J. J., & Doyle, J. L. 1987. CTAB DNA extraction in plants. *Phytochemical Bulletin*, *19*, 11-15.

Fishman, L., Aagaard, J., & Tuthill, J. C. 2008. Toward the evolutionary genomics of gametophytic divergence: patterns of transmission ratio distortion in monkeyflower (*Mimulus*) hybrids reveal a complex genetic basis for conspecific pollen precedence. *Evolution: International Journal of Organic Evolution*, *62*(12), 2958-2970.

Fishman, L., & Sweigart, A. L. 2018. When two rights make a wrong: the evolutionary genetics of plant hybrid incompatibilities. *Annual review of plant biology*, *69*, 707-731.

Fishman, L., & Willis, J. H. 2006. A cytonuclear incompatibility causes anther sterility in *Mimulus* hybrids. *Evolution*, *60*(7), 1372-1381.

Fox, J., Weisberg, S., Adler, D., Bates, D., Baud-Bovy, G., Ellison, S., Firth, D., Friendly, M., Gorjanc, G., Graves, S. and Heiberger, R. 2012. Package 'car'. *Vienna: R Foundation for Statistical Computing*

Gardner, M., & Macnair, M. 2000. Factors affecting the co-existence of the serpentine endemic *Mimulus nudatus* Curran and its presumed progenitor, *Mimulus guttatus* Fischer ex DC. *Biological Journal of the Linnean Society*, *69*(4), 443-459.

Garner, A. G., Kenney, A. M., Fishman, L., & Sweigart, A. L. 2016. Genetic loci with parent of-origin effects cause hybrid seed lethality in crosses between *Mimulus* species. *New Phytologist*, *211*(1), 319-331.

Gavrilets, S. 1997. Hybrid zones with Dobzhansky-type epistatic selection. *Evolution*, *51*(4), 1027-1035.

Grant, A.L. 1924. A monograph of the genus *Mimulus*. Ann. Missouri Bot. Gard. 11:99-389

Haig, D., & Westoby, M. 1989. Parent-specific gene expression and the triploid endosperm. *The American Naturalist*, *134*(1), 147-155.

Haig, D., & Westoby, M. 1991. Genomic imprinting in endosperm: its effect on seed development in crosses between species, and between different ploidies of the same species, and its implications for the evolution of apomixis. *Philosophical Transactions: Biological Sciences*, 1-13.

Hopkins, R. 2013. Reinforcement in plants. *New Phytologist*, *197*(4), 1095-1103.

Ishizaki, S., Abe, T., & Ohara, M. 2013. Mechanisms of reproductive isolation of interspecific hybridization between *Trillium camschatcense* and *T. tschonoskii* (Melanthiaceae). *Plant Species Biology*, *28*(3), 204-214.

Jacob, F., Vernaldi, S., & Maekawa, T. 2013. Evolution and conservation of plant NLR functions. *Frontiers in immunology*, *4*, 297.

Karasov, T. L., Horton, M. W., & Bergelson, J. 2014. Genomic variability as a driver of plant-pathogen coevolution? *Current opinion in plant biology*, *18*, 24-30.

Kenney, A. M., & Sweigart, A. L. 2016. Reproductive isolation and introgression between sympatric *Mimulus* species. *Molecular ecology*, *25*(11), 2499-2517.

Köhler, C., Scheid, O. M., & Erilova, A. 2010. The impact of the triploid block on the origin and evolution of polyploid plants. *Trends in Genetics*, *26*(3), 142-148.

Köhler, C., Wolff, P., & Spillane, C. 2012. Epigenetic mechanisms underlying genomic imprinting in plants. *Annual review of plant biology*, *63*, 331-352.

Kondrashov, A. S. 2003. Accumulation of Dobzhansky-Muller incompatibilities within a spatially structured population. *Evolution*, *57*(1), 151-153.

Kubo, T., Yamagata, Y., Eguchi, M., & Yoshimura, A. 2008. A novel epistatic interaction at two loci causing hybrid male sterility in an inter-subspecific cross of rice (*Oryza sativa* L.). *Genes & genetic systems*, *83*(6), 443-453.

Lafon-Placette, C., & Köhler, C. 2016. Endosperm-based postzygotic hybridization barriers: developmental mechanisms and evolutionary drivers. *Molecular Ecology*, *25*(11), 2620-2629.

Lai, Z., Nakazato, T., Salmaso, M., Burke, J. M., Tang, S., Knapp, S. J., & Rieseberg, L. H. 2005. Extensive chromosomal repatterning and the evolution of sterility barriers in hybrid sunflower species. *Genetics*, *171*(1), 291-303.

Lenth, R., & Lenth, M. R. 2018. Package 'lsmeans'. *The American Statistician*, *34*(4), 216-221.

Li, H., and Durbin, R. 2009. Fast and accurate short read alignment with Burrows-Wheeler transform. Bioinformatics 25:1754–1760.

Li, H., Handsaker, B., Wysoker, A., Fennell, T., Ruan, J., Homer, N., Marth, G., Abecasis, G & Durbin, R. 2009. The sequence alignment/map format and SAMtools. *Bioinformatics*, 25(16), 2078-2079.

Li, H. 2013. Aligning sequence reads, clone sequences and assembly contigs with BWA-MEM. arXiv 1303:3997v2.

Lowry, D. B., Modliszewski, J. L., Wright, K. M., Wu, C. A., & Willis, J. H. 2008. The strength and genetic basis of reproductive isolating barriers in flowering plants. *Philosophical Transactions of the Royal Society B: Biological Sciences*, *363*(1506), 3009-3021.

Lowry, D. B., Rockwood, R. C., & Willis, J. H. 2008. Ecological reproductive isolation of coast and inland races of *Mimulus guttatus*. *Evolution: International Journal of Organic Evolution*, *62*(9), 2196-2214.

Lowry, D.B., Sobel, J.M., Angert, A.L., Ashman, T.L., Baker, R.L., Blackman, B.K., Brandvain, Y., Byers, K.J., Cooley, A.M., Coughlan, J.M. and Dudash, M.R. 2019. The case for the continued use of the genus name *Mimulus* for all monkeyflowers. *Taxon*, *68*(4), pp.617-623.

Macnair, M. R., & Christie, P. 1983. Reproductive isolation as a pleiotropic effect of copper tolerance in *Mimulus guttatus*? *Heredity*, *50*(3), 295-302.

Mayr, E. 1942. Systematics and the origin of species. Columbia Univ. Press, New York.

McKenna, A., Hanna, M., Banks, E., Sivachenko, A., Cibulskis, K., Kernytsky, A., Garimella, K., Altshuler, D., Gabriel, S., Daly, M. & DePristo, M. A. 2010. The Genome Analysis Toolkit: a MapReduce framework for analyzing next-generation DNA sequencing data. *Genome research*, *20*(9), 1297-1303.

Morjan, C. L., & Rieseberg, L. H. 2004. How species evolve collectively: implications of gene flow and selection for the spread of advantageous alleles. *Molecular ecology*, *13*(6), 1341-1356.

Muir, C. D., & Hahn, M. W. 2015. The limited contribution of reciprocal gene loss to increased speciation rates following whole-genome duplication. *The American Naturalist*, *185*(1), 70-86.

Mukherjee, B. B., & Vickery, R. K. 1959. Chromosome counts in the section Simiolus of the genus *Mimulus* (Scrophulariaceae). III. *Madroño*, *15*(2), 57-62.

Mukherjee, B. B., & Vickery, R. K. 1960. Chromosome counts in the section Simiolus of the genus *Mimulus* (Scrophulariaceae). IV. *Madroño*, *15*(8), 239-245.

Mukherjee, B. B., & Vickery, R. K. 1962. Chromosome counts in the section Simiolus of the genus *Mimulus* (Scrophulariaceae). V. The chromosomal homologies of *M. guttatus* and its allied species and varieties. *Madroño*, *16*(5), 141-155.

Muller H. J. 1942. Isolating mechanisms, evolution, and temperature. Biological Symposium 6: 71–125.

Nesom, G. L. 2012. Taxonomy of *Erythranthe* sect. Simiola (Phrymaceae) in the USA and Mexico. *Phytoneuron*, *40*, 1-123.

Nesom, G.L. 2013. New distribution records for *Erythranthe* (Phrymaceae). Phytoneuron 2013, 67: 1–15.

Nesom, G.L. 2014. Updated classification and hypothetical phylogeny of *Erythranthe* sect. Simiola (Phrymaceae). *Phytoneuron*, *2014*, 1-6.

Nesom, G.L. 2019. Taxonomic status of *Erythranthe minor* (Phrymaceae). *Phytoneuron 2019*, 32: 1-7.

Nesom, G. L., Fraga, N. S., Barker, W. R., Beardsley, P. M., Tank, D. C., Baldwin, B. G., & Olmstead, R. G. 2019. Response to "The case for the continued use of the genus name *Mimulus* for all monkeyflowers".

Noor, M. A. 1999. Reinforcement and other consequences of sympatry. *Heredity*, *83*(5), 503-508.

Okonechnikov, K., Conesa, A., & García-Alcalde, F. 2015. Qualimap 2: advanced multi-sample quality control for high-throughput sequencing data. *Bioinformatics*, *32*(2), 292-294.

Oneal, E., Willis, J. H., & Franks, R. G. 2016. Disruption of endosperm development is a major cause of hybrid seed inviability between *Mimulus guttatus* and *Mimulus* nudatus. *New Phytologist*, *210*(3), 1107-1120.

Ostevik, K. L., Andrew, R. L., Otto, S. P., & Rieseberg, L. H. 2016. Multiple reproductive barriers separate recently diverged sunflower ecotypes. *Evolution*, *70*(10), 2322-2335.

Paradis, E., Claude, J., & Strimmer, K. 2004. APE: analyses of phylogenetics and evolution in R language. *Bioinformatics*, *20*(2), 289-290.

Pennell, F. W. 1951. *Mimulus*. *Illustrated flora of the Pacific states*, *3*, 688-731.

Ramsey, J., Bradshaw Jr, H. D., & Schemske, D. W. 2003. Components of reproductive isolation between the monkeyflowers *Mimulus lewisii* and *M. cardinalis* (Phrymaceae). *Evolution*, *57*(7), 1520-1534.

Rasband, W.S. 1997. ImageJ, U. S. National Institutes of Health, Bethesda, Maryland, USA, https://imagej.nih.gov/ij/.

Rebernig, C. A., Lafon-Placette, C., Hatorangan, M. R., Slotte, T., & Köhler, C. 2015. Non-reciprocal interspecies hybridization barriers in the *Capsella* genus are established in the endosperm. *PLoS genetics*, *11*(6).

Rieseberg, L. H. 2001. Chromosomal rearrangements and speciation. *Trends in ecology & evolution*, *16*(7), 351-358.

Rieseberg, L. H., & Willis, J. H. 2007. Plant speciation. *Science*, *317*(5840), 910-914.

Ritland, C. and Ritland, K., 1989. Variation of sex allocation among eight taxa of the *Mimulus guttatus* species complex (Scrophulariaceae). *American Journal of Botany*, *76*(12), pp.1731-1739.

Ritland, K. 1989. Genetic differentiation, diversity, and inbreeding in the mountain monkeyflower (*Mimulus* caespitosus) of the Washington Cascades. *Canadian Journal of Botany*, *67*(7), 2017-2024.

Roth, M., Florez-Rueda, A. M., Griesser, S., Paris, M., & Städler, T. 2018. Incidence and developmental timing of endosperm failure in post-zygotic isolation between wild tomato lineages. *Annals of botany*, *121*(1), 107-118.

Schliep, K. P. 2010. phangorn: phylogenetic analysis in R. *Bioinformatics*, *27*(4), 592-593.

Schluter, D. 2001. Ecology and the origin of species. *Trends in ecology & evolution*, *16*(7), 372-380.

Scott, R. J., Spielman, M., Bailey, J., & Dickinson, H. G. 1998. Parent-of-origin effects on seed development in Arabidopsis thaliana. *Development*, *125*(17), 3329-3341.

Sicard, A., Kappel, C., Josephs, E. B., Lee, Y. W., Marona, C., Stinchcombe, J. R., Wright, S.I. & Lenhard, M. 2015. Divergent sorting of a balanced ancestral polymorphism underlies the establishment of gene-flow barriers in *Capsella*. *Nature communications*, *6*, 7960.

Sobel, J. M., & Chen, G. F. 2014. Unification of methods for estimating the strength of reproductive isolation. *Evolution*, *68*(5), 1511-1522.

Sobel, J. M., Chen, G. F., Watt, L. R., & Schemske, D. W. 2010. The biology of speciation. *Evolution: International Journal of organic evolution*, *64*(2), 295-315.

Stebbins, G. L. 1958. The inviability, weakness and sterility of interspecific hybrids. Adv. Genet. 9:147–215.

Suni, S. S., & Hopkins, R. 2018. The relationship between postmating reproductive isolation and reinforcement in Phlox. *Evolution*, *72*(7), 1387-1398.

Sweigart, A. L., Fishman, L., & Willis, J. H. 2006. A simple genetic incompatibility causes hybrid male sterility in *Mimulus*. *Genetics*, *172*(4), 2465-2479.

Vickery, R.K., Jr. 1974. Crossing barriers in the yellow monkey flowers in the genus *Mimulus* (Scrophulariaceae). Genet. Lect. 3: 33–82.

Vickery, R.K., Jr. 1978. Case studies in the evolution of species complexes in *Mimulus. Evolutionary Biology.***11**: 405– 507.

Widmer, A., Lexer, C., & Cozzolino, S. 2009. Evolution of reproductive isolation in plants. *Heredity*, *102*(1), 31-38.

Wright, K. M., Lloyd, D., Lowry, D. B., Macnair, M. R., & Willis, J. H. 2013. Indirect evolution of hybrid lethality due to linkage with selected locus in *Mimulus guttatus*. *PLoS biology*, *11*(2).

Zheng, X. 2013. A Tutorial for the R Package SNPRelate. *University of Washington, Washington, USA*

Zuellig, M. P., & Sweigart, A. L. 2018. A two-locus hybrid incompatibility is widespread, polymorphic, and active in natural populations of *Mimulus*. *Evolution*, *72*(11), 2394-2405.

Zuellig, M. P., & Sweigart, A. L. 2018. Gene duplicates cause hybrid lethality between sympatric species of *Mimulus*. *PLoS genetics*, *14*(4)

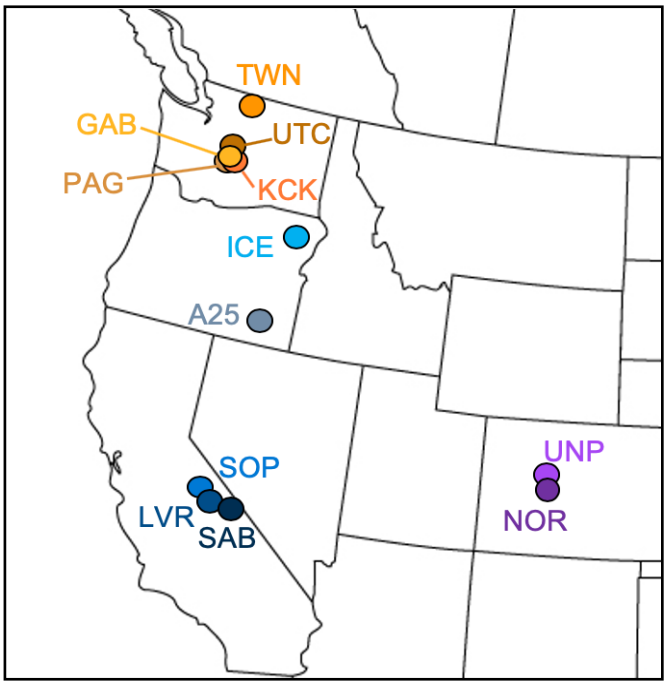

Figure 2.1. Distribution map of samples in the *Mimulus tilingii* species complex used in this study. Population identity is indicated by a three-letter population code and color. *Mimulus caespitosa* populations are colored in shades of orange, *M. minor* populations are colored in shades of purple, and *M. tilingii* populations are colored in shades of blue.

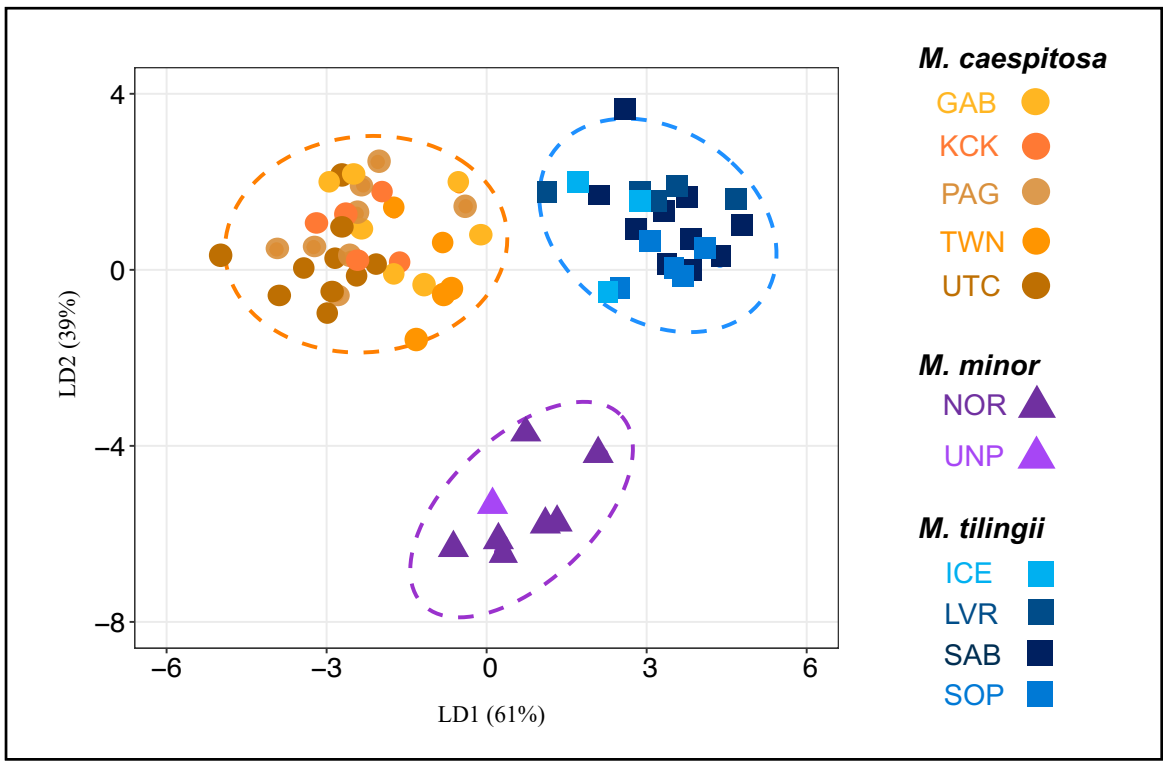

Figure 2.2. Linear discriminant analysis shows clear morphological differentiation based on floral and vegetative traits measured in a common garden among the three putative species in the *M. tilingii* complex. *M. caespitosa* samples are indicated with circles colored in shades of orange, *M. minor* samples are indicated with triangles colored in shades of purple, and *M. tilingii* samples are indicated with squares colored in shades of blue. Dashed ellipses represent 95% confidence intervals, with corresponding colors.

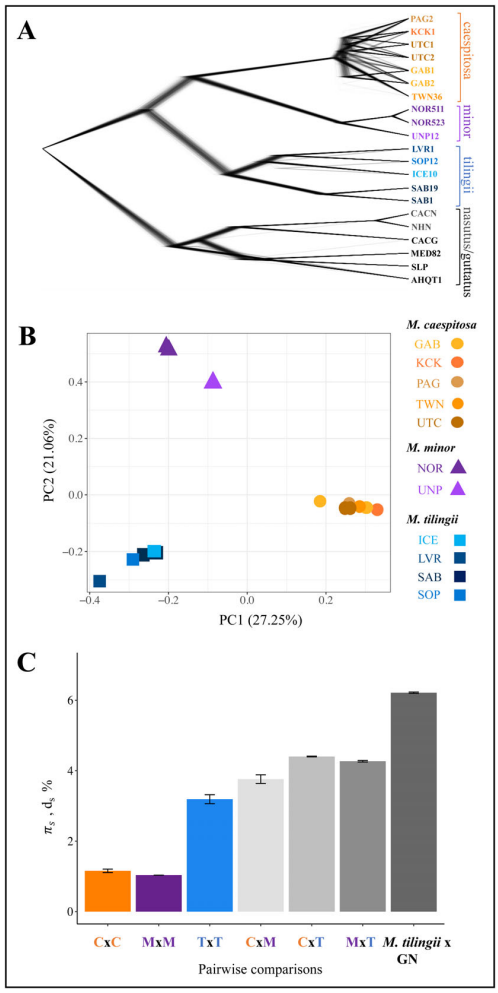

Figure 2.3. Whole-genome sequence analyses**. A.** Neighbor-joining tree representing the genetic relationships for seven *Mimulus caespitosa*, five *M. tilingii*, three *M. minor,* four *M. guttatus*, and two *M. nasutus* samples, rooted by one *M. dentilobus* sample. The consensus tree was based on 14,000 fourfold degenerate synonymous sites, plotted using a pairwise distance matrix with the nj function in the R package, ape, and smoothed with the function, chronopl, with λ = 1. The distribution of 1000 trees is plotted using the program DensiTree. **B.** Principal component analysis separates species in the *M. tilingii* complex based on genetic relatedness. The PCA uses the same SNP data as the nj tree, but excludes *M. guttatus, M. nasutus, and M. dentilobus. Mimulus caespitosa* samples are shown as round data points colored in shades of orange, *M. minor* samples are shown as triangular data points in shades of purple, and *M. tilingii* samples are shown as squared data points in shades of blue. Note that some populations have two maternal lines. **C.** Average pairwise sequence divergence and +/- SE at fourfold degenerate synonymous sites among *Mimulus* taxa: *M. caespitosa* (C), *M. minor* (M), *M. tilingii* (T). The darkest gray bar (*M. tilingii* x GN) includes all pairwise sequence comparisons between the three species within the *M. tilingii* complex and *M. guttatus* (G) and *M. nasutus* (N) samples.

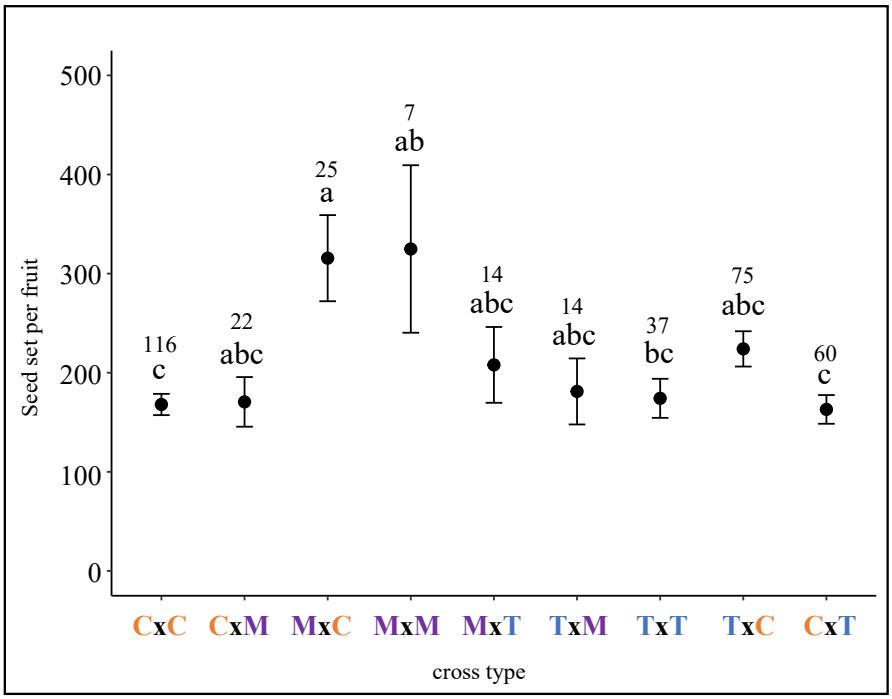

Figure 2.4. Intraspecific and interspecific seed set per fruit for cross types among *M. caespitosa* (C), *M. minor* (M), and *M. tilingii* (T). Crosses were performed three days after emasculating maternal parent. The first letter in each cross type indicates the maternal species. Least square means for each cross type are given with +/- SE. Least square means denoted by a different letter indicate significant differences among cross types (P <0.05) determined by post-hoc Tukey method. Sample sizes assessed for each cross type are listed above letters.

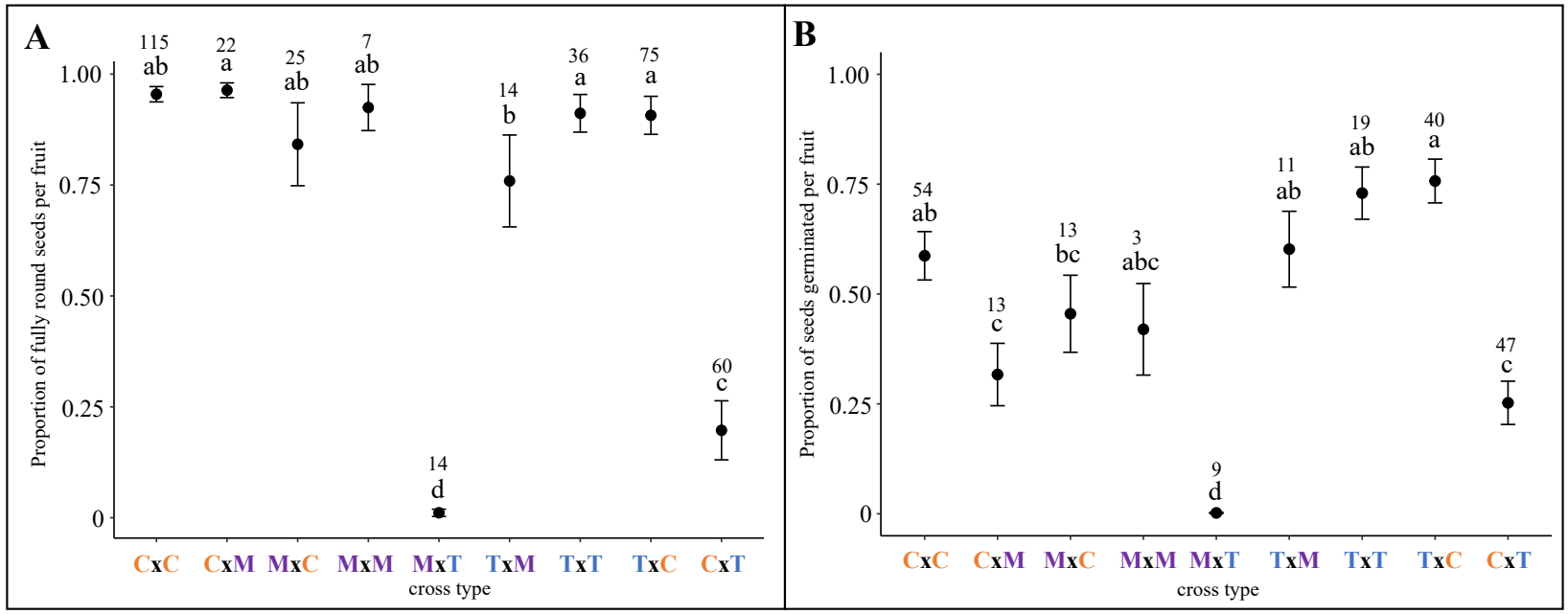

Figure 2.5. Intraspecific and interspecific seed viability for crosses among *M. caespitosa* (C), *M. minor* (M), and *M. tilingii* (T). The first letter in each cross type indicates the maternal species. Least square means for cross types are given with +/- SE. Least square means denoted by a different letter indicate significant differences among cross types (P <0.05) determined by post-hoc Tukey method. Sample sizes assessed for each cross type are listed above letters. **A.** Proportion of fully developed seeds per fruit (visual assessment). **B.** Proportion of seeds that germinated per fruit.

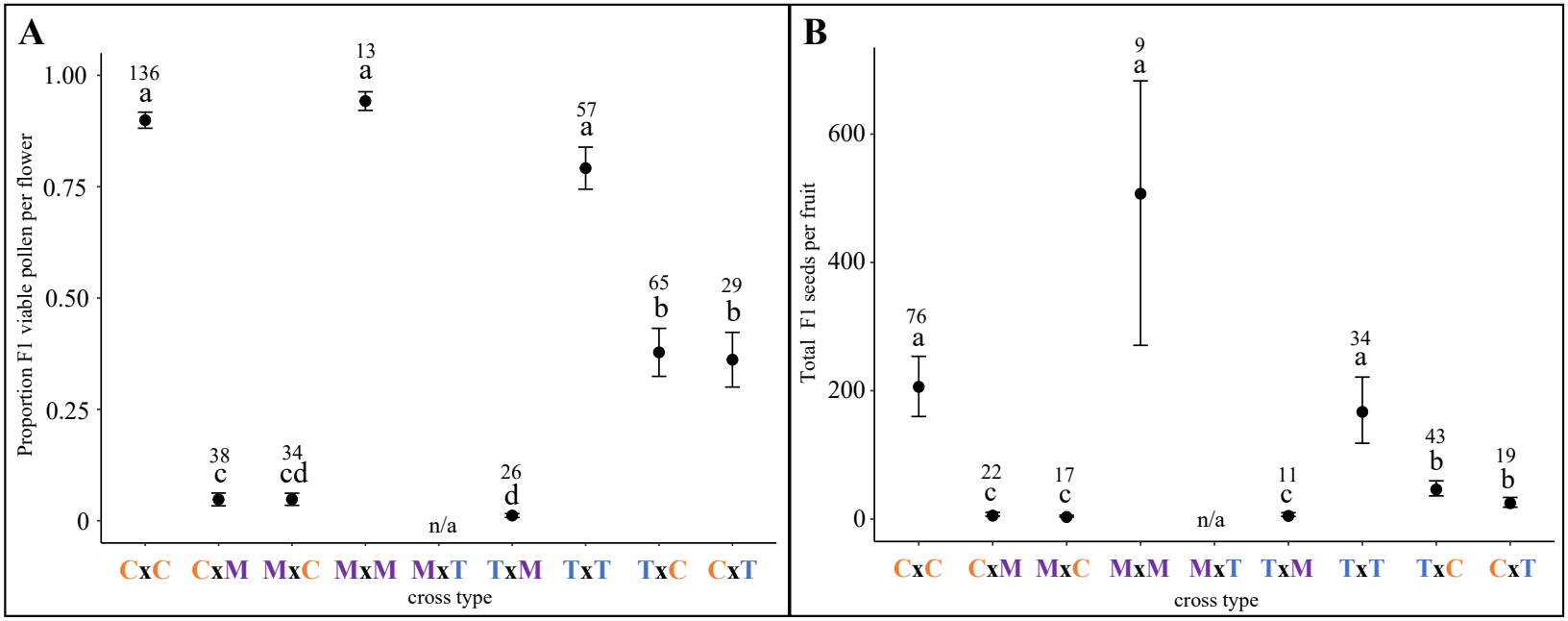

Figure 2.6. F1 intraspecific and interspecific fertility for crosses among *M. caespitosa* (C), *M. minor* (M), and *M. tilingii* (T). The first letter in each cross type indicates the maternal species. Least square means for each cross type are given with +/- SE. Least square means denoted by a different letter indicate significant differences among cross types (P <0.05) determined by post-hoc Tukey method. Sample sizes assessed for each cross type are listed above letters. There is no data for the M x T cross type due to the severe seed lethality phenotype. **A.** Proportion of F1 pollen viability per flower. **B.** Total F1 seeds produced per fruit. Crosses were performed using supplemental hand-pollinations on a subset of plants germinated from Figure 5B.

CHAPTER III

SEED DEVELOPMENT PHENOTYPES ARE POTENTIAL TARGETS FOR PARENTAL CONFLICT IN *MIMULUS*[2]

[2]Sandstedt, G.D. & A.L. Sweigart, To be submitted to *New Phytologist*.

ABSTRACT

When maternal and paternal genomes are unequally related to their offspring, theory predicts they might evolve different levels of resource acquisition (*i.e.*, parental conflict). In the seeds of flowering plants, the endosperm has been proposed as an important arena for parental conflict because it regulates nutrient transfer to the developing embryo. The endosperm is also often disrupted in inviable hybrid seeds between species presumed to have divergent histories of parental conflict. Nevertheless, despite the potential importance of parental conflict in plant speciation, we lack direct evidence of its action in endosperm functions or regions specifically involved in resource provisioning. To investigate whether parental conflict targets particular regions of the endosperm, we performed reciprocal crosses between pairs of three closely related, diploid yellow monkeyflower species (*Mimulus caespitosa*, *M. tilingii,* and *M. guttatus*). The severity of F1 hybrid seed viability varies among these crosses, which we determined was due to species divergence in endosperm balance number (EBN). By performing a detailed time series of intra- and interspecific seed development, we assessed whether specific regions in the endosperm were potential targets of parental conflict. Overall, we determined that the chalazal haustoria, a tissue within the endosperm that occurs at the maternal-filial boundary, is deregulated in all interspecific crosses, specifically when the paternal parent has the greater EBN (*i.e.*, "paternal excess"). Our results suggest that, within these *Mimulus* species, parental conflict might target the chalazal haustoria to control sucrose movement from the maternal parent into the endosperm, and conflict in this region is exposed in crosses between species. Our study provides evidence that parental conflict in the endosperm may function as a driver of speciation by targeting regions and developmental time points critical for resource allocation.

INTRODUCTION

The rampant diversification of flowering plants (angiosperms) has long fascinated evolutionary biologists, including Darwin himself, as he referred to this extensive radiation as "an abominable mystery" (Darwin 1903). Such incredible diversity is thought to be driven, in part, by reproductive characters unique to this clade, including the process of double fertilization and the nutritive endosperm (Soltis et al. 2019). In angiosperms, double fertilization occurs when a pollen tube releases two reproductive haploid sperm cells—one sperm fuses with the haploid egg cell to develop a zygote that forms a diploid embryo, while the other fuses with the homodiploid central cell to form a dosage sensitive, triploid endosperm with a relative contribution of two maternal to one paternal (2m:1p) genomes (Berger et al. 2008; Berger 2003). Within a seed, the endosperm plays a critical role in the acquisition and transfer of nutrients to the embryo (Brink and Cooper 1947), and crosses between species that cause genetic changes in the endosperm often fail due to defects in embryo development (Lafon-Placette and Köhler 2016). Despite its potential importance as a major arena for angiosperm diversification, endosperm development has only recently been studied in the context of reproductive isolation (Rebernig et al. 2015; Oneal et al. 2016, Lafon-Placette et al. 2017; Roth et al. 2018; Coughlan et al. 2020; İltaş et al. 2021), and we still lack a detailed understanding of its evolution within and between closely related lineages.

In early crossing studies, seed failure was often observed between plants of different ploidies. Many of these studies also reported pronounced reciprocal differences in seed growth and development (Håkasson 1952; Woodell and Valentine 1961; Nishiyama and Inomata 1966), leading to the hypothesis that seed failure is caused by a deviation from the usual dosage of

2m:1p genomes in the triploid endosperm (Nishiyama and Inomata 1966; Lin 1984). However, because these same parent-of-origin effects are also common in interspecific crosses of the same ploidy (Cooper and Brink 1942; Stephens 1949; Nishiyama and Yabuno 1978), it was later proposed that proper seed development depends on the balanced dosage of a discrete number of genetic factors in the endosperm, rather than on ploidy level of the entire genome (Johnston et al. 1980). Indeed, there is now broad support for the idea that cross compatibility is largely a function of species divergence in "endosperm balance number" (EBN; Hanneman 1993; Parrott and Smith 1986; Scott et al. 1998; Rebernig et al 2015; Roth et al. 2018; Coughlan et al. 2020; reviewed in Städler et al. 2021).

Classic theory suggests that species divergence in EBN reflects parental conflict over maternal investment in the endosperm (Haig and Westoby 1989). Inherently, the endosperm operates as a venue for parental conflict— maternal and paternal genomes evolve different levels of resource acquisition driven by unequal relatedness to offspring in non-monogamous systems (*i.e.*, co-developing offspring share the same maternal parent, but have different paternal parents; Hamilton 1964; Haig and Westoby 1989; Brandvain and Haig 2005). In a maternal (egg cell) parent, natural selection should favor gene expression in the endosperm that equalizes nutrient acquisition among all seeds, whereas in a paternal parent (pollen donor), selection should favor gene expression that maximizes resource acquisition in its own offspring at the expense of unrelated seeds (Haig and Westoby 1989). At a mechanistic level, this scenario is thought to play out through epigenetic modifications during male and female gametogenesis that regulate parent-of-origin biased gene expression in the endosperm (*i.e.*, genomic imprinting; Reik and Walter 2001; Haig and Westoby 1991; Kinoshita 2007; Batista and Köhler 2020). Within a population,

conflict should be resolved through a balance of loci that act to acquire resources from the seed parent and loci that moderate these acquisitive effects; however, species barriers may arise once this balance is disrupted in crosses between divergent populations (Haig and Westoby 1991).

According to the predictions of parental conflict theory, selection in the endosperm should target developmental timepoints or functions that are most important for nutrient uptake (Queller 1983). Most of what is known about the developmental phenotypes associated with hybrid seed inviability comes from crosses in *Arabidopsis* and other systems with nuclear-type endosperms (so called because the early endosperm forms a syncytium; Bushell et al. 2003; Rebernig et al. 2015; Floyd and Friedman 2000), where the timing of cellularization seems to be a major determinant of nutrient acquisition and seed size (Garcia et al. 2003; Luo et al. 2005; Kang et al. 2008; Hehenberger et al. 2012). Indeed, in interploidy crosses in these systems, endosperm cellularization is often precocious when the seed parent has higher ploidy and delayed when the pollen parent has higher ploidy, resulting in smaller or larger seeds, respectively (Scott et al. 1998; Pennington et al. 2008; Lu et al. 2012; Morgan et al. 2021). The fact that these same "maternal excess" and "paternal excess" effects on cellularization have been observed in crosses between species of the same ploidy in *Arabidopsis* and *Capsella* (Lafon-Placette et al. 2017; Rebernig et al. 2015; Lafon-Placette et al. 2018) has been taken as evidence for parental conflict in nuclear-type endosperms.

Although these disruptions in the timing of endosperm cellularization are certainly suggestive, we still lack definitive evidence of parental conflict operating directly on resource provisioning functions. Few studies of hybrid seed inviability have explicitly considered whether parental conflict differentially affects distinct regions of the endosperm – especially in systems

with non-nuclear modes of endosperm development (*i.e.*, cellular and helobial). In most angiosperms, the endosperm is not a homogeneous structure but rather differentiates into three spatially and functionally distinct domains: the micropylar domain that surrounds the embryo, the chalazal domain that occurs at maternal–filial interface, and the central peripheral domain that makes up the largest portion of the endosperm (Brown et al. 2003). Of these domains, the micropylar and chalazal regions appear to be directly involved in nutrient transfer from maternal to filial structures (Baud et al. 2005, Morley-Smith et al. 2008), making them potential targets of parental conflict and venues of EBN divergence.

Across the wildflower genus *Mimulus*, hybrid seed inviability has evolved repeatedly (Vickery 1978; Oneal et al. 2016; Garner et al. 2016; Coughlan et al. 2020; Kinser et al. 2021; Sandstedt et al. 2021), making it an outstanding system for dissecting the developmental and evolutionary mechanisms of this common isolating barrier. In *Mimulus,* the endosperm is of the cellular-type, meaning that cell walls develop following the initial division of the primary endosperm nucleus (Arekal 1965; Guilford and Fisk 1952; Oneal et al. 2016). After a few rounds of cell division, the three major endosperm domains form (*i.e.*, micropylar, chalazal, and central-peripheral endosperm), with the micropylar and chalazal regions giving rise to separate haustoria structures that likely act as channels for nutrient transfer between the maternal plant and developing seed (Nguyen et al. 2000; Mikesell 1990). The chalazal haustoria are ephemeral, composed of two cells extending from the ovule toward the micropylar domain that typically degenerate when the embryo is near a globular stage (Arekal 1965; Guilford and Fisk 1952; Oneal et al. 2016). On the opposite end of the seed, the two cells of the micropylar haustoria appear to penetrate the integuments (*i.e.*, precursors of the seed coat) and degenerate when the

embryo is nearly fully developed (Arekal 1965). Given their invasion of neighboring tissues to funnel nutrients to the developing embryo, we might expect deregulation of haustoria in hybrids if *Mimulus* species have diverged in their levels of parental conflict. Such phenotypes have been noted before in chalazal structures of interploidy crosses in *A. thaliana* (Scott et al. 1998), but they have not been described in a conflict scenario between species of the same ploidy.

In this study, we investigate developmental phenotypes associated with hybrid seed inviability among three closely related, diploid *Mimulus* species: *M. caespitosa* and *M. tilingii*, which shared a common ancestor ~382 kya, and *M. guttatus*, which diverged from the other two ~674 kya (Sandstedt et al. 2021). Populations of *M. caespitosa* and *M. tilingii* appear to be mostly allopatric and occur at high elevations – *M. caespitosa* is restricted high elevations in Washington state and *M. tilingii* grows throughout alpine regions in western North America. *M. guttatus* occupies a more diverse range in western North America, sometimes overlapping with populations of *M. caespitosa* and *M. tilingii* (Nesom 2012). Previously, we showed that crosses between *M. caespitosa* and *M. tilingii* result in severe hybrid seed inviability – but only when *M. tilingii* is the paternal parent (crosses in the reciprocal direction produce mostly viable seeds, Sandstedt et al. 2021). Hybrid seed inviability is even stronger between the more distantly related *M. tilingii* and *M. guttatus*, which produce very few (< 1%) viable seeds in either direction of the cross (Vickery, 1978; Garner et al. 2016). Despite this apparent similarity between reciprocal crosses of *M. tilingii* and *M. guttatus*, most of the underlying genetic loci affect seed viability only through the maternal or paternal parent (Garner et al. 2016). These parent-of-origin effects on seed viability and genetic loci are a hallmark of endosperm involvement but, until now, it has not been clear whether EBN differs among these *Mimulus* species. Here, we leverage this system

to explore divergence in EBN and to investigate whether and how parental conflict might manifest during *Mimulus* seed development. Our detailed developmental investigation provides strong evidence for parental conflict as a driver of reproductive isolation in this group of *Mimulus* species.

MATERIALS AND METHODS

Generation of Plant Material

Here, we used one inbred line (formed from $^{3}8$ generations of self-fertilization) for each focal species (*M. caespitosa*, *M. tilingii*, and *M. guttatus*). The same inbred lines were used in previous studies of hybrid seed inviability in *M. tilingii* and *M. guttatus* (Garner et al. 2016) and *M. caespitosa* (Sandstedt et al. 2021). The *M. caespitosa* inbred line TWN36 originates from a high-alpine population at 1594m in Twin Lakes, WA, and the *M. tilingii* inbred line LVR1 is derived from a population at 2751m in Yosemite Park, CA. The *M. guttatus* inbred line (DUN10) originates from a population in the Oregon Dunes National Recreation Area.

In this study, we considered three intraspecific crosses (CxC, TxT, and GxG, where C = *M. caespitosa*, T = *M. tilingii*, and G = *M. guttatus*) and six interspecific crosses (CxT, TxC, TxG, GxT, CxG, GxC; maternal parent is always listed first). To generate diploid, experimental plants, we sowed 20-30 seeds for each inbred line on damp paper towels in petri dishes sealed with parafilm and cold-stratified them for 7 days to disrupt seed dormancy. After cold stratification, we transferred petri dishes to a growth chamber with 16-h days at 23°C and 8-h nights at 16°C. We transplanted seedlings into 3.5” pots with moist Fafard 4P growing mix (Sun Gro Horticulture, Agawam, MA) and placed the pots in the same growth chamber. Once plants

began flowering, we randomly crossed within and between individuals (total plants: C = 19, T = 19, G = 15). For all crosses, we emasculated the maternal plant 1-3 days prior to each cross to prevent contamination from self-pollination.

In some experiments, we also included several interspecific, interploidy crosses (4N subscript indicates tetraploid: C_{4N}xT, TxC_{4N}; T_{4N}xG, GxT_{4N}; C_{4N}xG, GxC_{4N}). To generate synthetic tetraploid individuals, we treated 100-200 seeds of TWN36 and LVR1 with 0.1% or 0.2% colchicine and stored them in the dark for 24 hours 16 hours at 23°C and 8 hours at 16°C. The next day, we planted seeds onto Fafard 4P potting soil using a pipette and placed pots inside the growth chamber under typical light and temperature conditions (16-h days at 23°C and 8-h nights at 16°C). Once seeds germinated, we transplanted seedlings into 2.5" pots. After sufficient growth, we prepared samples for flow cytometry using a protocol adapted from Lu et al. 2017. Briefly, we extracted nuclei from one colchicine-treated sample and an internal control (2N *Mimulus* or *Arabidopsis thaliana,* Col-0) together in a single well. To extract nuclei, we chopped 100mg of leaf tissue (50mg colchicine-treated sample and 50 mg internal control) in 1mL of a pre-chilled lysis buffer (15mM Tris-HCl pH 7.5, 20mM NaCl, 80mM KCl, 0.5mM spermine, 5mM 2-ME, 0.2% TritonX-100). We stained nuclei with 4,6-Diamidino-2-phenylindole (DAPI), filtered nuclei for debris using a 40um Flowmi™ cell strainer, and aliquoted nuclei into a single well of a 96-well polypropylene plate. We assessed ploidy of each sample using a CytoFLEX (Beckman Coulter Life Sciences) flow cytometer. We calculated total DNA content with the following equation:

$$\text{2C DNA content (pg DNA)} = \frac{\text{sample G1 peak mean}}{\text{standard G1 peak mean}} * \text{standard 2C DNA content}$$

Overall, we recovered 3-5 polyploids for each maternal line tested (C_{4N} = 3, T_{4N} = 6). For each synthetic polyploid, 2C DNA content was nearly doubled compared to corresponding diploid lines (TWN36, 2C = 1.38 pg; $TWN36_{4N}$, 2C = 2.69 ± 0.09 pg; LVR1, 2C = 1.26 pg; $LVR1_{4N}$, 2C = 2.64 ± 0.05 pg). In some cases, we discovered that plants identified as 4N via flow cytometry were mixoploids. To ensure that the crosses we performed were indeed interploidy, we determined the ploidy of the resulting progeny. From each interploidy cross, we planted 5-10 seeds per fruit, isolated nuclei from the resulting plants, and assessed 2C content using a flow cytometer for a few offspring as described above (3N $TWN36_{4N}$xLVR1 = 1.92 ± 0.04, 3N LVR1xTWN36, 2C = 1.88 ± 0.01 pg; 3N $LVR1_{4N}$xDUN10, 2C = 1.95 ± 0.04 pg; 3N DUN10x$LVR1_{4N}$, 2C = 1.81 ± 0.01 pg). We included data from interploidy crosses only when their progenies were confirmed to be triploids, or if the tetraploid parent in the interploidy cross was a stable polyploid plant (*i.e.*, self-fertilized at least one generation). We note that all interspecific, interploidy crosses between *M. guttatus* and 4N *M. caespitosa* were performed with stable 4N *M. caespitosa* plants.

Measuring seed size and seed viability

To measure seed size, we collected three replicate fruits per cross, with each fruit collected from a distinct plant. We imaged 50 seeds per fruit under a dissecting scope, for a total of 150 seeds per cross (except for one CxG fruit for which only 35 seeds were measured for a total of 135 seeds). Seed area was measured using imageJ (Rasband 1997).

Using these same fruits, we assessed seed viability using two different methods (interploidy crosses were also included; 2-5 fruits per interploidy cross, where at least two fruits from each cross were collected from a distinct plant). First, we visually assessed mature seeds for irregular phenotypes (shriveled, wrinkled, or flat) associated with hybrid seed inviability in *Mimulus* (Garner et al. 2016, Oneal et al. 2016, Coughlan et al. 2020, Sandstedt et al. 2021). We scored the number of seeds that appeared round and plump (*i.e.*, fully-developed) versus irregularly shaped (*i.e.*, under-developed). Second, we immersed a subset of these same seeds (~100 seeds per fruit) in 1% Tetrazolium, which stains viable, living cells a dark red color (Fig. S1A). For fruits generated from interploidy crosses and fruits that produced <100 seeds, we stained on average 50 of the fruit's seeds with tetrazolium (32-63 seeds). For this method, we immersed seeds in a scarification solution (83.3% water, 16.6% commercial bleach, and 0.1% Triton X-100) and placed them on a shaker for 15 minutes. After scarification, we washed seeds five times with water and incubated seeds with 1% Tetrazolium at 30°C. Two days later, we scored the number of seeds that stained dark red (viable) versus pink or white (inviable).

Seed viability rescues

To assess whether aberrant endosperm development contributes to seed defects in interspecific crosses, we attempted to rescue seed viability with a sucrose-rich medium. We collected three fruits 8 to 12 days after pollination (DAP) from each intra- and interspecific cross (not including interploidy crosses), with each fruit collected from a distinct plant. On average, we dissected 40 whole immature seeds per fruit (range= 25-57) and placed them on petri dishes

with MS media containing 4% sucrose. We sealed petri dishes with parafilm and placed them at 23°C with constant light for 14 days before scoring germination.

Visualizing parent-of-origin effects during seed development

To compare trajectories of seed development, we performed intra- and interspecific crosses, and we collected fruits 3, 4, 5, 6, 8, and 10 DAP. For consistency, we performed crosses and collected fruits at the same time of day.

To visualize early seed development, we collected fruits 3 and 4 DAP (N = 1 to 2 fruits per DAP per cross) and prepared them for clearing with Hoyer's solution. We placed developing fruits in a 9 EtOH: 1 acetic acid fixative overnight. The following day, we washed fruits twice in 90% EtOH for 30 min per wash. We dissected immature seeds directly from the fruit onto a microscope slide with 100uL of 3 parts Hoyer's solution (70% chloral hydrate, 4% glycerol, 5% gum arabic): 1 part 10% Gum Arabic and sealed the slide with a glass cover slip. We stored the microscope slides containing cleared, immature seeds at 4°C overnight. The next day, we imaged slides using the differential interference contrast (DIC) setting with the 20x objective on a Leica DMRB microscope. For each fruit, we scored the number of developing seeds with and without an intact chalazal haustorium (15-56 seeds per fruit; 32-111 seeds per cross per DAP); only seeds with visible embryos were scored. Additionally, we imaged an average of 11 seeds per fruit (3-15 seeds per fruit, 10-27 seeds per cross per DAP) to assess size differences in the endosperm and chalazal haustoria at 3 and 4 DAP – for the interploidy T_{4N}xG cross, we imaged on average 18 seeds per fruit (14-26 seeds per fruit, 29-40 seeds per cross per DAP). We outlined and measured the endosperm in all seeds and the chalazal haustoria when present using ImageJ

(Rasband 1997). We selected and measured images that represented typical seed development at each time point.

We defined chalazal haustoria as two uninucleate cells that, together, form a continuous structure that penetrates towards the ovule hypostase cells (a group of tightly packed cells at the base of the ovule). To measure the chalazal haustoria, we began the outline near the epidermis of the seed (not including the hypostase cells) to where haustoria extended toward the micropylar region following Guilford and Fisk 1952 (see their Figure 27). In addition, when measuring the endosperm, we started the outline at the same region near the epidermis of the ovule to the opening of the micropylar haustoria.

To visualize later seed development (after 4 DAP when the seed coat is too thick to clear with Hoyer's solution), we collected whole fruits at 5, 6, 8, and 10 DAP and stored them in a Formaldehyde Alcohol Acetic Acid fixative (10%:50%:5% + 35% water) for a minimum of 48 hours. After fixation, we dehydrated developing fruits with increasing concentrations of Tert Butyl Alcohol. Next, we washed fruits three times for two hours each with paraffin wax at 65°C before embedding them into a wax block. We sectioned wax blocks containing whole fruits into ribbons using a LIPSHAW Rotary Microtome (Model 45). Fruits collected at 5 and 6 DAP were sectioned into 12-um ribbons for better visualization of micropylar and chalazal domains, and fruits collected at 8 and 12 DAP were sectioned into 8-um ribbons. Next, we gently placed ribbons in a warm (~40°C) water bath and positioned them onto a microscope slide. We placed slides on a slide warmer overnight to adhere sections completely to the glass. In a staining series, we first used Xylene as a clearing agent and performed several washes with increasing concentrations of EtOH to effectively stain nuclei and cytoplasm (1% Safranin-O and 0.5% Fast

Green, respectively). We further washed stained slides with EtOH and finished the series with Xylene. We sealed slides with a glass coverslip using Acrytol as the mounting medium.

We visualized slides using a Zeiss Axioskop 2 microscope with a 10x objective. For each fruit, we imaged at least 10 seeds with a developing embryo per fruit (except for severe embryo-lethal crosses: 10 DAP TxG, 8 seeds imaged; 10 DAP CxG, 1 seed imaged). We imaged at least five consecutive sections of each seed through the embryo. For all seeds imaged at 5 and 6 DAP, we scored the presence of the chalazal haustoria. Additionally, we categorized embryo development at 6, 8, and 10 DAP into four different stages: before globular to globular, late-globular to transition, early-heart to late-heart, and torpedo.

Data Analysis

We modeled the effect of cross on seed area using three separate linear mixed models, each with four comparisons including reciprocal interspecific crosses and the corresponding intraspecific crosses (CxC, CxT, TxC, TxT; TxT, TxG, GxT, GxG; and CxC, CxG, GxC, GxG). For each model, we fit a Gaussian distribution using the lmer command in the "lme4" package implemented in R (Bates et al. 2007). We assigned our fixed factor as cross, random factor as individual plant, and our response variable as seed area (mm^2). To determine whether there was an effect of cross on the variance of seed area, we computed an ANOVA test using the anova function in the R package "car" with type III sums of squares, which applies Wald chi-square tests for mixed models. We calculated least-squares means (lsmeans) using the emmeans function in the R package "emmeans", performed pairwise comparisons between all crosses, and

we used a post hoc Tukey method adjustment to determine which crosses differed significantly in seed area (Lenth and Lenth 2018).

We determined the effect of cross on seed viability using three generalized linear mixed models (GLMMs), for both measures of seed viability (visual and tetrazolium assessment). Each GLMM compared reciprocal interspecific crosses, and their corresponding interploidy and intraspecific crosses (CxC, CxT, TxC, TxT, C_{4N}xT, TxC_{4N}; TxT, TxG, GxT, GxG, T_{4N}xG, GxT_{4N}; and CxC, CxG, GxC, GxG, C_{4N}xG, GxC_{4N}). In these models, we fit GLMMs with a binomial distribution using the glmer command in the "lme4" package implemented in R (Bates et al. 2007). For our response variable, we combined the number of viable seeds (fully-developed or stained dark red) and the number of inviable seeds (under-developed or unstained) into a single variable using the R function cbind. We assigned our fixed factor as cross, and the individual plant was set as a random factor. We computed ANOVAs using the anova function to determine whether cross significantly affected the variance of seed viability. Then, we calculated lsmeans and performed pairwise comparisons between all crosses. We determined which crosses differed significantly in the number of viable seeds using a post hoc Tukey method adjustment.

To model the effect of cross on germination success of seed viability rescues with sucrose media, we performed three separate GLMMs, comparing only reciprocal interspecific crosses and their corresponding intraspecific crosses (CxC, CxT, TxC, TxT; TxT, TxG, GxT, GxG; and CxC, CxG, GxC, GxG). In these models, we fit GLMMs with a binomial distribution using the glmer command. For our response variable, we combined the number of seeds that germinated and the number of seeds that failed to germinate on a sucrose-rich medium into a single variable using

the R function cbind. We assigned our fixed factor as cross, and the individual plant was set as a random factor. We computed an ANOVA to determine which crosses significantly affected variance of germination success on a sucrose-rich medium using the anova function in R. Similar to prior analyses, we estimated lsmeans, performed pairwise comparisons of lsmeans between all crosses, and determined which crosses significantly differed in the number of seeds that germinated on a sucrose-rich medium using a post hoc Tukey method.

To determine whether cross had a significant effect on area of endosperm filled by a chalazal haustoria, we performed three separate linear models for both measurements, comparing only reciprocal interspecific crosses and their corresponding intraspecific crosses—except for T-G comparisons, in which case we also included measurements of the interploidy cross (CxC, CxT, TxC, TxT; TxT, TxG, GxT, GxG, T_{4N}xG; and CxC, CxG, GxC, GxG). We fit linear models using the lm function in R, assigning the response variable as either chalazal haustoria/endosperm area and fixed factors as cross, DAP, and their interaction. To determine whether these fixed factors affected the variance of the response variables, we computed ANOVAs with type III sums of squares. Then, we estimated lsmeans, performed pairwise comparisons of lsmeans, and determined which crosses at 3 and 4 DAP differed in embryo area and area of the endosperm filled by the chalazal haustoria.

RESULTS

Hybrid seed inviability is an exceptionally strong isolating barrier in crosses between *Mimulus guttatus*, *M. tilingii*, and *M. caespitosa* (Figs. 1A and S1). Consistent with our earlier work (Garner et al. 2014), *M. guttatus* and *M. tilingii* produced almost exclusively inviable F1

hybrid seeds in both directions of the cross. We found this same result in crosses between *M. guttatus* and *M. caespitosa*. On the other hand, as we have shown previously (Sandstedt et al. 2021), F1 hybrid seed inviability between the more closely related *M. tilingii* and *M. caespitosa* occurs in only one direction of the cross. However, even when reciprocal F1 hybrid seeds appear similar in terms of morphology (i.e., flat and shriveled), plating them on a nutritive sucrose medium revealed clear reciprocal differences in viability (Fig. 1B). With *M. guttatus* as the maternal parent, F1 hybrid seeds from crosses with *M. tilingii* or *M. caespitosa* showed viability levels on sucrose similar to seeds from parental crosses (Fig. 1B). In contrast, F1 hybrid seeds from the same crosses remained almost completely inviable on sucrose when *M. guttatus* acted as the paternal parent (Fig. 1B). Taken together, these stark reciprocal differences in F1 hybrid seed inviability point to a central role for the endosperm – and divergence in EBN – in driving reproductive isolation between these *Mimulus* species.

Crosses with synthetic polyploids provide further support for endosperm-based barriers and reveal the rank order of EBNs among the three *Mimulus* species (Figs. 1A and S1). Consistent with *M. caespitosa* having the lowest EBN, increasing its ploidy to 4N greatly improved hybrid seed viability in crosses with *M. tilingii* – but only when *M. caespitosa* acted as the seed parent. In the reciprocal direction, which normally produces viable seeds, 4N *M. caespitosa* pollen donors actually induced seed inviability. In crosses with *M. guttatus*, 4N *M. caespitosa* only partially restored F1 hybrid seed viability, pointing to an even wider divergence in EBN between these two species. The EBN of *M. tilingii* is apparently intermediate, with crosses between tetraploid *M. tilingii* and *M. guttatus* largely or completely restoring hybrid seed inviability. Taken together, these results demonstrate clear divergence in EBN: *M. guttatus* has

the highest EBN, followed by *M. tilingii*, and *M. caespitosa* has the lowest. To investigate whether parental conflict is the evolutionary force driving EBN divergence among these three *Mimulus* species, our next step was to take a closer look at parent-of-origin seed phenotypes.

One potential outcome of parental conflict is that seeds of reciprocal crosses might show marked differences in size. However, in these three species, parent-of-origin effects on hybrid seed area were subtle and not consistent across all species pairs (Fig. S2); only interspecific crosses involving *M. caespitosa* showed significant reciprocal differences in average hybrid seed size. Moreover, instead of showing any evidence of overgrowth in paternal excess crosses, hybrid seed area was nearly always reduced (except in CxT F1 hybrids, Fig. S2) compared to the progeny of intraspecific crosses. However, because mature hybrid seed size depends on a multitude of developmental processes, including embryo growth and early seed abortion, we focused on assessing parent-of-origin phenotypes at a finer scale.

Despite superficial similarities in seed size, we observed dramatic differences in the underlying development of all reciprocal pairs of F1 hybrid seeds. In early seed development, chalazal haustoria growth was strongly deregulated in all paternal excess crosses (CxT, TxG, CxG in Figs. 2A, S3). Whereas during normal seed development (*i.e.*, in the progeny of intraspecific crosses CxC, TxT, and GxG), the chalazal haustoria decrease in size early (3-4 DAP) and degenerate completely by 5 DAP, they occupy a significantly larger proportion of the endosperm in paternal excess crosses and are maintained much longer (Figs. 3, 4, S3). In the paternal excess cross between *M. caespitosa* and *M. tilingii*, the volume of endosperm devoted to chalazal haustoria at 4 DAP is nearly twice that of viable seeds (compare CxT to CxC, TxT, and TxC, Figs. 2A, 3, S3) and chalazal structures are maintained until 6 DAP (Fig. 4, S4).

Developmental irregularities in the chalazal haustoria were even clearer in paternal excess crosses involving *M. guttatus*, the species with the largest EBN. In the hybrid seeds of these interspecific crosses, the proportion of endosperm filled by the chalazal haustoria is ~3-4x greater than in the seeds of corresponding reciprocal and intraspecific crosses, and haustoria persist through 6 DAP (Figs. 2A, 3, 4, S4). Remarkably, this developmental defect was almost completely rescued by increasing maternal dosage: the volume of endosperm filled by chalazal haustoria is greatly reduced in 4N *M. tilingii* x *M. guttatus* hybrids (Figs. 2B, 3) and haustoria are almost entirely degenerated by 4 DAP (Fig. 4).

Parent-of-origin effects in the endosperm become even more apparent at later stages of development. At 6 DAP, most intraspecific seeds contain a globular-to-transition-stage embryo, which is surrounded by a cellularized endosperm with cells that appear largely empty (Figs. 5A, 6, S4). By 8 DAP in these normally developing seeds, the centrally-located endosperm cells begin to break down, while the peripheral endosperm lining the seed coat differentiates into cytoplasmically dense, starch-filled cells (Figs 5B, S4). However, in maternal excess crosses, especially those with *M. guttatus* as the seed parent, these differentiated endosperm cells appear earlier (6 DAP) and are tightly packed into a much smaller area, leaving little space for embryo progression. As a result, embryos of seeds from *M. guttatus* maternal excess crosses fail to transition from the heart to the torpedo stage (TxG, CxG in Figs. 5, 6, S4). Paternal excess crosses, on the other hand, produce hybrid seeds with delayed endosperm differentiation accompanied by stymied embryo development (CxT in Figs. 5, 6, S4). In the most severe paternal excess crosses (involving *M. guttatus* as the pollen parent), the endosperm cells of

hybrid seeds fail to differentiate at all and persist as large, empty cells unable to support embryo development past the globular stage (TxG and CxG in Figs. 5, 6, S4).

DISCUSSION

Crosses between individuals with different endosperm balance numbers, and histories of parental conflict, incur defects in endosperm development. However, empirical studies have not yet explicitly documented whether parental conflict targets specific regions within the heterogeneous endosperm and drives changes in EBN. Here, we determined that three closely related *Mimulus* species differ in EBN and crosses between any species pair results in nearly complete reproductive isolation. By performing a detailed time series of normal and F1 hybrid seed development, we uncovered prominent phenotypes with parent-of-origin effects that strongly implicate parental conflict in EBN divergence among *M. caespitosa*, *M. tilingii*, and *M. guttatus*. This study is one of the first to detail the disruption of nutrient acquiring tissues within the endosperm from hybridizations between species of the same ploidy.

Theory predicts that parental conflict targets developmental and genetic processes that regulate the vigor with which offspring acquire nutrients (Queller 1983; Haig and Westoby 1989). In flowering plants that undergo a nuclear mode of endosperm development, the timing of cellularization is a critical transition for proper seed formation and a key determinant of seed size (Garcia et al. 2003; Ohto et al. 2009; Hehenberger et al. 2012). In interploidy and interspecific crosses, parent-of-origin effects on the timing of cellularization are often observed. Precocious cellularization in maternal excess crosses limits nuclear proliferation in the endosperm accompanied by a reduction in seed size, whereas delayed cellularization in paternal excess

crosses results in over-proliferation of nuclei in the endosperm and enlarged seeds (Scott et al. 1998; Pennington et al. 2008; Rebernig et al. 2015; Lafon-Placette et al. 2017; Morgan et al. 2021). Given that the timing of cellularization is closely associated with seed size, it is possible that parental conflict targets this developmental process. Parent-of-origin effects on endosperm development have also been observed in crosses between species with cellular-type endosperms. In *Mimulus* and *Solanum*, maternal excess crosses develop small endosperm cells that are rapidly degraded by the growing embryo, resulting in smaller seeds than found in paternal excess crosses, which develop fewer, larger endosperm cells that contribute to increased seed sizes (Roth et al. 2018, Coughlan et al. 2020). Although these parent-of-origin effects on seed phenotypes are suggestive that parental conflict on resource allocation is driving differences in EBN, our study builds on these earlier findings by pointing to a distinct region (*i.e.*, the chalazal haustoria) and developmental time point that might be specifically targeted by parental conflict.

If there are different potential targets within a seed, why do we argue that parental conflict might manifest specifically within the chalazal haustoria? In species across the angiosperm phylogeny, this specialized region of the endosperm takes on diverse forms but invariably occurs at the maternal-filial boundary, where it often projects directly into maternal tissues (Povilus and Gehring 2022). In well-studied systems like *A. thaliana* and cereal crops (both with nuclear-type endosperm development), patterns of gene expression in chalazal tissues – or in analogous endosperm transfer cells – also point to their role in nutrient transfer, with upregulation of genes involved in sugar transport and metabolism (Thiel 2014, Zhan et al. 2015, Picard et al. 2021). In addition to this direct role in nutrient acquisition, the *Arabidopsis* chalazal endosperm appears to exert indirect effects on the process by producing the signaling protein

TERMINAL FLOWER1 (TFL1), which moves to the peripheral endosperm and initiates cellularization (Zhang et al. 2020). Thus, mounting evidence suggests genes expressed in the chalazal region are critical in determining the amount and timing of nutrient flow into the developing embryo.

Our finding that the chalazal endosperm is specifically deregulated in inviable, paternal-excess F1 hybrid *Mimulus* seeds also adds to a growing body of evidence suggesting this tissue is particularly sensitive to parental dosage and gene imprinting. Under a scenario of parental conflict in which maternally expressed genes (MEGs) and paternally expressed genes (PEGs) spar over the distribution of maternally-supplied resources to the developing seeds, the chalazal endosperm should be a key locus of paternal control (Povilus and Gehring 2022). In line with this prediction, gene expression for two key regulators of PEGs– *FIS2* and *MEA* – transitions from the syncytial endosperm to the chalazal cyst at the point of cellularization (Luo et al. 2000). *FIS2* and *MEA* are themselves MEGs and members of the Polycomb Repressive Complex 2 (PRC2) complex, which represses the maternal alleles of PEGs (Kinoshita et al. 1999; Luo et al. 2000; Köhler et al. 2005). In *fis2* mutants, endosperm cellularization fails, hexose accumulation in the central vacuole is prolonged (Hehenberger et al. 2012), and the chalazal endosperm is enlarged (sometimes filling ~50% of the endosperm; Sørenson et al. 2001). This type of evolutionary arms race between imprinted genes might help explain why EBN is positively correlated with the number and expression of PEGs in the endosperm of *Capsella* species (Lafon-Placette et al. 2018). Additionally, single nucleus RNA-sequencing in *Arabidopsis* shows that PEG expression is specifically enriched in the chalazal endosperm (Picard et al. 2021). Together with our study, this evidence points toward parental conflict driving rapid changes in

gene expression within the chalazal endosperm because it is a particularly effective venue for manipulating the transfer of maternal resources. In further support of this idea, chalazal-specific genes in two species of *Arabidopsis* show elevated rates of adaptive evolution compared to genes expressed in other regions of the seed (Geist et al. 2019).

Despite the chalazal haustoria being a promising target for parental conflict, there are other tissues within the developing seed that regulate nutrient transfer to the embryo and serve as potential additional targets, including the micropylar region that transfers sucrose from the integuments to the embryo (Morley-Smith et al. 2008). Micropylar haustoria typically degenerate before 10 DAP in intraspecific crosses, but persist in some paternal-excess crosses, especially *M. tilingii* as the seed parent and *M. guttatus* as the pollen parent – this region appears enlarged in developing seeds and is maintained at 10 DAP (Fig S4). While deregulation within the micropylar tissue might be shared across all paternal-excess crosses (*e.g.*, the micropylar haustoria is also observed in some CxT seeds at 10 DAP; Fig S4), irregularities are most obvious in this TxG cross; however, a more detailed investigation of seed development in the micropylar region is needed. Similar disruptions to the micropylar region have also been noted in paternal excess, interploidy crosses (Håkansson 1952; Scott et al. 1998), where micropylar haustoria vigorously invade seed integuments.

In addition to identifying the chalazal haustoria as a major target of parental conflict, our study is one of only a handful to investigate divergence in EBN between multiple, closely related species pairs. In this trio of *Mimulus* species, we find that EBN largely follows genetic distance – that is, the most closely related species pair, *M. caespitosa* and *M. tilingii*, has the least divergence between EBNs. However, patterns of hybrid seed inviability in this group also

suggest there have been lineage-specific changes in conflict. The fact that *M. guttatus* has the highest EBN suggests that parental conflict either increased in this species or decreased in the lineage leading to *M. caespitosa* and *M. tilingii*. Additionally, the higher EBN in *M. tilingii* vs. *M. caespitosa* suggests conflict might have relaxed specifically within *M. caespitosa*. Despite these divergence histories of conflict, disruption of the chalazal haustoria was observed in the F1 hybrid seeds of all species pairs, potentially suggesting parallel changes within lineages.

Our study provides strong developmental evidence that parental conflict acts as an evolutionary driver of divergence in EBN, but we do not yet know why levels of conflict vary among closely related *Mimulus* species. Often, mating system is found to be a strong predictor of the degree of parental conflict within species, where the strength of conflict is greater when there are more potential pollen donors, and therefore, relatedness among siblings decreases (weak inbreeder/strong outbreeder [WISO] hypothesis; Brandvain and Haig 2005). However, this might not be the case for this closely related *Mimulus* group because they share similar outcrossing floral morphologies while being hermaphroditic and self-compatible. Though, a morphological comparison between *M. tilingii* and *M. caespitosa* found that the anther-stigma distance was reduced in *M. caespitosa* (Sandstedt et al. 2021), suggesting possible mixed-mating differences. Aside from mating system, the strength of parental conflict within species may depend on other factors that influence effective population size (Coughlan et al 2020, reviewed in Städler et al. 2021), and in line with this expectation, *M. caespitosa*, *M. tilingii*, and *M. guttatus* differ in their levels of genetic variation (from lowest to highest, respectively; Sandstedt et al. 2021). Given that this trio of *Mimulus* species differ in EBN, it is possible that identifying the causal genes for

these developmental mishaps could shed light on the factors that drive differences in parental conflict throughout the speciation process.

REFERENCES

Arekal GD. 1965. Embryology of *Mimulus Ringens*. *Botanical Gazette* 126: 58–66.

Bates D, Sarkar D, Bates MD, Matrix L. 2007. The lme4 package. *R package version* 2: 74.

Batista RA, Köhler C. 2020. Genomic imprinting in plants-revisiting existing models. *Genes & development* 34: 24–36.

Baud S, Wuillème S, Lemoine R, Kronenberger J, Caboche M, Lepiniec L, Rochat C. 2005. The AtSUC5 sucrose transporter specifically expressed in the endosperm is involved in early seed development in Arabidopsis. *Plant Journal* 43: 824–836.

Berger F. 2003. Endosperm: the crossroad of seed development. *Current opinion in plant biology* 6: 42–50

Berger F, Hamamura Y, Ingouff M, Higashiyama T. 2008. Double fertilization – caught in the act. *Trends in Plant Science* 13: 437–443.

Brandvain Y, Haig D. 2005. Divergent Mating Systems and Parental Conflict as a Barrier to Hybridization in Flowering Plants. *The American Naturalist* 166: 30–338.

Brink RA, Cooper DC. 1947. The Endosperm in Seed Development. *The Botanical Review* 13: 479–541

Brown RC, Lemmon BE, Nguyen H. 2003. Events during the first four rounds of mitosis establish three developmental domains in the syncytial endosperm of *Arabidopsis thaliana*. *Protoplasma* 222: 167–174.

Bushell C, Spielman M, Scott RJ. 2003. The basis of natural and artificial postzygotic hybridization barriers in *Arabidopsis* species. *Plant Cell* 15: 1430–1442.

Cooper DC, and Brink RA. 1942. The endosperm as a barrier to interspecific hybridization in flowering plants. *Science* 95: 75-76

Coughlan JM, Wilson Brown M, Willis JH. 2020. Patterns of Hybrid Seed Inviability in the *Mimulus guttatus* sp. Complex Reveal a Potential Role of Parental Conflict in Reproductive Isolation. *Current Biology* 30: 83–93.

Darwin C, 1903. *More letters of Charles Darwin: a record of his work in a series of hitherto unpublished letters* (Vol. 2). D. Appleton.

Floyd SK, Friedman WE. 2000. Evolution of endosperm developmental patterns among basal flowering plants. *International Journal of Plant Sciences* 161: S57–S81.

Garcia D, Saingery V, Chambrier P, Mayer U, Jürgens G, Berger F. 2003. Arabidopsis *haiku* mutants reveal new controls of seed size by endosperm. *Plant Physiology* 131: 1661–1670.

Garner AG, Kenney AM, Fishman L, Sweigart, AL. 2016. Genetic loci with parent-of-origin effects cause hybrid seed lethality in crosses between Mimulus species. *New Phytologist* 211: 319–331.

Geist KS, Strassmann JE, Queller DC. 2019. Family quarrels in seeds and rapid adaptive evolution in Arabidopsis. *Proceedings of the National Academy of Sciences* 116: 9463-9468

Guilford VB, Fisk EL. 2016. Torrey Botanical Society Megasporogenesis and Seed Development in *Mimulus tigrinus* and *Torenia fournieri*. *Bulletin of the Torrey Botanical Club*. 79: 6–24.

Haig D, Westoby M. 1989. Parent-Specific Gene Expression and the Triploid Endosperm. *The American Naturalist* 134: 147–155.

Haig D, Westoby M. 1991. Genomic Imprinting in Endosperm: Its Effect on Seed Development in Crosses between Species, and between Different Ploidies of the Same Species, and Its Implications for the Evolution of Apomixis. *Philosophical Transactions: Biological Sciences* 1–13.

Håkansson A. 1952. Seed development after 2x, 4x crosses in Galeopsis pubescens. *Hereditas* 38:425–448

Hamilton WD. 1964. The genetical theory of kin selection. *J. Theor. Biol*, 7: 1–52.

Hanneman RE. 1993. Assignment of Endosperm Balance Numbers to the tuber.bearing nums and their close non-tuber-bearing relatives. *Euphytica* 74: 19–25.

Hehenberger E, Kradolfer D, Köhler C. 2012. Endosperm cellularization defines an important developmental transition for embryo development. *Development* 139: 2031–2039.

İltaş Ö, Svitok M, Cornille A, Schmickl R, Lafon Placette C. 2021. Early evolution of reproductive isolation: A case of weak inbreeder/strong outbreeder leads to an intraspecific hybridization barrier in *Arabidopsis lyrata*. *Evolution* 75: 1466–1476

Johnston SA, den Nijs TPM, Peloquin SJ, Hanneman RE. 1980. The Significance of Genic Balance to Endosperm Development in Interspecific Crosses. *Theoretical and applied genetics* 57: 5–9

Kang IH, Steffen JG, Portereiko MF, Lloyd A, Drews GN. 2008. The AGL62 MADS domain protein regulates cellularization during endosperm development in Arabidopsis. *Plant Cell* 20: 635–647.

Kinoshita T. 2007. Reproductive barrier and genomic imprinting in the endosperm of flowering plants. *Genes & genetic systems* 82: 177–186.

Kinser TJ, Smith RD, Lawrence AH, Cooley AM, Vallejo-Marín M, Conradi Smith GD, Puzey JR. 2021. Endosperm-based incompatibilities in hybrid monkeyflowers. *The Plant Cell* 33: 2235–2257

Lafon-Placette C, Hatorangan MR, Steige KA, Cornille A, Lascoux M, Slotte T, Köhler C. 2018. Paternally expressed imprinted genes associate with hybridization barriers in Capsella. *Nature Plants* 4: 352–357.

Lafon-Placette C, Johannessen IM, Hornslien KS, Ali MF, Bjerkan KN, Bramsiepe J, Glöckle BM, Rebernig CA, Brysting AK, Grini PE, Köhler C. 2017. Endosperm-based hybridization barriers explain the pattern of gene flow between Arabidopsis lyrata and Arabidopsis arenosa in Central Europe. *Proceedings of the National Academy of Sciences of the United States of America* 114: E1027–E1035.

Lafon-Placette C, Köhler C. 2016. Endosperm-based postzygotic hybridization barriers: developmental mechanisms and evolutionary drivers. *Molecular ecology* 25: 2620–2629.

Lenth R, Lenth MR. 2018. Package 'lsmeans'. *The American Statistician*, 34: 216–221.

Lin B-Y. 1984. Ploidy barrier to endosperm development in maize. *Genetics* 107: 103–115

Lu J, Zhang C, Baulcombe DC, Chen ZJ. 2012. Maternal siRNAs as regulators of parental genome imbalance and gene expression in endosperm of Arabidopsis seeds. *Proceedings of the National Academy of Sciences of the United States of America* 109: 5529–5534.

Luo M, Bilodeau P, Dennis ES, Peacock WJ, Chaudhury A. 2000. Expression and parent-of-origin effects for FIS2, MEA, and FIE in the endosperm and embryo of developing Arabidopsis seeds. *Proceedings of the National Academy of Sciences* 97: 10637–10642.

Luo M, Dennis ES, Berger F, Peacock WJ, Chaudhury A. 2005. MINISEED3 (MINI3), a WRKY family gene, and HAIKU2 (IKU2), a leucine-rich repeat (LRR) KINASE gene, are regulators of seed size in Arabidopsis. *Proceedings of the National Academy of Sciences* 102: 17531–17536.

Mikesell J. 1990. Anatomy of terminal haustoria in the ovule of plantain (Plantago major L.) with taxonomic comparison to other angiosperm taxa. *Botanical Gazette*, 151: 452–464.

Morgan EJ, Čertner M, Lučanová M, Deniz U, Kubíková K, Venon A, Kovářík O, Lafon Placette C, Kolář, F. 2021. Disentangling the components of triploid block and its fitness consequences in natural diploid–tetraploid contact zones of *Arabidopsis arenosa*. *New Phytologist* 232: 449–1462.

Morley-Smith ER, Pike MJ, Findlay K, Köckenberger W, Hill LM, Smith AM, Rawsthorne S. 2008. The transport of sugars to developing embryos is not via the bulk endosperm in oilseed rape seeds. *Plant Physiology* 147: 2121–2130.

Nesom GL. 2012. Taxonomy of *Erythranthe* sect. *Simiola* (Phrymaceae) in the USA and Mexico. *Phytoneuron* 40: 1–123.

Nguyen H, Brown RC, Lemmon, BE. 2000. The specialized chalazal endosperm in Arabidopsis thaliana and Lepidium virginicum (Brassicaceae). *Protoplasma*, 212: 99–110.

Nishiyama I, Inomata N. 1966. Embryological studies on cross-incompatibility between 2x and 4x in Brassica. *The Japanese journal of genetics* 41: 27–42.

Nishiyama I, Yabuno T. 1978. Causal Relationships between the Polar Nuclei in Double Fertilization and Interspecific Cross-incompatibility in Avena. *Cytologia*, 43: 453–466.

Ohto MA, Floyd SK, Fischer RL, Goldberg RB, Harada JJ. 2009. Effects of APETALA2 on embryo, endosperm, and seed coat development determine seed size in Arabidopsis. *Sexual plant reproduction* 22: 277–289.

Oneal E, Willis JH, Franks RG. 2016. Disruption of endosperm development is a major cause of hybrid seed inviability between Mimulus guttatus and Mimulus nudatus. *New Phytologist* 210: 1107–1120.

Parrott WA, and Smith RR. 1986. Evidence for the existence of endosperm balance number in the true clovers (*Trifolium* spp.). *Canadian journal of genetics and cytology* 28: 581–586.

Pennington PD, Costa LM, Gutierrez-Marcos JF, Greenland AJ, Dickinson HG. 2008. When genomes collide: Aberrant seed development following maize interploidy crosses. *Annals of botany* 101: 833–843.

Picard CL, Povilus RA, Williams BP, Gehring M. 2021. Transcriptional and imprinting complexity in Arabidopsis seeds at single-nucleus resolution. *Nature plants* 7: 730–738.

Povilus RA, Gehring M. 2022. Maternal-filial transfer structures in endosperm: A nexus of nutritional dynamics and seed development. *Current opinion in plant biology* 65: 102121.

Queller DC. 1983. Kin Selection and Conflict in Seed Maturation. *Journal of Theoretical Biology* 100: 153–172.

Rasband WS. 1997. ImageJ, U. S. National Institutes of Health, Bethesda, Maryland, USA, https://imagej.nih.gov/ij/.

Rebernig CA, Lafon-Placette C, Hatorangan MR, Slotte T, Köhler C. 2015. Non-reciprocal interspecies hybridization barriers in the Capsella genus are established in the endosperm. *PLoS genetics* 11:1005295

Reik W, Walter J. 2001. Genomic imprinting: parental influence on the genome. *Nature Reviews Genetics* 2: 21–32.

Roth M, Florez-Rueda AM, Griesser S, Paris M, Städler T. 2018. Incidence and developmental timing of endosperm failure in post-zygotic isolation between wild tomato lineages. *Annals of Botany* 121: 107–118.

Sandstedt GD, Wu CA, Sweigart AL. 2021. Evolution of multiple postzygotic barriers between species of the Mimulus tilingii complex*. *Evolution* 75: 600–613.

Scott RJ, Spielman M, Bailey J, Dickinson HG. 1998. Parent-of-origin effects on seed development in Arabidopsis thaliana. *Development* 125: 3329–3341.

Soltis PS, Folk RA, Soltis DE. 2019. Darwin review: Angiosperm phylogeny and evolutionary radiations. *Proceedings of the Royal Society B: Biological Sciences* 286.

Sørensen MB, Chaudhury AM, Robert H, Banchare E, Berger F. 2001. Polycomb group genes control pattern formation in plant seed. *Current Biology* 11: 277–281.

Städler T, Florez-Rueda AM, Roth M. 2021. A revival of effective ploidy: the asymmetry of parental roles in endosperm-based hybridization barriers. *Current Opinion in Plant Biology* 61: 102015

Stephens SG. 1949. The cytogenetics of speciation in Gossypium. I. Selective elimination of the donor parent genotype in interspecific backcrosses. *Genetics* 34: 627.

Thiel J. 2014. Development of endosperm transfer cells in barley. *Frontiers in Plant Science* 5: 108.

Vickery RK. 1978. Case studies in the evolution of species complexes in *Mimulus*. *Evolutionary biology* 405–507. Springer, Boston, MA.

Woodell SRJ, Valentine DH. 1961. Studies in British Primulas IX. Seed Incompatibility in Diploid-Autotetraploid Crosses. *New Phytologist* 282–294.

Zhan J, Thakare D, Ma C, Lloyd A, Nixon NM, Arakaki AM, Burnett WJ, Logan KO, Wang D, Wang X, Drews GN. 2015. RNA sequencing of laser-capture microdissected compartments of the maize kernel identifies regulatory modules associated with endosperm cell differentiation. *The Plant Cell*, 27: 513–531.

Zhang B, Li C, Li Y, and Yu, H. 2020. Mobile TERMINAL FLOWER1 determines seed size in Arabidopsis. *Nature Plants* 6: 1146–1157.

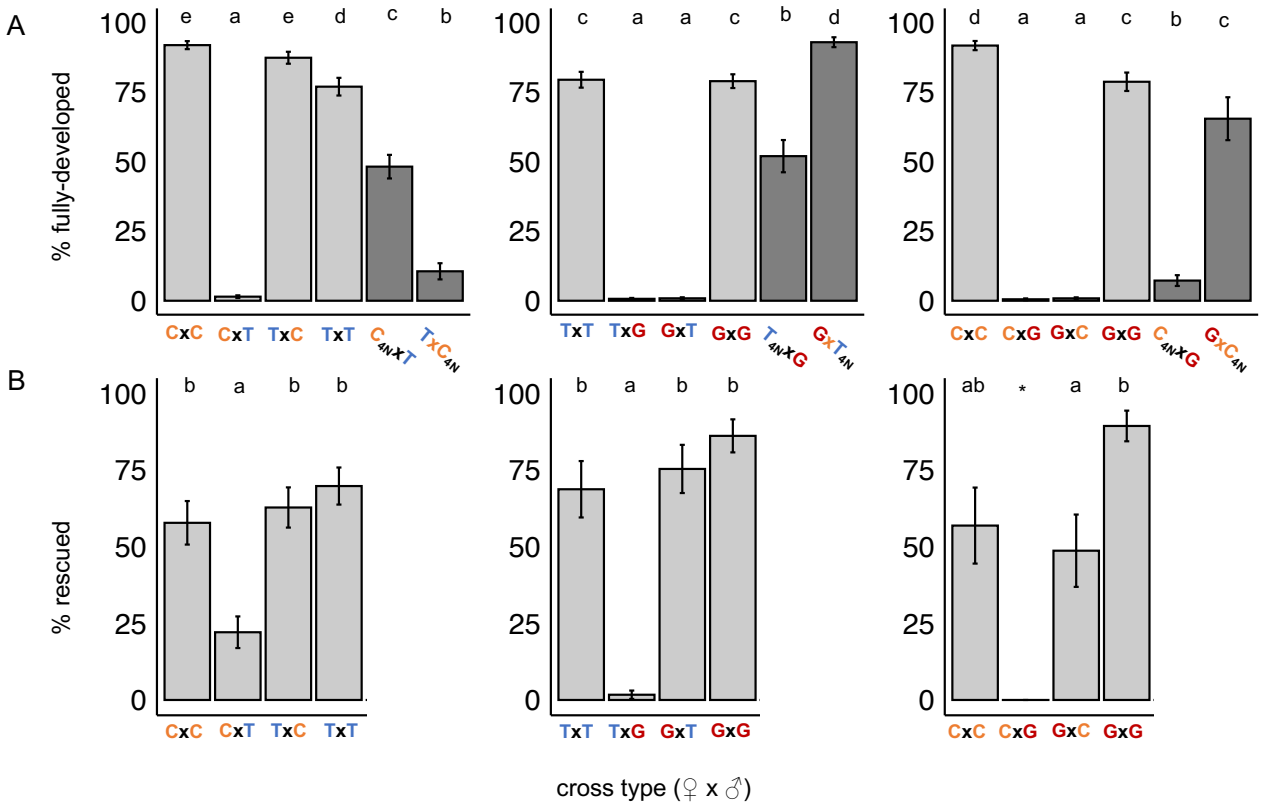

Figure 3.1. Percentage of viable seeds from morphological assessments and embryo rescues in intra- and interspecific crosses among *M. caespitosa* (C), *M. tilingii* (T), and *M. guttatus* (G). The first letter of each cross indicates the maternal species. Least squares means given with +/- SE. Light gray bars represent cross types between diploid parents, and dark gray bars represent crosses where one parent is a synthetic tetraploid, as denoted by the "4N" subscript in the cross. Different letters indicate significant differences in lsmeans among crosses ($P<0.05$) determined by a post hoc Tukey method. Analyses were performed separately, only comparing reciprocal interspecific crosses and their corresponding intraspecific (and interploidy crosses for 1A). **A**. Percentage of seeds per fruit that appeared fully-developed. **B.** Percentage of developing seeds (8-12 DAP) per fruit that germinated on a sucrose-rich medium. Asterisk denotes lack of variation in response variable to determine statistical differences.

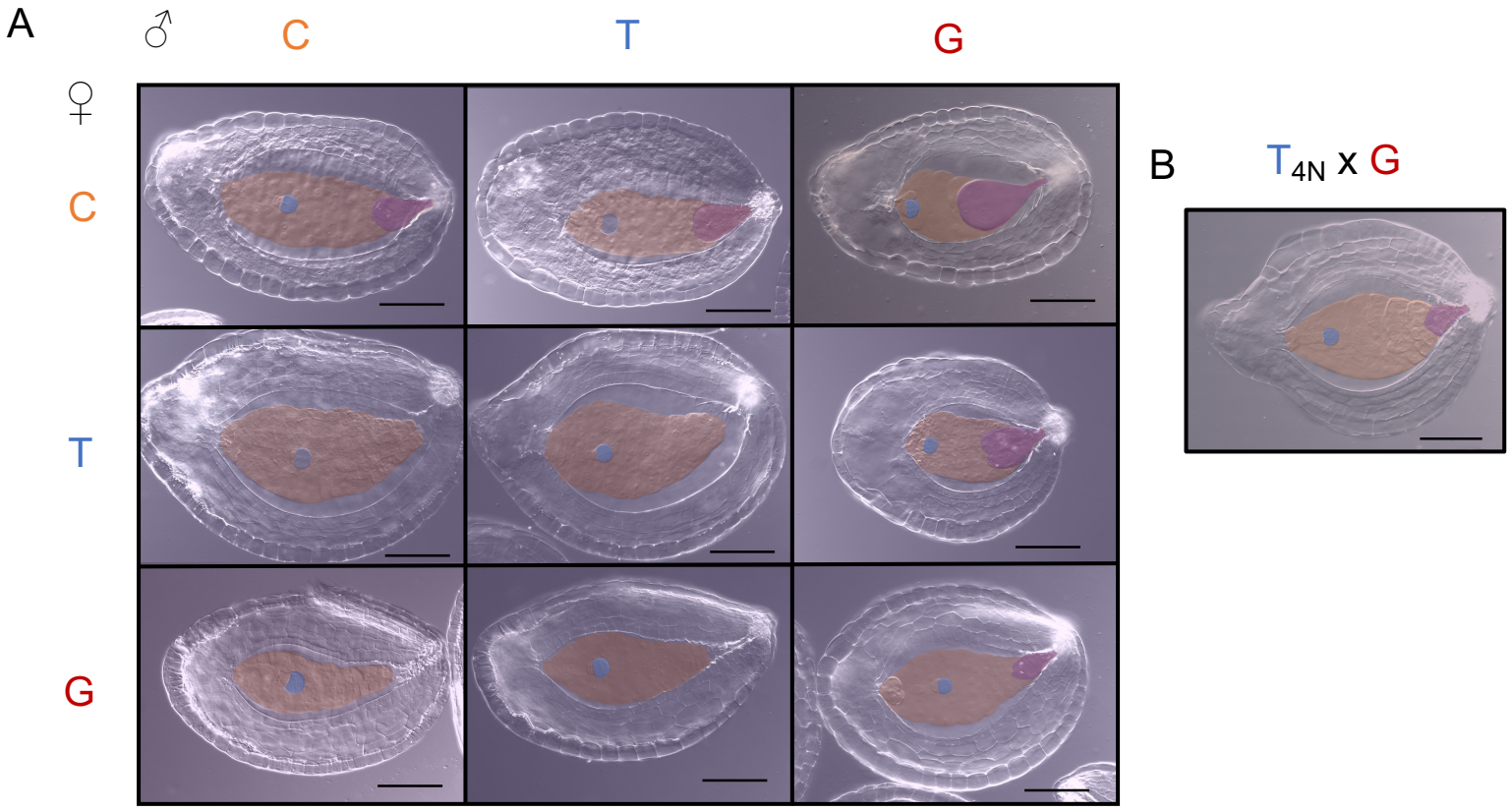

Figure 3.2. Developing seeds four days after pollination (DAP) in crosses among *M. caespitosa* (C), *M. tilingii* (T), and *M. guttatus* (G). Seeds were cleared with Hoyer's solution. Blue shading represents embryo, orange shading represents endosperm region, and purple shading represents chalazal haustoria. Scale bar is 0.1mm. A) Seeds 4DAP of intra- and interspecific crosses. Maternal parent is listed along the left side, and paternal parent is listed along the top. Along the diagonal are the intraspecific crosses (CxC, TxT, and GxG), below diagonal are maternal excess crosses (CxT, GxT, and GxC), and above diagonal are paternal excess crosses (CxT, TxG, and CxG). B) Representative seed of interploidy cross at 4 DAP. "4N" subscript denotes tetraploid maternal parent.

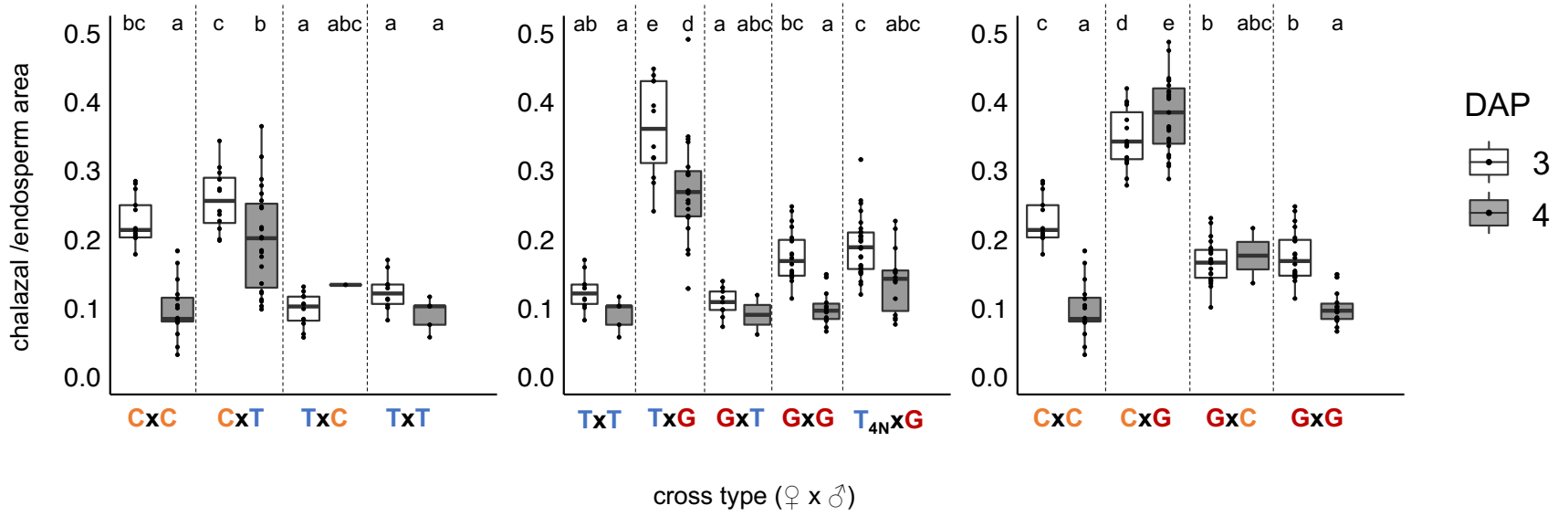

Figure 3.3. Proportion of endosperm filled by a chalazal haustorium at 3 and 4 days after pollination in intra- and interspecific crosses among *M. caespitosa* (C), *M. tilingii* (T), and *M. guttatus* (G). The first letter of each cross indicates the maternal species. In the T4NxG cross, 4N indicates a synthetic tetraploid *M. tilingii* parent. Different letters above boxes indicate significant differences in lsmeans among crosses ($P<0.05$) determined by a post hoc Tukey method. Analyses were performed separately, comparing reciprocal interspecific and corresponding intraspecific crosses, except for the T–G cross, where comparisons with T_{4N}xG were also included – "4N" subscript denotes tetraploid maternal parent.

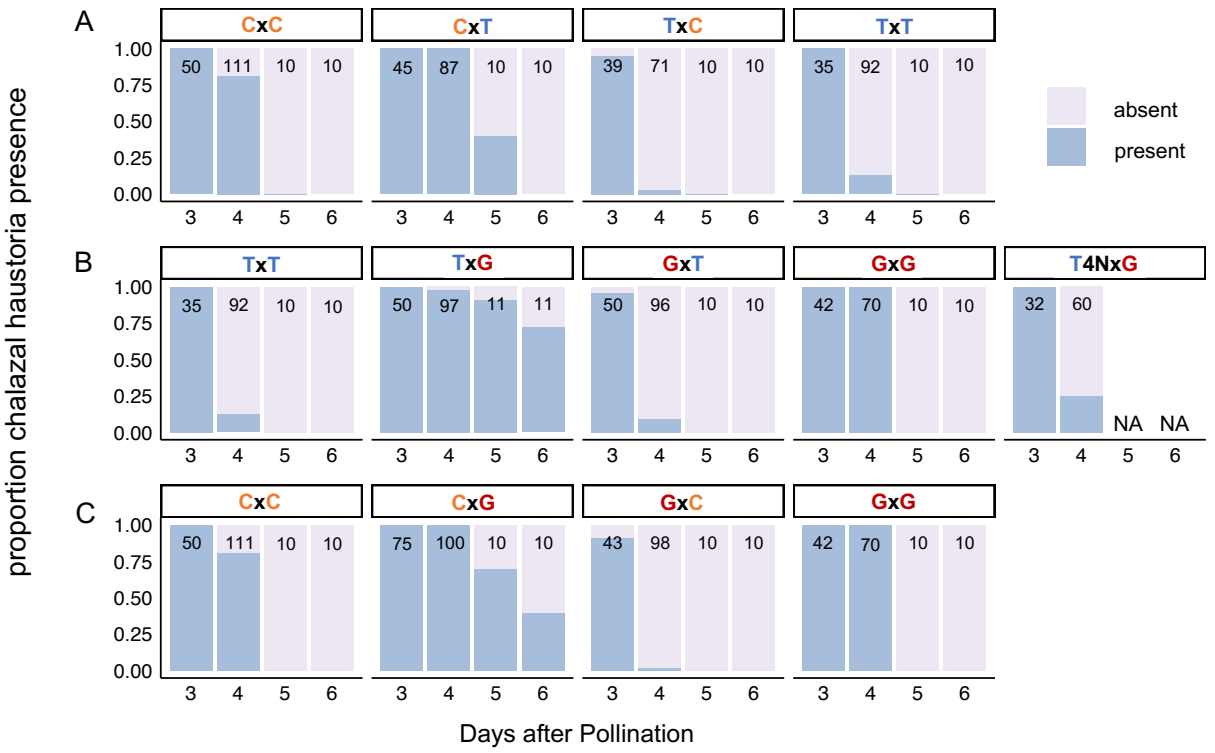

Figure 3.4. Proportion of chalazal haustoria presence and absence in developing seeds (3, 4, 5, and 6 days after pollination) from intra- and interspecific crosses among *M. caespitosa* (C), *M. tilingii* (T), and *M. guttatus* (G). The first letter of each cross indicates the maternal species. Numbers in bars represent the total number of developing seeds scored for an intact chalazal haustorium, where seeds were scored from 1-2 fruits per cross type per DAP. Seeds were only scored and imaged if they contained a visible embryo. The blue color indicates the proportion of seeds with intact chalazal haustoria, and the purple color indicates the proportion of seeds where chalazal haustoria were absent. In the T_{4N}xG cross type, "4N" subscript denotes synthetic tetraploid *M. tilingii* maternal parent. In days 3 and 4, chalazal haustoria presence/absence were scored after dissecting developing seeds from whole ovules and clearing with Hoyer's solution. In days 5 and 6, this phenotype was scored from whole fruit histological sections. A) *M. caespitosa* and *M. tilingii* B) *M. tilingii* and *M. guttatus* C) *M. caespitosa* and *M. guttatus.*

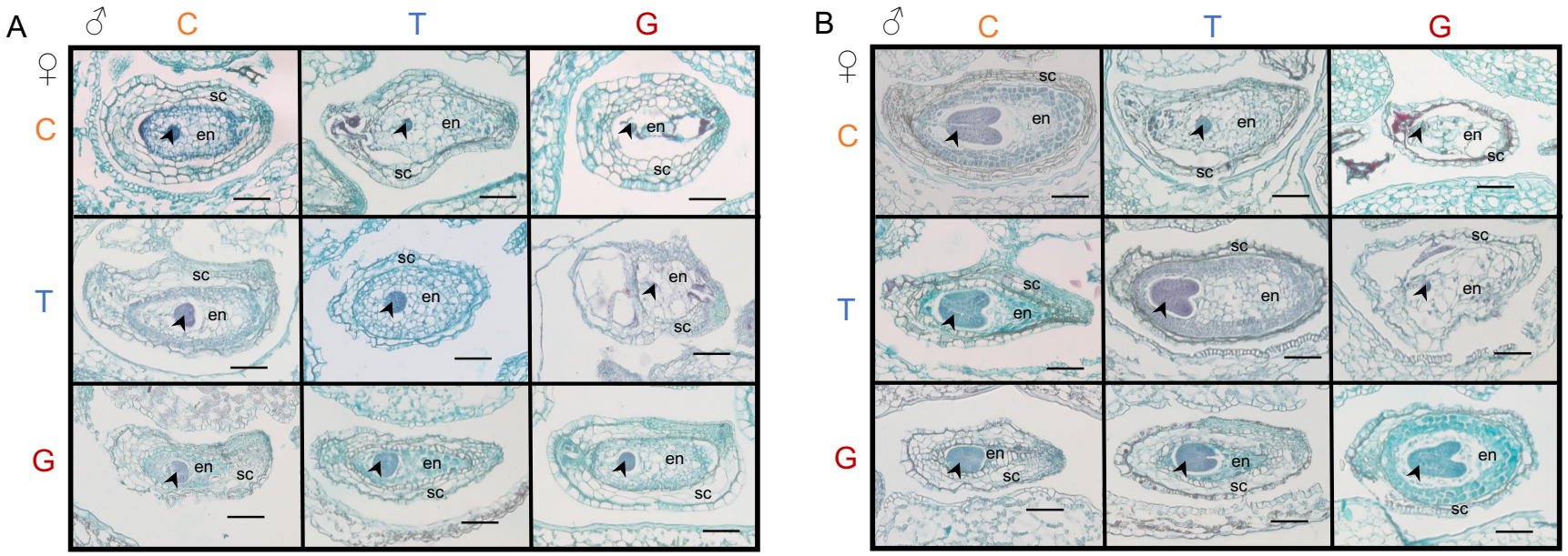

Figure 3.5. Histological sections of whole fruits from intra- and interspecific crosses among *M. caespitosa* (C), *M. tilingii* (T), and *M. guttatus* (G). Maternal parent is listed along the left side, and paternal parent is listed along the top. Along the diagonal are the intraspecific crosses (CxC, TxT, and GxG), below diagonal are maternal excess crosses (CxT, GxT, and GxC; maternal parent always listed first), and above diagonal are putative paternal excess crosses (CxT, TxG, and CxG). Arrowhead = embryo, en = endosperm, sc = seed coat. Scale bar is 0.1mm. A) 6 DAP. Intraspecific and paternal excess endosperms are mostly composed of large empty cells, whereas maternal excess cross types (especially GxT and GxC) develop endosperms that are small and composed of darkly stained, dense cells. B) 8 DAP. Intraspecific endosperm cells begin to differentiate into cytoplasmically dense, starch-filled cells along the peripheral region near the seed coat. However, in GxT and GxC crosses, the whole endosperm is composed of these dense cell types, and the endosperm remains very small and compact. Paternal excess endosperms appear abnormal and do not show evidence of cell differentiation by 8 DAP.

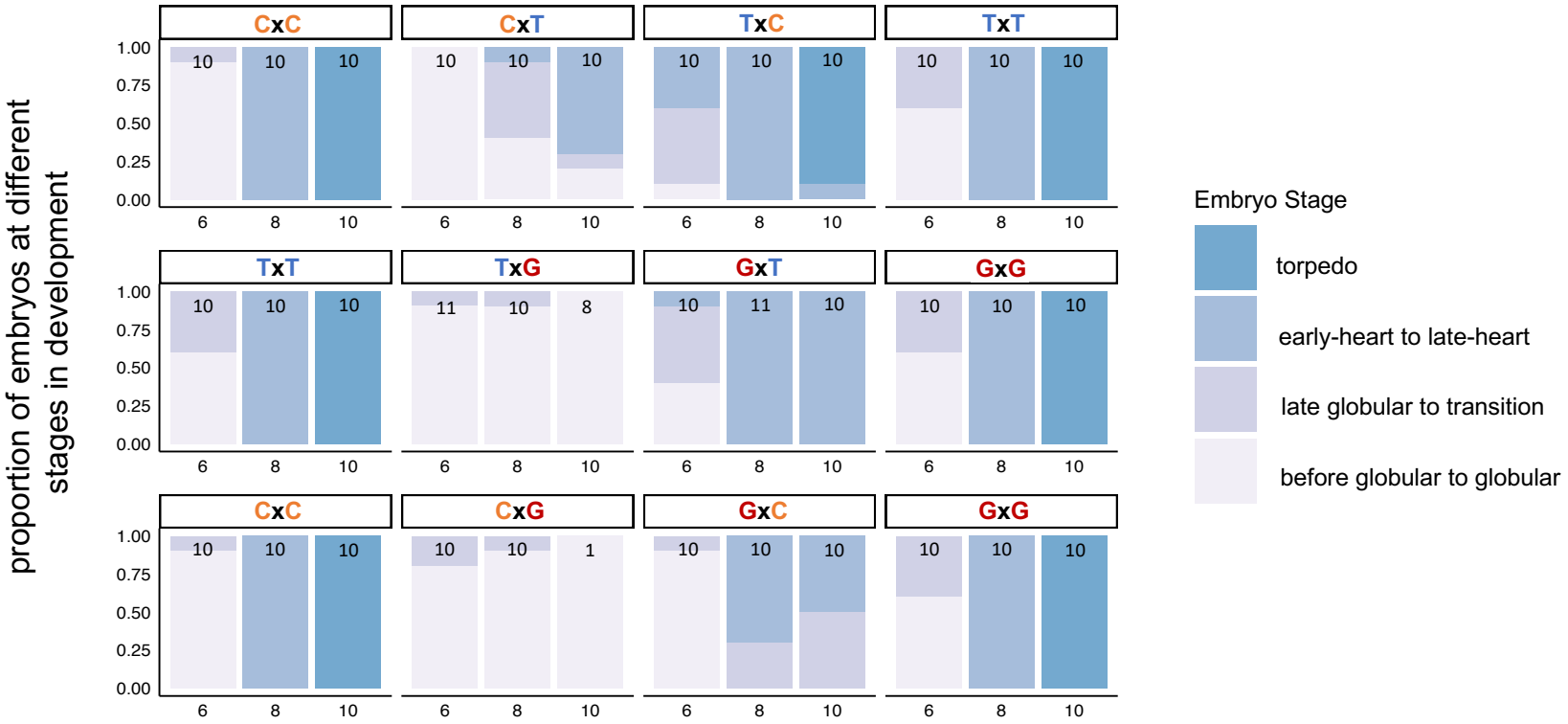

Figure 3.6. Proportion of embryos at a particular developmental stage at different time points (6, 8, 10 DAP) in intra- and interspecific crosses among *M. caespitosa* (C), *M. tilingii* (T), and *M. guttatus* (G). The first letter of each cross type indicates the maternal species. Numbers in bars represent the total number of embryos scored per cross type, where less than 10 embryo suggests severe embryo lethality for a particular cross type. Colors in each bar indicates stage of embryo development: the light purple color represents early to globular embryos, the dark purple color represents late globular to transition embryos, the light blue color represents early to late heart stage embryos, and the dark blue color represents torpedo embryos. Stages of embryo development determined from whole fruit histological sections.

CHAPTER IV

CHROMOSOMAL REARRANGEMENTS CAUSE SEVERE F1 HYBRID STERILITY BETWEEN SPECIES IN THE *MIMULUS TILINGII* COMPLEX[3]

[3]Sandstedt, G.D. & A.L. Sweigart, To be submitted to *Evolution.*

ABSTRACT

A formidable question in evolutionary biology is understanding how and why postzygotic barriers, such as hybrid inviability and sterility, evolve. In this study, we investigated the genetic basis of severe F1 hybrid male and female sterility in two pairs of closely related, diploid species in the *Mimulus tilingii* complex. We performed a classic experiment – artificially doubling hybrid genomes – to determine whether genetic incompatibilities or chromosomal rearrangements are the cause of F1 hybrid sterility between *Mimulus* species. If hybrid sterility results from the production of unbalanced gametes due to aberrant pairing of rearranged chromosomes during meiosis, doubling the genome should restore fertility because each divergent homolog now has a collinear partner. If, instead, hybrid sterility is due to genetic incompatibilities, doubling the genomic content will have little impact on fertility because the same dysfunctional, heterospecific genotype combinations will still be present. Strikingly, we found an increase in both male and female fertility in synthetic tetraploid F1 hybrids of crosses between species in the *M. tilingii* complex, with male fertility nearly fully rescued. These results provide strong evidence that underdominant chromosomal rearrangements are directly disrupting meiosis in F1 hybrids. This study highlights the importance of characterizing the genetic basis of F1 hybrid sterility because it is a critical first step toward understanding the evolutionary mechanisms of species divergence.

INTRODUCTION

In *On the Origin of Species* (1859), Darwin discussed hybrid sterility at great length because he understood that the production of dysfunctional hybrids could not possibly be favored

by natural selection. Given his ignorance of Mendelian genetics and evolutionary processes such as genetic drift, he struggled to explain how or why hybrid sterility could evolve if selection was not directly playing a role. This puzzle was solved during the first half of the twentieth century, as biologists demystified the mechanisms of inheritance and gained a deeper understanding of evolution. Two broad genetic mechanisms were proposed to explain the formation of intrinsic hybrid sterility: chromosomal rearrangements and epistatic interactions among loci (Dobzhansky 1937). Because these two mechanisms require the action of very different evolutionary processes, determining the genetic basis of hybrid sterility is an important first step toward understanding postzygotic reproductive isolation and the origin of species.

Heterozygous underdominant chromosomal rearrangements, such as inversions or reciprocal translocations, are predicted to disrupt meiosis and gametogenesis (White 1948). A single underdominant rearrangement can yield aneuploid gametes up to fifty percent of the time (White 1973), but the strength of underdominance may vary for any given rearrangement. If we consider a pericentric inversion, which includes a centromere, a crossover event within the rearranged region produces unbalanced recombinant gametes with zero or two centromeres, thereby reducing fertility (Navarro and Ruiz 1997). In contrast, inversions that are small and/or do not include a centromere (*i.e.*, paracentric) are thought to have weaker deleterious effects when heterozygous (White 1973; Kirkpatrick 2010). Moreover, when individuals are heterozygous for a reciprocal translocation, fifty percent of their gametes are expected to be unbalanced under random segregation. Still, a bias towards alternate versus adjacent segregation can give rise to an increased proportion of viable gametes (Auger and Sheridan 2012). Despite

their promising role as species barriers, it is difficult to imagine how underdominant rearrangements may spread without invoking a large role of genetic drift.

The second major mechanism of hybrid sterility, genetic incompatibilities, does not need to rely solely on genetic drift. To describe how the breakdown of hybrid fitness might be tolerated by natural selection, Dobzhansky (1937) and Muller (1942) independently formulated a model without either species needing to pass through an adaptive valley. For example, suppose that prior to the species split, an "*aa*" genotype existed at one locus and "*bb*" at a second, unlinked locus. When the species diverge in allopatry, an "*A*" mutation arises in one species and fixes due to neutral or adaptive processes – this species now has the genotype "*AAbb*". Similarly, a "*B*" allele evolves and fixes in the other species, which now carries the genotype "*aaBB*". These mutations are compatible in their own native genetic backgrounds. However, when these two species hybridize, the mutations are now "tested" against a new, foreign genetic background – the "*A*" allele may negatively interact with the "*B*" allele, resulting in hybrid sterility or inviability. Indeed, there is now broad empirical support in plants and animals for genetic incompatibilities as a major source of hybrid sterility (reviewed in: Rieseberg and Blackman 2010; Blackman 2016; Fishman and Sweigart 2018).

Despite widespread support for the Dobzhansky-Muller model, a handful of recent studies in plants have reopened the debate about whether chromosomal rearrangements can sometimes play a primary role in hybrid sterility. For instance, in self-incompatible sunflower species with large effective population sizes (Strasburg et al. 2011), nine of 11 pollen viability QTL genetically mapped to chromosomal rearrangements (Lai et al. 2005). Additionally, pollen sterility was mapped to two large-effect translocations in closely related *Mimulus* species

(Stathos and Fishman 2014). Aside from genetic drift, an underdominant chromosomal rearrangement might spread if it is linked to a meiotic driver or confers a fitness advantage due to novel variation created by the breakpoint itself (Hoffman and Rieseberg 2008), but there is little empirical support for such mechanisms. Theory also suggests that costly rearrangements might spread if natural selection favors suppression of recombination (Kirkpatrick and Barton 2006). In brief, this model suggests that in the absence of geographical barriers, adaptive alleles within an underdominant rearrangement might be protected against recombination if their benefits outweigh maladaptive gene flow (Rieseberg 2001; Noor et al. 2001; Kirkpatrick and Barton 2006). Given the prevalence of gene flow during plant species divergence (Arnold 2004; Rieseberg and Willis 2007; Abbott et al. 2013), it is possible that a role for chromosomal rearrangements in causing postzygotic reproductive isolation was dismissed too soon.

In this study, we investigate whether chromosomal rearrangements or genetic incompatibilities cause severe F1 hybrid sterility between yellow monkeyflower species in the *Mimulus tilingii* complex. Members of this complex – *M. caespitosa*, *M. minor*, and *M. tilingii* – are primarily allopatric and restricted to high-elevation sites of western North America. *Mimulus caespitosa* grows in Washington state, *M. minor* grows exclusively in Colorado, and *M. tilingii* occupies a wider distribution across several western states (Nesom 2012). The three species in this complex are morphologically and genetically distinct, and they split within the last 400ky (Sandstedt et al. 2021). Reciprocal crosses among species in this group have revealed several strong intrinsic postzygotic barriers that affect F1 hybrids, including severe seed inviability, necrosis, male sterility, and female sterility. In terms of the fertility effects, F1 hybrids from crosses between *M. caespitosa* and *M. tilingii* produce <40% viable pollen and F1 hybrids from

any interspecific cross involving *M. minor* produce only ~1% viable pollen. Similarly, female fertility is severely disrupted, with F1 hybrids between *M. tilingii* and *M. caespitosa* producing <20% of the seeds set by parental species, and any cross with *M. minor* producing only ~1% (Sandstedt et al. 2021).

In this system, we aim to determine whether chromosomal rearrangements or genetic incompatibilities are the primary cause of hybrid sterility. Classic and recent studies have utilized genome doubling to resolve this problem (Dobzhansky 1933; Stebbins 1950; Stathos and Fishman 2014). If chromosomal rearrangements underlie hybrid sterility, doubling the genomic content should restore abnormal pairing in meiosis by providing divergent homologues with a collinear partner, thereby rescuing fertility. On the other hand, genome doubling should not rescue hybrid sterility if it is caused by genetic incompatibilities because the same incompatible alleles should still be present. Using this approach, we explore the genetic basis of male and female sterility between species in the *M. tilingii* complex to provide insight into the evolutionary forces underlying divergence in this group of closely related species.

MATERIALS AND METHODS

Plant Material and Care

In this study, we used inbred lines formed by more than six generations of self-fertilization to represent each focal species in the *M. tilingii* complex (*M. tilingii, M. caespitosa*, and *M. minor*). Previously, we showed crosses between these inbred lines result in severe F1 hybrid male and female sterility (Sandstedt et al. 2021). The inbred lines originated from three distinct, high-elevation populations: LVR1 (*M. tilingii*) originated from Lee Vining and

Yosemite National Park, CA at 2751m, TWN36 (*M. caespitosa*) was derived from Twin Lakes, WA at 1594m, and NOR523 (*M. minor*) was derived from North Pole Basin, CO at 3349m. Using these three lines, we performed intraspecific crosses to generate pure species progeny, which we designate as follows: T, C, and M (T = *M. tilingii*, C = *M. caespitosa*, and M = *M. minor*). We also performed interspecific crosses using *M. tilingii* as the seed parent and either *M. caespitosa* or *M. minor* as the pollen donor to create two classes of F1 hybrid: TC and TM (maternal parent is always listed first; the reciprocal direction of these crosses generates mostly inviable seeds: Sandstedt et al. 2021). For all crosses, we emasculated maternal plants 2-3 days prior to crossing to prevent contamination from self-pollination.

We planted pure species and F1 hybrid seeds onto petri dishes containing damp paper towels and sealed them with parafilm. We cold-stratified petri dishes to disrupt seed dormancy, and after one week, we transferred petri dishes into a growth chamber set to 16-h at 23°C and 8-h at 16°C. After germination, we transplanted 10 seedlings from each of the three pure species and two F1 hybrid classes into 2.5" pots with moist Fafard 4P growing mix (Sun Gro Horticulture, Agawam, MA). To generate tetraploid plants, we treated F1 TC and F1 TM hybrid seeds with 0.2% colchicine (~400 seeds per F1 class) in 1.8mL Eppendorf tubes. We wrapped tubes in foil to prevent light exposure and incubated them for 24 hours in the same growth chamber as above. We planted colchicine-treated seeds directly into 3.5" pots with moist Fafard 4P growing mix (Sun Gro Horticulture, Agawam, MA) and placed them in the same growth chamber.

Once pure species and F1 hybrids began to grow their first true leaf pair, we transferred seedlings into 3.5" pots in the greenhouse, which was set to 16-h days at 23°C and 8-h nights at 16°C. Across 10 flats, we randomized individuals from each of the seven following genotypes:

three pure species (T, C, and M), two diploid F1 ($F1_{TC}$-2n, $F1_{TM}$-2n), and two tetraploid F1 ($F1_{TC}$-4n; $F1_{TM}$-4n). In total, there were 10 individuals for each of the pure species, diploid F1 classes, and tetraploid F1 classes.

Ploidy Assessment

To assess ploidy, we used flow cytometry to estimate genome size. We performed flow cytometry on three random diploid plants from each pure species and F1 hybrid class (Table 1). To confirm that colchicine treated plants were tetraploids and not diploids or mixoploids, we performed flow cytometry on colchicine-treated F1 TC plants (*N = 60*) and F1 TM plants (*N* = 24). To prepare samples for flow cytometry, we used a protocol adapted from Lu et al. 2017. In brief, we extracted nuclei by chopping ~50mg of leaf tissue from each experimental sample with ~50mg of leaf tissue from an internal control (*Arabidopsis thaliana*, accession Col-0) into 1mL of a pre-chilled lysis buffer (15mM Tris-HCl pH 7.5, 20mM NaCl, 80mM KCl, 0.5mM spermine, 5mM 2-ME, 0.2% TritonX-100). We stained nuclei with 4,6-Diamidino-2-phenylindole (DAPI) and filtered nuclei for debris using a 40um Flowmi™ cell strainer into a single well of a 96-well polypropylene plate. Using a CytoFLEX (Beckman Coulter Life Sciences) flow cytometer, we determined ploidy and calculated total DNA content of each sample with the following equation (Table 1):

$$\text{2C DNA content (pg DNA)} = \frac{\text{sample G1 peak mean}}{\text{standard G1 peak mean}} * \text{standard 2C DNA content}$$

Assessment of Pollen Fertility

Once plants began to flower, we collected pollen from the first two open flowers into a lacto-phenol aniline blue stain (viable pollen grains stain a dark blue color). We estimated pollen viability by scoring the proportion of viable pollen from a haphazard sample of 100 pollen grains per flower. Once we collected flowers from colchicine-treated individuals, we labeled the flowering stems with tape, so that we could test genome size on adjacent leaves using flow cytometry given the potential for chimera or mixoploid plants.

To determine whether genome doubling rescues pollen viability, we performed two separate generalized linear models (GLM) using the glm function in the 'lme4' package implemented in R with a quasibinomial distribution to correct for overdispersion (Bates et al. 2007). In Model 1, we included T, C, $F1_{TC}$-2n hybrids, and $F1_{TC}$-4n hybrids (θ=11.8; theta represents overdispersion parameter). In Model 2, we compared T, M, $F1_{TM}$-2n hybrids, and $F1_{TM}$-4n hybrids (θ=11.4). For each model, we combined the number of viable and inviable pollen grains into a single variable using the R function cbind and set this as the response variable, while genotype class was set as our fixed variable. We computed an ANOVA to test whether genotype significantly contributed to variation in pollen viability using the anova function in the 'car' package in R with type III sums of squares, which implements likelihood-ratio chi-square tests for GLMs (Fox et al. 2012). Using the emmeans function in the 'emmeans' package in R, we calculated least-squares means (lsmeans) and compared lsmeans among all genotype classes (Lenth and Lenth 2018). We further tested which of the four genotypes for each model significantly differed in pollen viability using a post-hoc Tukey method adjustment.

Assessment of Female Fertility

To estimate female fertility, we emasculated 1-2 flowers per experimental plant, performed hand-pollinations, and counted the total number of seeds per fruit (for experimental plants with more than one fruit, we calculated the average). For pure species, we used the same inbred line as the pollen donor and assessed female fertility in 8-9 individuals (C = 9, T = 9, M = 8). For diploid F1 hybrids, we used one or both parental lines as pollen donors and assessed female fertility in 10 $F1_{TC}$-2n hybrids and seven $F1_{TM}$-2n. For tetraploid F1 hybrids, we used diploid parental lines as pollen donors, as well as synthetic tetraploid lines of *M. tilingii* and *M. caespitosa* generated in CHIII (4N *M. tilingii* pollen donor for $F1_{TC}$-4n and $F1_{TM}$-4n hybrids and 4N *M. caespitosa* pollen donor for $F1_{TC}$-4n hybrids). We pollinated tetraploid F1 hybrids with both 2n and 4n pollen because interploidy crosses often result in strong triploid block (i.e., hybrid seed inviability: see CHIII), which might affect levels of seed production. We assessed female fertility in nine $F1_{TC}$-4n hybrids and six $F1_{TM}$-4n hybrids. We also scored seed viability by eye for each fruit and determined whether seeds were round and plump (*i.e.*, "fully-developed"), or dark and shriveled (*i.e.*, "underdeveloped").

To model female fertility, we performed two separate GLMs using a Gamma distribution for seed count. Because parental line of the pollen donor had no significant effects on seed production in any of the hybrid classes (data not shown), we pooled seed count regardless of which parental species was used in supplemental pollinations. However, to disentangle seed production and triploid block, we separated each tetraploid hybrid class ($F1_{TC}$-4n, and $F1_{TM}$-4n) into two groups based on ploidy of the pollen donor. Thus, in Model 1, we included T, C, $F1_{TC}$-2n hybrids, and $F1_{TC}$-4n hybrids with a 2n or with a 4n pollen donor. In Model 2, we compared

T, M, $F1_{TM}$-2n hybrids, and $F1_{TM}$-4n hybrids with a 2n or 4n pollen donor. In Model 2, we set "0" values to "0.01" to fit a Gamma distribution (only the $F1_{TM}$-2n hybrid class had zero values and these represented <10% of all data). For both models, we set the total number of seeds per fruit as the response variable and combined genotype class and ploidy level of the pollen donor into a single fixed factor. To test whether the fixed factor significantly contributed to variation in seed number per fruit, we performed an ANOVA with type III sums of squares. We calculated and performed lsmeans comparisons among all crosses and tested which crosses and ploidy level of pollen donor significantly differed in seeds per fruit using a post-hoc Tukey method adjustment.

To assess differences in hybrid seed viability due to triploid block, we performed two separate GLMs using a quasibinomial distribution to correct for overdispersion (Model 1: T, C, $F1_{TC}$-2n hybrids, and $F1_{TC}$-4n hybrids with 2n or 4n pollen donor, $\theta = 7.04$; Model 2: T, M, $F1_{TM}$-2n hybrids, and $F1_{TM}$-4n hybrids with 2n or 4n pollen donor, $\theta = 3.95$). We combined genotype class and ploidy level of the pollen donor into a single fixed factor. Additionally, we set the response variable to the number of viable and inviable seeds per fruit combined into a single variable using the R function cbind. We performed an ANOVA and performed pairwise comparisons of lsmeans using a post-hoc Tukey method.

RESULTS

In our previous study (Sandstedt et al. 2021), crosses between *M. tilingii* and *M. caespitosa* or *M. minor* produced highly sterile reciprocal F1 hybrid offspring (severe hybrid

seed viability in MT F1 hybrids precludes assessment of hybrid sterility). Here, we recapitulate these results, finding that pollen viability significantly differs among genotype classes (Figure 1A: $\chi2 = 284.61$, $df = 3$, $p < 2.2e\text{-}16$; Figure 1B: $\chi2 = 410.05$, $df = 3$, $p < 2.2e\text{-}16$). While all pure species were highly fertile (pollen viability = 74%–94%), pollen viability was much lower in diploid F1 hybrids between *M. tilingii* and *M. caespitosa* (pollen viability of $F1_{TC}$-2n = 28%) and between *M. tilingii* and *M. minor* (pollen viability of $F1_{TM}$-2n = 2%). However, upon genome doubling, male fertility in both of these hybrids increased dramatically: pollen viability was restored to 94% in $F1_{TC}$-4n hybrids and to 70% in $F1_{TM}$-4n hybrids (Figure 1). These results strongly implicate chromosomal rearrangements as the primary cause of F1 hybrid male sterility in these *Mimulus* species.

Genome doubling also had a strong effect on female fertility, resulting in higher seed production in tetraploid F1 hybrids than in their diploid counterparts (Figure 2). For *M. tilingii* and *M. caespitosa*, both hybrid classes had significantly lower seed production than parental lines (Figure 2A: $\chi2 = 98.7$, $df = 4$, $p < 2.2e\text{-}16$), but tetraploids ($F1_{TC}$-4n) produced 60% or 32% more seeds than diploids ($F1_{TC}$-2n), depending on the ploidy of the pollen donor (note that these increases are not significant in post hoc Tukey comparisons, see Figure 2). For *M. tilingii* and *M. minor*, seed production was also lower in hybrid than in parental classes, but the effect of genome doubling on hybrid seed set was highly significant: seed production in $F1_{TM}$-4n hybrid plants was 146 times higher (diploid pollen donor) or 78 times higher (tetraploid pollen donor) than in $F1_{TM}$-2n hybrid plants (Figure 2B: $\chi2 = 237.85$, $df = 4$, $p < 2.2e\text{-}16$). Consistent with strong triploid block in interploidy crosses, we discovered highly significant effects of pollen

donor ploidy on tetraploid hybrid seed viability in *M. tilingii-M. caespitosa* comparisons (Figure 2C: $\chi 2 = 350.68$, $df = 4$, $p < 2.2e\text{-}16$) and in *M. tilingii-M. minor* comparisons (Figure 2D: $\chi 2 = 907.97$, $df = 4$, $p < 2.2e\text{-}16$). In both cases, tetraploid F1 hybrids pollinated with pollen from diploid parents produced almost exclusively inviable triploid seeds (Figure 2C-D), which, if subject to lower maternal investment than viable seeds, might explain why they were also produced in higher numbers (Figure 2A-B). Despite this additional complexity due to triploid block, our results show that genome doubling produces a consistent increase in F1 hybrid seed production, providing strong evidence for chromosomal rearrangements as a direct cause of hybrid female sterility between species in the *M. tilingii* complex.

DISCUSSION

In this study, we add to a growing body of evidence that chromosomal rearrangements can play a direct role in hybrid sterility, suggesting that the field's dismissal of chromosomal rearrangements as a major driver in species barriers was potentially premature. While it is clear how hybrid incompatible alleles rise in frequency via drift or selection and evade an adaptive valley (Dobzhansky 1937, Muller 1942), chromosomal rearrangements present a conundrum for speciation via natural selection. Below, we discuss the potential for strong underdominant rearrangements to evolve and contribute to F1 hybrid sterility between species in the *M. tilingii* complex.

Given the clear challenges to fix strong underdominant chromosomal rearrangements in natural populations, how might they evolve within the *M. tilingii* species complex? Underdominant rearrangements can spread within a population if they reach intermediate

frequencies (Futuyma and Mayer 1980), which might be possible when the population size is small and genetic drift is strong ($N_e < 50$; Walsh 1982). A new underdominant rearrangement might also spread if it has a large homozygous advantage or participates in meiotic drive (White 1978). Under a meiotic drive scenario, chromosomal rearrangements that include or are linked to meiotic drivers will have a >50% chance of being transmitted into any given gamete (Sandler and Novitski 1957); however, this scenario appears to occur infrequently (Coyne 1989).

Alternative models have proposed that chromosomal rearrangements do not need to rely on strong genetic drift or meiotic drive to spread within a population (Rieseberg 2001; Noor et al. 2001; Kirkpatrick and Barton 2006). In the presence of gene flow, the cost of underdominant rearrangements can be outweighed by the selective advantage of suppressed recombination if crossovers within a rearranged region break up favorable allelic combinations (Kirkpatrick and Barton 2006). While this local adaptation model is consistent with the common observation in plants that locally adaptive or life-history traits genetically map to chromosomal inversions (Lowry and Willis 2010; Fang et al. 2012; Oneal et al 2014; Lee et al. 2017; Coughlan and Willis 2019), many of these studies do not show a direct loss in fitness. Instead, such inversions probably suppress recombination via mechanical pairing problems and not by a loss of unbalanced gametes (Searle 1993; reviewed in Huang and Rieseberg 2020).

This local adaptation model might explain, in part, the evolution of underdominant rearrangements in some taxa. For instance, in *Mimulus*, *M. lewisii* and *M. cardinalis* strongly differ in their ecogeographic distributions and are specialized to different pollinators (Ramsey and Schemske 2003). In addition to their ecological differences, lab-generated F1 hybrids are largely sterile, and F1 hybrid male sterility has been genetically mapped to two large-effect

reciprocal translocations that suppress recombination (Stathos and Fishman 2014). Considering hybridization is possible, but rare, in natural populations (Ramsey and Schemske 2003), and a closely related selfer does not have any unique chromosomal rearrangements (*M. parishii*; Fishman et al. 2013), it is difficult to explain underdominance in this system by drift alone. Indeed, Stathos and Fishman (2014) speculate that a combination of selection for suppressed recombination during periods of gene flow and genetic drift likely contributed to the evolution of these underdominant reciprocal translocations. Because members of the *M. tilingii* complex are currently allopatric and grow exclusively at high elevations, it is tempting to rule out the possibility that chromosomal rearrangements evolved due to suppressed recombination between locally adapted loci. However, current distributions are unlikely to reflect their geographic ranges over evolutionary time. It is possible that during the Pleistocene glaciation, incipient species in the *M. tilingii* complex experienced some degree of gene flow, which facilitated the evolution of underdominant chromosomal rearrangements holding together locally adaptive loci.

Although chromosomal rearrangements contribute to both male and female sterility between species in the *M. tilingii* complex, dominant genetic incompatibilities might still be involved. Whereas pollen viability in $F1_{TC}$-4n hybrids was nearly completely restored, $F1_{TM}$-4n hybrids continued to show partial sterility (pollen viability = 69%). It is also important to note that our measure of female fertility, which relied on seed counts instead of estimates of ovule viability, was somewhat indirect. Consequently, it is unclear whether lower seed counts in tetraploid hybrids relative to pure species is due to genic female sterility or to post-mating, prezygotic barriers, such as pollen-pistil incompatibilities. In addition, when assessing female

fertility, we observed a classic trade-off in seed number and seed size (Smith and Fretwell 1974). Interploidy crosses that develop shriveled, underdeveloped triploid seeds (*i.e*, $F1_{TC}$-4n, $F1_{TM}$-4n hybrid plants x 2n pollen donor) produced a greater number of seeds than intraploidy crosses, which produced fewer seeds that are viable and fully-developed (*i.e.*, $F1_{TC}$-4n, $F1_{TM}$-4n hybrid plants x 4n pollen donor). Even with these potential caveats in our measurements and modest contributions from genetic incompatibilities, our results are nevertheless unequivocal in implicating chromosomal rearrangements as a major contributor to hybrid sterility between *M. tillingi* species.

Because the maximum fitness loss resulting from a single rearrangement is typically 50% (White 1973), the fact that we see >65% rescue in pollen viability for both F1-2n hybrid classes suggests the involvement of more than one underdominant chromosomal rearrangement. Additionally, our study did not address whether chromosomal rearrangements might also explain the severe F1 hybrid sterility we have observed in a third species pair in this group: *M. caespitosa* and *M. minor* (Sandstedt et al. 2021). The results here set the stage for future comparative mapping experiments to determine the number, type (inversion versus translocation), and evolutionary origin of rearrangements in this species group. What is clear is that chromosomal rearrangements currently cause strong postzygotic isolation – through both male and female functions – between species of the *M. tilingii* complex, even if the evolutionary mechanisms leading to the initial fixation of such strong barriers remain mysterious.

REFERENCES

Abbott, R., Albach, D., Ansell, S., Arntzen, J.W., Baird, S.J., Bierne, N., Boughman, J., Brelsford, A., Buerkle, C.A., Buggs, R. & Butlin, R.K., 2013. Hybridization and speciation. *Journal of evolutionary biology*, *26*(2), 229-246.

Arnold, M.L., 2004. Transfer and origin of adaptations through natural hybridization: were Anderson and Stebbins right?. *The Plant Cell*, *16*(3), 562-570.

Auger, D.L. & Sheridan, W.F. 2012. Plant chromosomal deletions, insertions, and rearrangements. In *Plant cytogenetics* (pp. 3-36). Springer, New York, NY.

Bates, D., Sarkar, D., Bates, M. D., & Matrix, L. 2007. The lme4 package. *R package version*, *2*(1), 74.

Blackman, B.K. 2016. Speciation genes. *Encyclopedia of Evolutionary Biology*, *4*, 66-175.

Coyne, J.A. 1989. A test of the role of meiotic drive in fixing a pericentric inversion. *Genetics*, *123*(1), 241.

Coughlan, J.M., & Willis, J.H., 2019. Dissecting the role of a large chromosomal inversion in life history divergence throughout the Mimulus guttatus species complex. *Molecular ecology*, *28*(6), 1343-1357.

Darwin, C. R. 1859. The Origin of species. 6th ed. John Murray, London.

Dobzhansky, T. 1933. On the sterility of the interracial hybrids in Drosophila pseudoobscura. *Proceedings of the National Academy of Sciences of the United States of America*, *19*(4), 397.

Dobzhansky, T. 1937. Genetic nature of species differences. *The American Naturalist*, *71*(735), 404-420.

Fang, Z., Pyhäjärvi, T., Weber, A.L., Dawe, R.K., Glaubitz, J.C., González, J.D.J.S., Ross-Ibarra, C., Doebley, J., Morrell, P.L. & Ross-Ibarra, J. 2012. Megabase-scale inversion polymorphism in the wild ancestor of maize. *Genetics*, *191*(3), 883-894.

Fishman, L., Stathos, A., Beardsley, P.M., Williams, C.F., & Hill, J.P. 2013. Chromosomal rearrangements and the genetics of reproductive barriers in Mimulus (monkey flowers). *Evolution*, *67*(9), 2547-2560.

Fishman, L. & Sweigart, A.L. 2018. When two rights make a wrong: the evolutionary genetics of plant hybrid incompatibilities. *Annual review of plant biology*, *69*, 707-731.

Fox, J., Weisberg, S., Adler, D., Bates, D., Baud-Bovy, G., Ellison, S., Firth, D., Friendly, M., Gorjanc, G., Graves, S. & Heiberger, R. 2012. Package 'car'. *Vienna: R Foundation for Statistical Computing*

Futuyma, D.J. & Mayer, G.C. 1980. Non-allopatric speciation in animals. *Systematic Biology*, *29*(3), 254-271.

Hedrick, P.W. 1981. The establishment of chromosomal variants. *Evolution*, 322-332.

Hoffmann, A.A. & Rieseberg, L.H. 2008. Revisiting the impact of inversions in evolution: from population genetic markers to drivers of adaptive shifts and speciation?. *Annual review of ecology, evolution, and systematics*, *39*, 21-42.

Huang, K. & Rieseberg, L.H. 2020. Frequency, origins, and evolutionary role of chromosomal inversions in plants. *Frontiers in plant science*, *11*, 296.

Kirkpatrick, M. & Barton, N. 2006. Chromosome inversions, local adaptation and speciation. *Genetics*, *173*(1), 419-434.

Kirkpatrick, M. 2010. How and why chromosome inversions evolve. *PLoS biology*, *8*(9), e1000501.

Lai, Z., Nakazato, T., Salmaso, M., Burke, J.M., Tang, S., Knapp, S.J. and Rieseberg, L.H. 2005. Extensive chromosomal repatterning and the evolution of sterility barriers in hybrid sunflower species. *Genetics*, *171*(1), 291-303.

Lee, C.R., Wang, B., Mojica, J.P., Mandáková, T., Prasad, K.V., Goicoechea, J.L., Perera, N., Hellsten, U., Hundley, H.N., Johnson, J, & Grimwood, J. 2017. Young inversion with multiple linked QTLs under selection in a hybrid zone. *Nature ecology & evolution*, *1*(5), 1-13.

Lenth, R., & Lenth, M. R. 2018. Package 'lsmeans'. *The American Statistician*, *34*(4), 216-221.

Lowry, D.B. & Willis, J.H. 2010. A widespread chromosomal inversion polymorphism contributes to a major life-history transition, local adaptation, and reproductive isolation. *PLoS biology*, *8*(9), e1000500.

Muller H. J. 1942. Isolating mechanisms, evolution, and temperature. Biological Symposium 6: 71–125.

Navarro, A. & Ruiz, A. 1997. On the fertility effects of pericentric inversions. *Genetics*, *147*(2), 931.

Nesom, G. L. 2012. Taxonomy of *Erythranthe* sect. Simiola (Phrymaceae) in the USA and Mexico. *Phytoneuron*, *40*, 1-123.

Noor, M.A., Grams, K.L., Bertucci, L.A. & Reiland, J. 2001. Chromosomal inversions and the reproductive isolation of species. *Proceedings of the National Academy of Sciences*, *98*(21), 12084-12088.

Oneal, E., Lowry, D.B., Wright, K.M., Zhu, Z., & Willis, J.H., 2014. Divergent population structure and climate associations of a chromosomal inversion polymorphism across the *Mimulus guttatus* species complex. *Molecular ecology*, *23*(11), pp.2844-2860.

Ramsey, J., Bradshaw Jr, H.D. & Schemske, D.W. 2003. Components of reproductive isolation between the monkeyflowers Mimulus lewisii and M. cardinalis (Phrymaceae). *Evolution*, *57*(7), 1520-1534.

Rieseberg, L.H. & Blackman, B.K. 2010. Speciation genes in plants. *Annals of botany*, *106*(3), pp.439-455.

Rieseberg, L. H. 2001. Chromosomal rearrangements and speciation. *Trends in ecology & evolution*, *16*(7), 351-358.

Sandler, L. & Novitski, E. 1957. Meiotic drive as an evolutionary force. *The American Naturalist*, *91*(857), 105-110.

Sandstedt, G.D., Wu, C.A. & Sweigart, A.L. 2021. Evolution of multiple postzygotic barriers between species of the *Mimulus tilingii* complex. *Evolution*, *75*(3), 600-613.

Searle, J.B. 1993. Chromosomal hybrid zones in eutherian mammals. *Hybrid zones and the evolutionary process*, 309-353.

Smith, C.C. & Fretwell, S.D. 1974. The optimal balance between size and number of offspring. *The American Naturalist*, *108*(962), 499-506.

Stathos, A. & Fishman, L. 2014. Chromosomal rearrangements directly cause underdominant F1 pollen sterility in Mimulus lewisii–Mimulus cardinalis hybrids. *Evolution*, *68*(11), 3109-3119.

Stebbins, G.L., 1950. Variation and evolution in plants. In *Variation and evolution in plants*. Columbia University Press.

Strasburg, J.L., Kane, N.C., Raduski, A.R., Bonin, A., Michelmore, R. & Rieseberg, L.H. 2011. Effective population size is positively correlated with levels of adaptive divergence among annual sunflowers. *Molecular biology and evolution*, *28*(5), 1569-1580.

Walsh, J.B. 1982. Rate of accumulation of reproductive isolation by chromosome rearrangements. *The American Naturalist*, *120*(4), 510-532.

White, M.J.D. 1973. *Animal cytology & evolution*. Cambridge university press.

White, M.J.D. 1978. Chain processes in chromosomal speciation. *Systematic zoology*, *27*(3), 285-298.

Table 4.1. 2C DNA content of each genotype class (pure species: C = *M. caespitosa*, M = *M. minor*, T = *M. tilingii*; diploid F1 hybrids: $F1_{TC}$ -2n, $F1_{TM}$-2n; tetraploid F1 hybrids: $F1_{TC}$ -4n, $F1_{TM}$-4n).

genotype class	line(s)	genome size mean (pg) ± SE	*N*
C	TWN36	1.31 ± 0.04	3
T	LVR1	1.17 ± 0.05	3
M	NOR523	1.1 ± 0.04	3
$F1_{TC}$-2n	LVR1 x TWN36	1.24 ± 0.05	3
$F1_{TC}$-4n	LVR1 x TWN36	2.46 ± 0.06	10
$F1_{TM}$-2n	LVR1 x NOR523	1.14 ± 0.01	3
$F1_{TM}$-2n	LVR1 x NOR523	2.32 ± 0.08	10

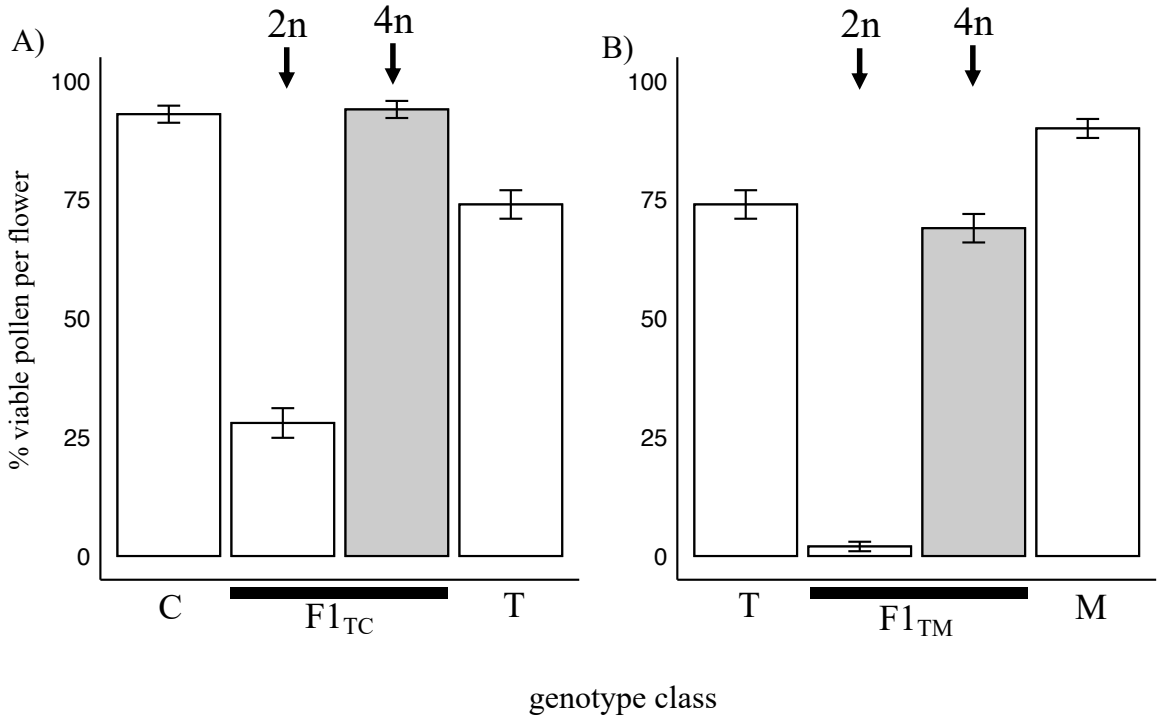

Figure 4.1. Pollen fertility among genotype classes in the *M. tilingii* complex (pure species: C = *M. caespitosa*, M = *M. minor*, T = *M. tilingii*; diploid F1 hybrids: $F1_{TC}$ -2n, $F1_{TM}$-2n; tetraploid F1 hybrids: $F1_{TC}$ -4n, $F1_{TM}$-4n). Bars are shaded white or gray corresponding to 2n and 4n genotype classes, respectively. Additionally, arrows denote bars that represent 2n or 4n F1 hybrids. Error bars correspond to +/- standard error. Differences in least squares means (lsmeans) among classes were determined using a post-hoc Tukey method. We report statistically different groups ($p<0.05$) with letters that correspond to each box, left to right in each description. A) Lsmeans pollen fertility in C, T pure species, and $F1_{TC}$-2n and $F1_{TC}$-4n F1 hybrid plants. Group: c, a, c, b. B) Lsmeans pollen fertility in T, M pure species, and $F1_{TM}$-2n and $F1_{TM}$-4n F1 hybrid plants. Group: b, a, b, c.

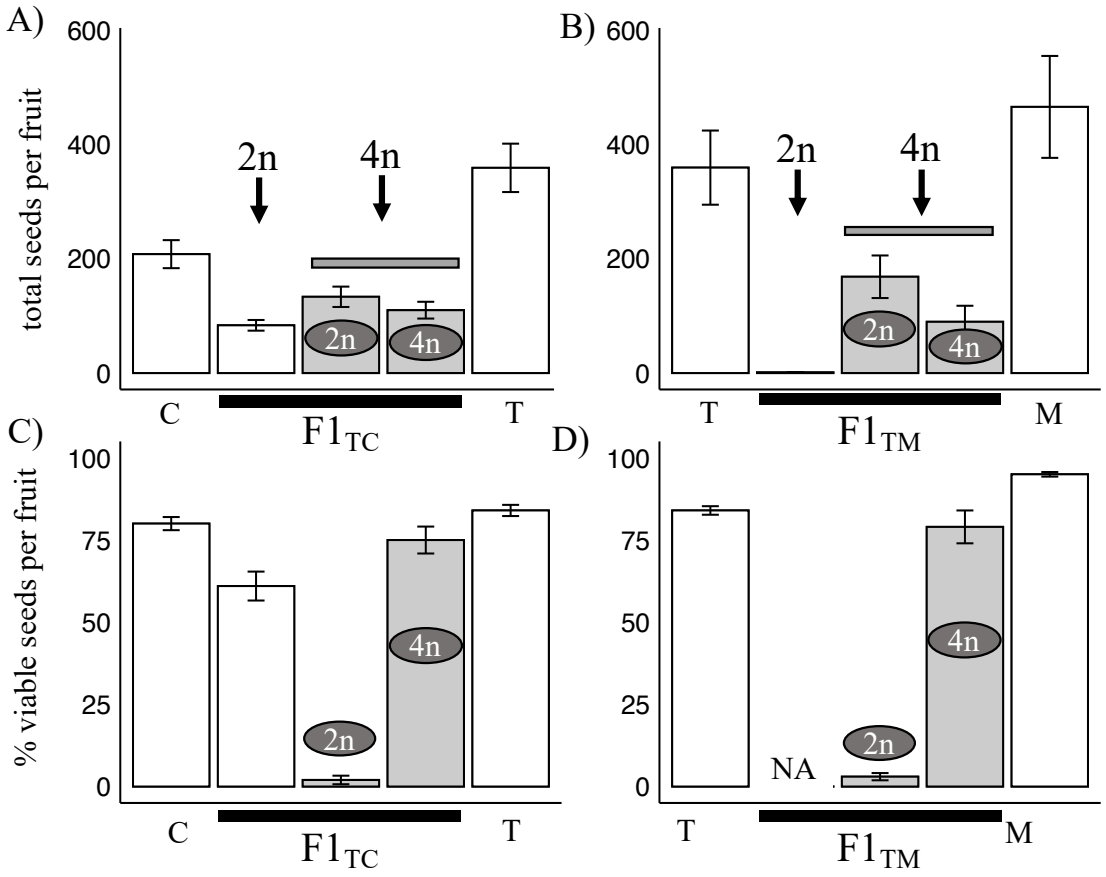

Figure 4.2. Female fertility among genotype classes in the *M. tilingii* complex (pure species: C = *M. caespitosa*, M = *M. minor*, T = *M. tilingii*; diploid F1 hybrids: $F1_{TC}$ -2n, $F1_{TM}$-2n; tetraploid F1 hybrids: $F1_{TC}$ -4n, $F1_{TM}$-4n). Bars are shaded white or gray corresponding to 2n and 4n genotype classes, respectively. Additionally, arrows denote bars that represent 4n F1 hybrids. Circles within bars label the ploidy of the pollen donor with either 2n or 4n for a F1-4n class. Error bars correspond to +/- standard error. Differences in least squares means (lsmeans) among classes were determined using a post-hoc Tukey method. We report statistically different groups ($p<0.05$) with letters that correspond to each box, left to right in each description. A) Lsmeans seed count per fruit for C, T pure species, and $F1_{TC}$-2n and $F1_{TC}$-4n F1 hybrid plants. Group: b, a, a, ab, c. B) Lsmeans seed count per fruit for T, M pure species, and $F1_{TM}$-2n and $F1_{TM}$-4n F1 hybrid plants. Group: bc, a, b, bc, c. C) Lsmeans viable seeds per fruit corresponding to fruits in A. Group: c, b, a, bc, c. D) Lsmeans viable seeds per fruit corresponding to fruits in B. Group: b, NA, a, b, c.

CHAPTER V

CONCLUSION AND FUTURE DIRECTIONS

Although it has been argued that postzygotic barriers are not as important for plant species divergence as prezygotic barriers (Lowry et al. 2008), this dissertation provides empirical support that postzygotic barriers can, indeed, be quite strong and evolve rapidly between closely related species. Additionally, this work adds to the growing body of work showing how investigating the developmental and genetic mechanisms underlying individual reproductive barriers can provide insight into the potential evolutionary drivers of species divergence. We discuss below the findings of each chapter and follow-up investigations that may further illuminate the speciation process in the *Mimulus tilingii* complex.

In Chapter II, we investigated patterns of morphological and genetic variation and reproductive isolation among three species in the *M. tilingii* complex: *M. caespitosa, M. minor,* and *M. tilingii*. We determined that these three species were, indeed, morphologically and genetically distinct. Although species within the *M. tilingii* complex split within the last 400ky, reproductive isolation is nearly complete between any two species in this complex by several postzygotic barriers, including: hybrid seed inviability, F1 hybrid necrosis, F1 hybrid male and female sterility. We predict that because species in the *M. tilingii* complex are largely allopatric and restricted to high elevations, alleles that are incompatible in hybrids might have readily evolved without the removal by selection in areas of geographic overlap. Although we cannot

rule out the possibility of premating barriers, which might be likely given that these species occupy geographically distinct alpine regions, postzygotic barriers appear important for species divergence in this complex. Future work will need to elucidate whether premating barriers, such as habitat isolation, flowering time differences, or pollinator isolation contribute to reproductive isolation in this system. To fully assess the importance of pre- vs postzygotic barriers in this system, a powerful approach would be to quantify the strength of reproductive barriers across life-history in areas of sympatry and allopatry. However, because it is not yet known whether species co-occur, efforts must be made to identify and sample additional natural populations. Determining whether *M. tilingii* species geographically overlap and characterizing the strength of unmeasured premating barriers will be a key step toward understanding the relative importance of postzygotic barriers among these species. To understand how and why strong intrinsic barriers may have evolved between species in the *M. tilingii* complex, we took a closer look at individual barriers in Chapters III and IV.

In Chapter III, we characterized the developmental basis of hybrid seed inviability between diploid species in the *M. tilingii* complex, as well as a more distantly related species, *M. guttatus*. In this study, we described seed phenotypes during development that were disrupted in crosses between species with different histories of parental conflict (as measured by endosperm balance number). A major insight of this study is that, early in seed development, a specific region within the endosperm that likely funnels nutrients from the ovule to the endosperm (*i.e.*, chalazal haustorium) was strongly deregulated in all paternal excess crosses (*i.e.*, paternal parent has greater degree of conflict). We predicted that parental conflict potentially targets this region in the endosperm within species and drives differences in gene expression between species,

causing deregulated nutrient allocation in F1 hybrids. Further investigations will need to determine how gene expression might have diverged in tissues responsible for nutrient acquisition between species, which might reveal genes that are potential targets of parental conflict. In particular, we hope to characterize patterns of imprinted gene expression and determine whether paternally-expressed imprinted genes are specifically deregulated in the chalazal haustoria of hybrid seeds.

Furthermore, in Chapter IV, we investigated whether chromosomal rearrangements or genic incompatibilities explained severe F1 hybrid sterility between species in the *M. tilingii* complex. We utilized a classic approach to determine whether doubling the genome of F1 hybrids restores sterility. If underdominant chromosomal rearrangements underlie this sterility barrier, doubling the genome should restore fertility by providing divergent homologues with a collinear partner. Indeed, this approach increased F1 hybrid male and female fertility between two species pairs in the *M. tilingii* species complex, with pollen fertility almost completely rescued. Although this experiment provided unequivocal evidence that underdominant chromosomal rearrangements contribute to hybrid sterility in this group, additional work will be needed to investigate how many and what types of rearrangements distinguish the three species. In addition, how underdominant chromosomal rearrangements evolved in this or any other system is not yet understood, though it remains a large question in speciation genetics.

As a whole together, this dissertation highlights the immense value of investigating the genetics of reproductive isolation among diverse taxa at different stages of divergence to address the long-standing question of how and why new species evolve.

REFERENCES

Lowry, D. B., Rockwood, R. C., & Willis, J. H. 2008. Ecological reproductive isolation of coast and inland races of *Mimulus guttatus*. *Evolution: International Journal of Organic Evolution*, *62*(9), 2196-2214.

Table S2.1. Description of all samples within the *Mimulus tilingii* species complex analyzed in this study.

		Population location										
Species	**Population Code**	**Elevation (m)**	**State**	**(LAT, LONG)**	**Maternal Family**	**Generations inbred**	**# plants/maternal family[‡]**	**Crossing barriers tested?**	**Million Paired-End Reads**	**% Heterozygosity[§]**	**% Coverage @ 14k Sites**	**SRA**
M. caespitosa	GAB	2350	WA	(46.88297, -121.72335)	GAB1	1	5	X	11.1	0.97	55.09	SRR12424423
					GAB2	1	2		14.7	1.17	85.45	SRR12424422
M. caespitosa	KCK	1090	WA	(46.84036, -121.56115)	KCK1	1	5	X	17.2	1.39	89.59	SRR12424416
M. caespitosa	PAG	1880	WA	(46.79924, -121.71255)	PAG1	1	3	X	not sequenced	NA	NA	NA
					PAG2	1	5	X	12.8	1.08	75.89	SRR12424413
M. caespitosa	TWN	1594	WA	(48.57026, -121.38164)	TWN36	7	5	X	15.6	0.64	85.12	SRR12424421
M. caespitosa	UTC	1025	WA	(46.8004, -121.87111)	UTC1	1	5	X	12.7	1.01	71.91	SRR12424419
					UTC2	1	5	X	12.1	0.79	73.45	SRR12424418
M. minor	NOR	3349	CO	(39.015033, -107.045033)	NOR511	3	2	X	16.2	0.63	93.72	SRR12424415
					NOR523	4	5	X	15.5	0.63	90.75	SRR12424414
M. minor	UNP	3728	CO	(39.019639, -107.096053)	UNP12	2	1		14.9	2	86.01	SRR12424420
M. tilingii	A25	2343[†]	OR	(42.6364, -118.5767)	A25	0	0		9.2	1.33	NA	SRX6914883[¶]
M. tilingii	ICE	2369	OR	(45.13553, -117.16067)	ICE10	6	3	X	12.5	0.86	74.77	SRR12424417
M. tilingii	LVR	2751	CA	(37.57049, -119.13544)	LVR1	8	5	X	54.2	0.82	99.79	SRX1532174[¶]
M. tilingii	SAB	2778	CA	(37.12720, -118.36627)	SAB1	6	5	X	14	0.73	72.28	SRR12424411
					SAB19	5	5		11.6	0.91	83.52	SRR12424412
M. tilingii	SOP	1025	CA	(38.266753, -119.617981)	SOP12	6	5	X	13.7	0.72	84.54	SRR12424410

[†]Elevation estimated from https://www.mapcoordinates.net/en
[‡]Number of individuals measured for floral and vegetative traits.
[§]Values from this column are estimated from fourfold degenerate synonymous sites
[¶]SRAs obtained from previously generated sequence data

Table S2.2. Lsmeans and standard error (SE) for 16 morphological traits of *M. tilingii* subgroups

Trait	Subgroups						Data transformation for LDA
	M. caespitosa		*M. minor*		*M. tilingii*		
	Lsmeans	SE	Lsmeans	SE	Lsmeans	SE	
Trichomes	24.05	0.94	1.9	0.49	344.68	3.34	Normal-Quantile
Petiole Length (mm)	3.48	0.38	6.74	1.56	3.08	0.42	Log
Leaf Length (mm)	18.05	0.79	22.91	2.09	31.02	1.68	Cube-Root
Leaf Width (mm)	12.16	0.54	14.14	1.32	17.57	0.97	None
Corolla Height (mm)	19.02	0.52	12.39	0.71	18.58	0.63	None
Corolla Width (mm)	16.41	0.45	14.76	0.85	21.14	0.72	None
Tube Length (mm)	14.6	0.55	12.95	1.01	16.65	0.77	None
Tube Width (mm)	10.14	0.29	10	0.6	11.74	0.42	None
Pistil Length (mm)	16.72	0.36	14.25	0.64	19.83	0.53	None
Stamen Length (mm)	13.63	0.31	13.23	0.62	15.58	0.43	None
Pedicel Length (mm)	17.52	0.91	9.37	1.01	21.51	1.37	None
Capsule Length (mm)	4.35	0.11	4.54	0.25	5.41	0.17	None
Calyx Length (mm)	10.68	0.3	11.98	0.7	13	0.45	Log
Calyx Nodding (°)	134.82	2	105.73	3.52	144.76	2.66	Square-Root
Number of Stolons	3.83	0.33	1.38	0.41	3.3	0.38	None
Stolon Length (mm)	22.93	1.72	7.05	1.28	13.85	1.28	Square-Root

Note: We fit a GLM with a gamma distribution (except trichomes and stolon branches, which used a Poisson distribution), where the trait measurements were the response variable and *M. tilingii* species was the predictor variable. We used the emmeans command in R to calculate lsmeans for the model.

Table S2.3. Description of *Mimulus* maternal lines obtained from Brandvain *et al.* 2014

Species	Population Code	Million Paired-End Reads	% heterozygosity	% Coverage @ 14k sites	SRA
M. dentilobus	DENT	12.1	0.53	65.25	SRX030541
M. guttatus	AHQT1	34.9	0.73	98.83	SRX142379
M. guttatus	CACG6	70.2	0.88	99.62	SRX525044
M. guttatus	MED82	44.8	0.92	99.5	SRA166889
M. guttatus	SLP	41.9	0.89	99.39	SRX142377
M. nasutus	CACN9	46.6	0.6	99.6	SRX525048
M. nasutus	NHN	46.1	0.61	99.39	SRX525051

Table S2.4. Comparisons of crosses performed within maternal lines and between maternal lines of the same species.

Barrier	Species	Type	Lsmean	SE	Estimate	SE	Z-ratio	P-value
Seed Set	*M. caespitosa*	between-lines	171.2	13.39	-6.93E-04	1.28E-03	-0.54	0.59
		within-lines	153.06	28.08				
	M. minor	between-lines	337.5	119.11	-1.63E-04	1.26E-03	-0.13	0.9
		within-lines	319.8	71.38				
	M. tilingii	between-lines	165.22	18.78	9.70E-04	9.92E-04	0.98	0.33
		within-lines	196.73	27.7				
Morphological Seed Viability	*M. caespitosa*	between-lines	0.94	0.01	1.77	0.13	7.66	<0.001
		within-lines	0.9	0.02				
	M. minor	between-lines	0.93	0.03	0.96	0.2	-0.22	0.82
		within-lines	0.93	0.03				
	M. tilingii	between-lines	0.91	0.02	1.5	0.13	4.8	<0.001
		within-lines	0.87	0.02				
Germination Success	*M. caespitosa*	between-lines	0.56	0.07	1.47	0.1	6	<0.001
		within-lines	0.46	0.07				
	M. minor	between-lines	0.68	0.06	19.36	5.85	9.8	<0.001
		within-lines	0.1	0.02				
	M. tilingii	between-lines	0.63	0.13	0.94	0.14	-0.39	0.7
		within-lines	0.64	0.13				
F1 Seed Set	*M. caespitosa*	between-lines	214.96	1.89	6.48E-05	7.96E-04	0.081	0.94
		within-lines	218	3.58				
	M. minor	between-lines	511.5	67.37	-1.40E-03	5.57E-04	-2.512	0.01
		within-lines	298.13	43.9				
	M. tilingii	between-lines	234.28	2.95	-8.71E-04	1.34E-03	-0.648	0.52
		within-lines	194.57	5.27				
F1 Pollen Viability	*M. caespitosa*	between-lines	0.96	0.02	4.06	0.49	11.55	<0.001
		within-lines	0.87	0.07				
	M. minor	between-lines	0.95	0.01	1.38	0.23	1.94	0.053
		within-lines	0.93	0.01				
	M. tilingii	between-lines	0.73	0.06	0.38	0.02	-17.54	<0.001
		within-lines	0.88	0.03				

Table S2.5. Crosses performed within and between populations and species of the *Mimulus tilingii* complex.

Unique Crosses[†]	Number of fruits per cross[‡]	Number of fruits assayed for seed germination[§]
CxC	**116**	**54**
GAB1xGAB1	2	2
GAB1xKCK1	3	1
GAB1xPAG1	2	
GAB1xTWN36	2	
GAB1xUTC1	3	1
GAB1xUTC2	2	2
KCK1xGAB1	1	1
KCK1xKCK1	4	2
KCK1xPAG1	1	
KCK1xPAG2	3	2
KCK1xTWN36	5	2
KCK1xUTC1	2	1
KCK1xUTC2	1	1
PAG1xKCK1	1	1
PAG1xPAG1	1	
PAG1xTWN36	1	
PAG1xUTC2	1	1
PAG2xKCK1	4	1
PAG2xPAG1	3	1
PAG2xPAG2	2	2
PAG2xTWN36	5	1
PAG2xUTC1	6	2
PAG2xUTC2	2	
TWN36xGAB1	2	1
TWN36xKCK1	3	1
TWN36xPAG1	2	1
TWN36xPAG2	3	1
TWN36xTWN36	5	2
TWN36xUTC1	4	2
TWN36xUTC2	4	1
UTC1xGAB1	2	1
UTC1xKCK1	4	1
UTC1xPAG1	1	
UTC1xPAG2	1	1
UTC1xTWN36	2	2
UTC1xUTC1	4	2
UTC1xUTC2	2	2
UTC2xGAB1	3	3
UTC2xKCK1	3	1
UTC2xPAG1	1	
UTC2xPAG2	4	2
UTC2xTWN36	3	2
UTC2xUTC1	3	2
UTC2xUTC2	3	2

CxM	**22**	**13**
GAB1xNOR511	1	1
KCK1xNOR511	1	
PAG1xNOR511	2	1
PAG2xNOR511	3	1
PAG2xNOR523	1	1
TWN36xNOR511	3	2
TWN36xNOR523	3	2
UTC1xNOR511	2	
UTC2xNOR511	4	3
UTC2xNOR523	2	2
MxC	**25**	**13**
NOR511xGAB1	1	
NOR511xKCK1	3	3
NOR511xPAG1	2	1
NOR511xPAG2	2	
NOR511xTWN36	1	
NOR511xUTC1	2	1
NOR511xUTC2	4	
NOR523xGAB1	2	2
NOR523xKCK1	2	2
NOR523xTWN36	2	2
NOR523xUTC1	2	2
NOR523xUTC2	2	
MxM	**7**	**3**
NOR511xNOR511	2	1
NOR511xNOR523	1	
NOR523xNOR511	1	1
NOR523xNOR523	3	1
MxT	**14**	**9**
NOR511xICE10	3	1
NOR511xLVR	1	1
NOR511xSAB	1	
NOR511xSOP12	1	1
NOR523xICE10	2	1
NOR523xLVR	2	2
NOR523xSAB	2	2
NOR523xSOP12	2	1
TxM	**14**	**11**
ICE10xNOR511	3	3
ICE10xNOR523	1	1
LVRxNOR511	3	1
LVRxNOR523	2	2
SABxNOR511	2	2
SOP12xNOR511	2	1
SOP12xNOR523	1	1

TxT	37	19
ICE10xICE10	4	2
ICE10xLVR	3	2
ICE10xSOP12	3	3
LVRxLVR	5	3
LVRxSAB	3	
LVRxSOP12	1	
SABxICE10	4	3
SABxLVR	2	
SABxSAB	2	2
SABxSOP12	2	
SOP12xICE10	2	1
SOP12xLVR	2	1
SOP12xSAB	1	
SOP12xSOP12	3	1
TxC	**75**	**40**
ICE10xGAB1	1	1
ICE10xKCK1	3	3
ICE10xPAG1	2	2
ICE10xPAG2	2	2
ICE10xTWN36	3	1
ICE10xUTC1	3	2
ICE10xUTC2	2	2
LVRxGAB1	1	
LVRxKCK1	1	
LVRxTWN36	7	2
LVRxUTC1	1	1
LVRxUTC2	2	4
SABxGAB1	2	1
SABxKCK1	3	1
SABxPAG2	8	3
SABxTWN36	2	
SABxUTC1	4	4
SABxUTC2	2	1
SOP12xGAB1	3	2
SOP12xKCK1	5	1
SOP12xPAG1	5	4
SOP12xPAG2	1	
SOP12xTWN36	5	
SOP12xUTC1	5	2
SOP12xUTC2	2	1

CxT	60	47
GAB1xICE10	2	1
GAB1xLVR	1	1
GAB1xSAB	2	1
GAB1xSOP12	1	1
KCK1xICE10	3	3
KCK1xLVR	2	2
KCK1xSAB	3	3
KCK1xSOP12	2	2
PAG1xICE10	1	1
PAG2xICE10	2	1
PAG2xLVR	1	1
PAG2xSOP12	4	4
TWN36xICE10	3	1
TWN36xLVR	4	2
TWN36xSAB	2	
TWN36xSOP12	3	1
UTC1xICE10	3	3
UTC1xLVR	2	2
UTC1xSAB	2	1
UTC1xSOP12	3	3
UTC2xICE10	4	4
UTC2xLVR	4	4
UTC2xSAB	3	2
UTC2xSOP12	3	3

[†]Unique cross combinations of maternal families, female parent listed first.
[‡]Numbers of fruits listed in this column were used to assess postmating, prezygotic isolation and hybrid seed inviability.
[§]Numbers of fruits listed in this column were used to assess seed germination rates.

Table S2.6. Assessment of hybrid inviability and hybrid sterility between species of the *Mimulus tilingii* complex.

Unique Crosses	No. F1 seedlings tansplanted per cross	No. F1s that flowered	Proportion flowering progeny	Proportion necrotic progeny	Average days to flower (from seedling)	Individuals with pollen viability measured†	No. F1 individuals used for backcross	Pollen donor	Total F1 crosses
CxC	**199**	**199**	**1**	**0**	**49.56**	**136**	**76**		**95**
GAB1xGAB1	15	15	1	0	50.13	10	2	GAB1	3
KCK1xKCK1	10	10	1	0	49.7	7	3	KCK1	3
KCK1xPAG2	16	16	1	0	42.75	11	9	PAG2	10
KCK1xUTC1	8	8	1	0	57	4	3	KCK1	4
PAG1xTWN36	10	10	1	0	51.4	7	4	TWN36	5
PAG2xPAG2	4	4	1	0	57.5	2	1	PAG2	2
PAG2xUTC1	15	15	1	0	54.53	7	7	UTC1	8
PAG1xUTC2	16	16	1	0	53.31	8	6	UTC2	8
UTC1xPAG2	10	10	1	0	42.5	8	4	UTC1	5
UTC1xUTC1	12	12	1	0	56.75	10	3	UTC1	4
UTC2xPAG2	11	11	1	0	38.27	8	5	PAG2	6
UTC2xUTC1	6	6	1	0	63.67	6	3	UTC2	5
UTC2xUTC2	11	11	1	0	49.45	8	5	UTC2	5
TWN36xPAG1	16	16	1	0	46.13	14	6	TWN36	8
TWN36xPAG2	12	12	1	0	50.8	11	5	PAG2	7
TWN36xTWN36	15	15	1	0	46.73	7	3	TWN36	4
TWN36xUTC1	12	12	1	0	31.9	17	7	UTC1	8
CxM	**57**	**57**	**1**	**0**	**36.23**	**38**	**22**		**27**
PAG1xNOR511	12	12	1	0	35.5	8	4	NOR511	5
PAG2xNOR511	15	15	1	0	36.13	8 (2)	5	PAG2	6
TWN36xNOR511	7	7	1	0	36.86	4	4	TWN36	5
UTC2xNOR511	13	13	1	0	35.54	9	4	UTC2	5
UTC2xNOR523	10	10	1	0	37.1	9	5	UTC2	6
MxC	**56**	**56**	**1**	**0**	**47.64**	**34**	**17**		**26**
NOR511xKCK1	16	16	1	0	46.63	13	6	NOR511/KCK1	11
NOR511xPAG1	16	16	1	0	47.81	10	3	NOR511/PAG1	5
NOR511xUTC1	9	9	1	0	58.33	4	4	UTC1	6
NOR523xGAB1	15	15	1	0	37.8	7 (1)	4	GAB1	4

MxM	**23**	**23**	**1**	**0**	**42.07**	**13**	**9**		**12**
NOR511xNOR511	11	11	1	0	47.64	7	4	NOR511	6
NOR523xNOR511	12	12	1	0	36.5	6	5	NOR511	6
TxM	**54**	**54**	**1**	**0**	**43.4**	**26**	**11**		**12**
ICE10xNOR511	13	13	1	0	45.31	7 (4)	3	ICE10	3
SAB1xNOR511	23	23	1	0	44.7	9	3	NOR511	4
SAB1xNOR523	3	3	1	0	42	3	3	SAB1	3
SOP12xNOR511	15	15	1	0	41.6	7	2	NOR511	2
TxT	**93**	**93**	**1**	**0**	**45.06**	**57**	**34**		**38**
ICE10xICE10	11	11	1	0	61.91	7	2	ICE10	2
ICE10xLVR1	10	10	1	0	36.2	8	7	LVR1	7
ICE10xSOP12	15	15	1	0	42.47	7	3	SOP12	4
LVR1xLVR1	16	16	1	0	51.5	7	2	LVR1	2
LVR1xSOP12	5	5	1	0	36	5	4	SOP12	5
SOP12xICE10	12	12	1	0	32.25	8	7	SOP12	9
SOP12xLVR1	11	11	1	0	45.18	6	6	SOP12	6
SOP12xSOP12	13	13	1	0	55	9	3	SOP12	3
TxC	**107**	**93**	**0.87**	**0.13**	**43.44**	**65**	**43**		**63**
ICE10xGAB1	16	8	0.5	0.5	49.13	7	2	ICE10	3
ICE10xKCK1	16	16	1	0	43	8	5	KCK1	6
ICE10xPAG2	13	13	1	0	49	7	4	PAG2	6
ICE10xTWN36	13	13	1	0	48.64	8	7	TWN36	10
ICE10xUTC1	11	5	0.45	0.55	52.2	4	5	UTC1	12
LVR1xUTC2	12	12	1	0	31.58	8	6	LVR1	6
SAB1xPAG2	8	8	1	0	38.88	8	4	PAG2	7
SAB1xUTC1	8	8	1	0	37.13	8	5	UTC1	6
SAB1xUTC2	10	10	1	0	41.4	7	5	UTC2	7
CxT	**60**	**44**	**0.73**	**0.27**	**51.38**	**29**	**19**		**24**
GAB1xICE10	8	6	0.75	0.25	44.67	6	3	GAB1	4
GAB1xLVR1	16	16	1	0	45.44	7 (2)	7	LVR1	8
KCK1xSAB1	11	11	1	0	67.09	5 (5)	4	KCK1	5
PAG2xSOP12	3	3	1	0	52.67	3	1	KCK1	2
TWN36xLVR1	1	1	1	0	56	1	--	--	--
UTC1xICE10	14	0	0	1	--	--	--	--	--
UTC2xLVR1	7	7	1	0	42.43	7	4	LVR1	5
Total	**649**	**619**	**--**	**--**	**--**	**399**	**231**	**--**	**297**

†In parentheses are the number of individuals with anthers that were either shriveled and/or produced no pollen

Table S2.7. Trait coefficients for each linear discriminant. Largest coefficient (positive or negative) indicate traits that contribute most to the discriminant function.

Trait	LD1	LD2	Total †
Trichomes	0.99	0.34	1.32
Petiole Length	-0.23	-0.35	0.58
Leaf Length	1.32	-0.59	1.91
Leaf Width	-0.17	0.56	0.73
Corolla Height	-0.83	0.49	1.32
Corolla Width	0.35	-0.43	0.78
Tube Length	-0.44	0.22	0.66
Tube Width	-0.11	-0.31	0.42
Pistil Length	0.01	1.63	1.64
Stamen Length	-0.03	-0.56	0.6
Pedicel Length	-0.47	0.34	0.81
Capsule Length	0.5	-0.74	1.24
Calyx Length	0.62	0.1	0.72
Calyx Nodding	0.65	1	1.65
Stolon Branches	0.13	0.49	0.63
Stolon Branch Length	-0.62	0.16	0.78

†Absolute value of LD1 and LD2

Table S2.8. LDA model prediction based on probability that individual belongs to a given class.

Maternal line	Individual	Proposed Species	Class Probability		
			M. t. caespitosa	*M. t. minor*	*M. t. tilingii*
GAB1	1	C	9.77E-01	7.76E-09	2.28E-02
GAB1	2	C	1.00E+00	2.21E-15	1.09E-07
GAB1	3	C	1.00E+00	7.29E-09	3.00E-06
GAB1	4	C	9.95E-01	2.40E-12	4.63E-03
GAB1	5	C	1.00E+00	2.15E-07	4.86E-05
GAB2	1	C	1.00E+00	1.45E-15	8.97E-09
GAB2	2	C	1.00E+00	3.31E-12	1.44E-07
KCK1	1	C	1.00E+00	2.56E-10	5.69E-08
KCK1	2	C	1.00E+00	4.50E-09	4.51E-06
KCK1	3	C	1.00E+00	1.60E-13	2.63E-08
KCK1	4	C	1.00E+00	1.80E-13	1.84E-09
KCK1	5	C	1.00E+00	8.49E-14	1.51E-06
PAG1	1	C	1.00E+00	1.14E-10	3.39E-08
PAG1	2	C	1.00E+00	9.98E-16	1.40E-06
PAG1	3	C	1.00E+00	6.35E-13	1.86E-11
PAG2	1	C	9.93E-01	5.27E-11	7.42E-03
PAG2	2	C	1.00E+00	3.49E-12	8.50E-10
PAG2	3	C	1.00E+00	1.12E-14	2.51E-07
PAG2	4	C	1.00E+00	8.67E-09	5.64E-09
PAG2	5	C	1.00E+00	3.84E-13	9.75E-08
TWN36	1	C	1.00E+00	2.14E-12	4.62E-06
TWN36	2	C	1.00E+00	2.68E-06	3.52E-04
TWN36	3	C	1.00E+00	3.12E-04	1.10E-05
TWN36	4	C	9.99E-01	2.68E-06	7.78E-04
TWN36	5	C	9.99E-01	2.65E-09	5.09E-04
UTC1	1	C	1.00E+00	5.84E-10	1.47E-11
UTC1	2	C	1.00E+00	9.74E-14	5.04E-14
UTC1	3	C	1.00E+00	6.33E-08	2.03E-09
UTC1	4	C	1.00E+00	6.84E-09	4.46E-09
UTC1	5	C	1.00E+00	7.64E-13	1.98E-08
UTC2	1	C	1.00E+00	1.41E-09	4.27E-08
UTC2	2	C	1.00E+00	7.15E-11	1.30E-08
UTC2	3	C	1.00E+00	1.10E-15	3.05E-08
UTC2	4	C	1.00E+00	3.45E-11	2.62E-10
UTC2	5	C	1.00E+00	1.11E-09	4.20E-07

NOR511	1	M	1.84E-10	1.00E+00	1.44E-14
NOR511	2	M	3.11E-11	1.00E+00	3.46E-13
NOR523	1	M	7.21E-12	1.00E+00	7.24E-14
NOR523	2	M	2.56E-11	1.00E+00	7.40E-11
NOR523	3	M	2.80E-05	1.00E+00	9.73E-06
NOR523	4	M	1.87E-08	1.00E+00	1.38E-05
NOR523	5	M	3.93E-11	1.00E+00	5.66E-11
UNP12	3	M	7.40E-09	1.00E+00	3.71E-11
ICE10	1	T	1.77E-06	4.22E-13	1.00E+00
ICE10	2	T	1.61E-04	2.09E-06	1.00E+00
ICE10	3	T	8.35E-04	7.76E-13	9.99E-01
LVR1	1	T	1.98E-06	2.67E-13	1.00E+00
LVR1	2	T	3.31E-02	1.99E-11	9.67E-01
LVR1	3	T	3.93E-08	1.76E-14	1.00E+00
LVR1	4	T	1.49E-10	5.86E-15	1.00E+00
LVR1	5	T	7.28E-07	4.95E-13	1.00E+00
SAB1	1	T	8.12E-11	2.52E-13	1.00E+00
SAB1	2	T	1.30E-08	2.75E-11	1.00E+00
SAB1	3	T	2.12E-08	7.46E-14	1.00E+00
SAB1	4	T	3.03E-07	5.31E-13	1.00E+00
SAB1	5	T	2.86E-08	2.38E-09	1.00E+00
SAB19	1	T	4.72E-06	3.34E-18	1.00E+00
SAB19	2	T	1.06E-09	1.04E-10	1.00E+00
SAB19	3	T	3.67E-06	7.76E-11	1.00E+00
SAB19	4	T	2.92E-07	2.58E-09	1.00E+00
SAB19	5	T	1.06E-04	2.38E-12	1.00E+00
SOP12	1	T	3.90E-08	4.97E-09	1.00E+00
SOP12	2	T	8.91E-08	4.50E-09	1.00E+00
SOP12	3	T	1.05E-06	1.30E-10	1.00E+00
SOP12	4	T	5.25E-09	5.37E-11	1.00E+00
SOP12	5	T	4.34E-05	1.08E-06	1.00E+00

Table S2.9. Pairwise nucleotide diversity comparisons among *Mimulus* species (C=*M. caespitosa*, M= *M. minor*, T = *M. tilingii*, G = *M. guttatus*, N= *M. nasutus*, D = *M. dentilobus*).

Sample 1	Sample 2	Comparison	Intra-population?	No. sites	No. polymorphic sites	Dxy/pi
GAB1	GAB2	C x C	X	478593	5711	0.012
GAB1	KCK1	C x C		542249	6291	0.012
GAB1	PAG2	C x C		379433	5205	0.014
GAB1	TWN36	C x C		479699	6428	0.013
GAB1	UTC1	C x C		346059	4742	0.014
GAB1	UTC2	C x C		363270	4920	0.014
GAB2	KCK1	C x C		1179245	11391	0.01
GAB2	PAG2	C x C		792455	8692	0.011
GAB2	TWN36	C x C		1044661	12428	0.012
GAB2	UTC1	C x C		719855	8238	0.011
GAB2	UTC2	C x C		764229	8251	0.011
KCK1	PAG2	C x C		926215	9325	0.01
KCK1	TWN36	C x C		1208062	13666	0.011
KCK1	UTC1	C x C		843450	7498	0.009
KCK1	UTC2	C x C		885378	8327	0.009
PAG2	TWN36	C x C		815627	10539	0.013
PAG2	UTC1	C x C		579476	6653	0.011
PAG2	UTC2	C x C		608203	6698	0.011
TWN36	UTC1	C x C		739034	9475	0.013
TWN36	UTC2	C x C		780572	9606	0.012
UTC1	UTC2	C x C	X	552896	5794	0.01
NOR511	NOR523	M x M	X	1892185	4682	0.002
NOR511	UNP12	M x M		1617266	16895	0.01
NOR523	UNP12	M x M		1467315	15726	0.011
A25	ICE10	T x T		86786	2927	0.034
A25	LVR	T x T		152911	5679	0.037
A25	SAB	T x T		101043	3691	0.037
A25	SAB19	T x T		80550	3016	0.037
A25	SOP12	T x T		104890	3616	0.034
ICE10	LVR	T x T		1466657	43164	0.029
ICE10	SAB	T x T		848641	28434	0.034
ICE10	SAB19	T x T		654113	22176	0.034
ICE10	SOP12	T x T		889458	23633	0.027
LVR	SAB	T x T		1836031	54519	0.03
LVR	SAB19	T x T		1416846	42896	0.03
LVR	SOP12	T x T		1918602	50227	0.026
SAB	SAB19	T x T	X	832066	12603	0.015
SAB	SOP12	T x T		1088685	34531	0.032
SAB19	SOP12	T x T		841431	27514	0.033

GAB1	NOR511	C x M		607861	25591	0.042
GAB1	NOR523	C x M		551162	23136	0.042
GAB1	UNP12	C x M		486262	16734	0.034
GAB2	NOR511	C x M		1385590	55454	0.04
GAB2	NOR523	C x M		1253335	50202	0.04
GAB2	UNP12	C x M		1093456	35142	0.032
KCK1	NOR511	C x M		1622882	66563	0.041
KCK1	NOR523	C x M		1464066	60192	0.041
KCK1	UNP12	C x M		1271905	42747	0.034
PAG2	NOR511	C x M		1076027	44631	0.041
PAG2	NOR523	C x M		972227	40381	0.042
PAG2	UNP12	C x M		847868	28851	0.034
TWN36	NOR511	C x M		1434096	59212	0.041
TWN36	NOR523	C x M		1296349	53658	0.041
TWN36	UNP12	C x M		1120902	38441	0.034
UTC1	NOR511	C x M		965764	40341	0.042
UTC1	NOR523	C x M		877295	36740	0.042
UTC1	UNP12	C x M		764191	26224	0.034
UTC2	NOR511	C x M		1022333	42498	0.042
UTC2	NOR523	C x M		925376	38654	0.042
UTC2	UNP12	C x M		807475	27551	0.034
GAB1	A25	C x T		52916	2229	0.042
GAB1	ICE10	C x T		372174	16491	0.044
GAB1	LVR	C x T		758041	34179	0.045
GAB1	SAB	C x T		454908	19571	0.043
GAB1	SAB19	C x T		350240	15664	0.045
GAB1	SOP12	C x T		471532	20998	0.045
GAB2	A25	C x T		95464	4050	0.042
GAB2	ICE10	C x T		811522	34532	0.043
GAB2	LVR	C x T		1757250	76026	0.043
GAB2	SAB	C x T		1000513	41712	0.042
GAB2	SAB19	C x T		766543	33065	0.043
GAB2	SOP12	C x T		1043626	44709	0.043
KCK1	A25	C x T		107586	4702	0.044
KCK1	ICE10	C x T		935428	40901	0.044
KCK1	LVR	C x T		2074880	92339	0.045
KCK1	SAB	C x T		1159386	49588	0.043
KCK1	SAB19	C x T		893729	39593	0.044
KCK1	SOP12	C x T		1210030	53039	0.044
PAG2	A25	C x T		78468	3439	0.044
PAG2	ICE10	C x T		634316	28411	0.045
PAG2	LVR	C x T		1367191	61742	0.045
PAG2	SAB	C x T		779241	33751	0.043
PAG2	SAB19	C x T		602992	26812	0.044
PAG2	SOP12	C x T		811659	36229	0.045

TWN36	A25	C x T		97548	4230	0.043
TWN36	ICE10	C x T		834223	36881	0.044
TWN36	LVR	C x T		1824278	81433	0.045
TWN36	SAB	C x T		1031616	44284	0.043
TWN36	SAB19	C x T		790395	35220	0.045
TWN36	SOP12	C x T		1076907	47770	0.044
UTC1	A25	C x T		70457	2958	0.042
UTC1	ICE10	C x T		571105	25413	0.044
UTC1	LVR	C x T		1226757	55219	0.045
UTC1	SAB	C x T		700213	30371	0.043
UTC1	SAB19	C x T		543723	24187	0.044
UTC1	SOP12	C x T		736565	32717	0.044
UTC2	A25	C x T		74417	3197	0.043
UTC2	ICE10	C x T		602891	26806	0.044
UTC2	LVR	C x T		1296909	58507	0.045
UTC2	SAB	C x T		743663	32260	0.043
UTC2	SAB19	C x T		573713	25668	0.045
UTC2	SOP12	C x T		776483	34557	0.045
NOR511	A25	M x T		122624	5226	0.043
NOR511	ICE10	M x T		1139922	49550	0.043
NOR511	LVR	M x T		2603770	113778	0.044
NOR511	SAB	M x T		1425235	60643	0.043
NOR511	SAB19	M x T		1090892	47409	0.043
NOR511	SOP12	M x T		1484611	64642	0.044
NOR523	A25	M x T		112815	4883	0.043
NOR523	ICE10	M x T		1032201	44986	0.044
NOR523	LVR	M x T		2322219	101896	0.044
NOR523	SAB	M x T		1285273	54622	0.042
NOR523	SAB19	M x T		983031	42622	0.043
NOR523	SOP12	M x T		1342275	58638	0.044
UNP12	A25	M x T		101119	4254	0.042
UNP12	ICE10	M x T		895121	37593	0.042
UNP12	LVR	M x T		1980730	83730	0.042
UNP12	SAB	M x T		1109875	45479	0.041
UNP12	SAB19	M x T		851447	36084	0.042
UNP12	SOP12	M x T		1160148	48941	0.042
AHQT1	CACG	G x G		3416204	148002	0.043
AHQT1	MED84	G x G		3361660	187971	0.056
AHQT1	SLP	G x G		3328696	189792	0.057
CACG	MED84	G x G		3570377	193520	0.054
CACG	SLP	G x G		3528904	197570	0.056
MED84	SLP	G x G		3500980	164704	0.047
CACN	NHN	N x N		3554430	48909	0.014
AHQT1	CACN	G x N		3349682	195561	0.058
AHQT1	NHN	G x N		3324482	193062	0.058

CACG	CACN	G x N		3590384	170754	0.048
CACG	NHN	G x N		3551846	172971	0.049
MED84	CACN	G x N		3523489	177903	0.05
MED84	NHN	G x N		3491227	176917	0.051
SLP	CACN	G x N		3483131	185615	0.053
SLP	NHN	G x N		3452238	183961	0.053
AHQT1	GAB1	G x C		730827	45239	0.062
AHQT1	GAB2	G x C		1682290	102780	0.061
AHQT1	KCK1	G x C		1981058	123066	0.062
AHQT1	PAG2	G x C		1312094	81888	0.062
AHQT1	TWN36	G x C		1746066	109325	0.063
AHQT1	UTC1	G x C		1171205	73499	0.063
AHQT1	UTC2	G x C		1241732	77929	0.063
CACG	GAB1	G x C		760699	47408	0.062
CACG	GAB2	G x C		1764329	108089	0.061
CACG	KCK1	G x C		2082881	130312	0.063
CACG	PAG2	G x C		1373288	86595	0.063
CACG	TWN36	G x C		1830691	115224	0.063
CACG	UTC1	G x C		1231268	77515	0.063
CACG	UTC2	G x C		1301649	82176	0.063
MED84	GAB1	G x C		750439	47567	0.063
MED84	GAB2	G x C		1737986	109016	0.063
MED84	KCK1	G x C		2052312	131200	0.064
MED84	PAG2	G x C		1354279	86877	0.064
MED84	TWN36	G x C		1803934	115526	0.064
MED84	UTC1	G x C		1212922	78315	0.065
MED84	UTC2	G x C		1284219	82746	0.064
SLP	PAG2	G x C		1345396	86463	0.064
SLP	GAB1	G x C		745670	47215	0.063
SLP	GAB2	G x C		1725197	108074	0.063
SLP	KCK1	G x C		2036038	130234	0.064
SLP	TWN36	G x C		1789942	114991	0.064
SLP	UTC1	G x C		1203888	77469	0.064
SLP	UTC2	G x C		1273984	82306	0.065
AHQT1	NOR511	G x M		2480788	157418	0.063
AHQT1	NOR523	G x M		2216473	141265	0.064
AHQT1	UNP12	G x M		1894887	115160	0.061
CACG	NOR511	G x M		2615338	166314	0.064
CACG	NOR523	G x M		2331722	149064	0.064
CACG	UNP12	G x M		1986719	121191	0.061
MED84	NOR511	G x M		2575152	166881	0.065
MED84	NOR523	G x M		2296411	149358	0.065
MED84	UNP12	G x M		1959497	122176	0.062

SLP	NOR511	G x M		2558097	165848	0.065
SLP	NOR523	G x M		2281789	148129	0.065
SLP	UNP12	G x M		1947407	121339	0.062
AHQT1	A25	G x T		148261	8524	0.057
AHQT1	ICE10	G x T		1396059	84872	0.061
AHQT1	LVR	G x T		3334869	207273	0.062
AHQT1	SAB	G x T		1746019	106372	0.061
AHQT1	SAB19	G x T		1343681	82582	0.061
AHQT1	SOP12	G x T		1820733	110965	0.061
CACG	A25	G x T		152530	8879	0.058
CACG	ICE10	G x T		1462769	89166	0.061
CACG	LVR	G x T		3571672	221848	0.062
CACG	SAB	G x T		1830294	111735	0.061
CACG	SAB19	G x T		1413398	87674	0.062
CACG	SOP12	G x T		1911775	116626	0.061
MED84	A25	G x T		150840	8851	0.059
MED84	ICE10	G x T		1444032	89288	0.062
MED84	LVR	G x T		3498051	220313	0.063
MED84	SAB	G x T		1807001	111857	0.062
MED84	SAB19	G x T		1393434	87345	0.063
MED84	SOP12	G x T		1885911	116496	0.062
SLP	A25	G x T		149701	8783	0.059
SLP	ICE10	G x T		1432212	88588	0.062
SLP	LVR	G x T		3461730	217689	0.063
SLP	SAB	G x T		1792636	111337	0.062
SLP	SAB19	G x T		1380936	86550	0.063
SLP	SOP12	G x T		1871832	115994	0.062
CACN	GAB1	N x C		751709	47408	0.063
CACN	GAB2	N x C		1745259	109145	0.063
CACN	KCK1	N x C		2060090	130991	0.064
CACN	PAG2	N x C		1357932	86984	0.064
CACN	TWN36	N x C		1810024	116139	0.064
CACN	UTC1	N x C		1216126	78151	0.064
CACN	UTC2	N x C		1287524	82629	0.064
NHN	GAB1	N x C		748160	47344	0.063
NHN	GAB2	N x C		1733297	108370	0.063
NHN	KCK1	N x C		2044043	130055	0.064
NHN	PAG2	N x C		1348265	86428	0.064
NHN	TWN36	N x C		1796888	115252	0.064
NHN	UTC1	N x C		1207186	77584	0.064
NHN	UTC2	N x C		1278836	82111	0.064

CACN	NOR511	N x M		2589288	167347	0.065
CACN	NOR523	N x M		2309461	149560	0.065
CACN	UNP12	N x M		1969078	122719	0.062
NHN	NOR511	N x M		2569555	165887	0.065
NHN	NOR523	N x M		2292474	148195	0.065
NHN	UNP12	N x M		1955006	121669	0.062
CACN	A25	N x T		3554430	48909	0.014
CACN	ICE10	N x T		1447148	89359	0.062
CACN	LVR	N x T		3512330	220243	0.063
CACN	SAB	N x T		1813000	111797	0.062
CACN	SAB19	N x T		1398633	87410	0.062
CACN	SOP12	N x T		1890361	116666	0.062
NHN	A25	N x T		149589	8831	0.059
NHN	ICE10	N x T		1435901	88500	0.062
NHN	LVR	N x T		3477790	217948	0.063
NHN	SAB	N x T		1800013	110997	0.062
NHN	SAB19	N x T		1388316	86634	0.062
NHN	SOP12	N x T		1876577	115751	0.062
DENT	AHQT1	D x G		1152795	86528	0.075
DENT	CACG	D x G		1187840	89586	0.075
DENT	MED84	D x G		1180682	92151	0.078
DENT	SLP	D x G		1176385	91810	0.078
CACN	DENT	D x N		1179364	92160	0.078
DENT	NHN	D x N		1171388	91453	0.078
DENT	GAB1	D x C		273822	18870	0.069
DENT	GAB2	D x C		637372	44037	0.069
DENT	KCK1	D x C		749612	52618	0.07
DENT	PAG2	D x C		512725	36198	0.071
DENT	TWN36	D x C		665863	47162	0.071
DENT	UTC1	D x C		458721	32477	0.071
DENT	UTC2	D x C		481807	34237	0.071
DENT	NOR511	D x M		930364	65313	0.07
DENT	NOR523	D x M		839748	59184	0.07
DENT	UNP12	D x M		723134	49397	0.068
DENT	A25	D x T		63920	4190	0.066
DENT	ICE10	D x T		531642	37223	0.07
DENT	LVR	D x T		1179931	83547	0.071
DENT	SAB	D x T		656016	45578	0.069
DENT	SAB19	D x T		508440	35781	0.07
DENT	SOP12	D x T		687169	48051	0.07

Table S2.10. Pairwise differences in seed set per fruit assessed using a post-hoc Tukey method. Cross types involved *M. caespitosa* (C), *M. minor* (M), and *M. tilingii* (T), with the maternal parent in each cross listed first. N_{cross} = number of unique maternal family combinations per cross type, and N_{total} = total number of fruits scored per cross type. Values on diagonal are lsmeans +/- standard error. In each box below the diagonal, the uppermost value is the model estimate, the middle value is the z-ration, and the bottom value is the *P*-value. Upper right: GLM type III ANOVA results of intra- and interspecific seed set with the likelihood ratio $\chi 2$ values for "Maternal Species" and "Paternal Species" (fixed effects) and "Maternal*Paternal" species interaction effect. Below ANOVA table: pairwise differences drive by maternal species. Shades of light gray denotes a $P<0.05$, medium gray denotes $P<0.01$, and dark gray denotes a $P<0.001$.

C x C N_{cross} = 43 N_{total} = 116	167.97 ± 10.73								
C x M N_{cross} = 10 N_{total} = 22	9.16e-05 0.097 1.0	170.59 ± 25.03							
M x C N_{cross} = 12 N_{total} = 25	2.79e-03 4.81 0.0001	-2.69e-03 -2.79 0.12	315.60 ± 43.44						
M x M N_{cross} = 4 N_{total} =7	2.88e-03 3.24 0.032	2.78e-03 2.37 0.30	9.03e-05 0.10 1.0	324.86 ± 84.50					
M x T N_{cross} = 8 N_{total} = 14	1.14e-03 1.19 0.96	1.05e-3 0.85 1.0	-1.64e-03 -1.66 0.77	-1.73e-03 -1.45 0.88	207.93 ± 38.29				
T x M N_{cross} = 7 N_{total} = 14	4.33e-04 0.40 1.0	3.41e-04 0.26 1.0	-2.35e-03 -2.13 0.45	-2.44e-03 -1.89 0.62	7.11e-04 0.53 1.0	181.14 ± 3.32			
T x T N_{cross} = 14 N_{total} = 37	2.13e-04 0.28 1.0	1.21e-04 0.11 1.0	-2.57e-03 -3.28 0.028	-2.66e-03 -2.58 0.19	-9.32e-04 -0.85 1.0	-2.20e-04 -0.18 1.0	174.19 ± 19.71		
T x C N_{cross} = 25 N_{total} = 75	1.49e-03 2.87 0.09	-1.40e-03 -1.50 -0.85	-1.29e-03 -2.30 0.34	1.38e-03 1.58 0.82	-3.46e-04 -0.36 1.0	-1.06e-03 -0.98 0.99	-1.28e-03 -1.73 0.73	224.05 ± 17.80	
C x T N_{cross} = 24 N_{total} = 60	-1.81e-04 -0.27 1.0	-2.73e-04 -0.27 1.0	-2.97e-03 -4.25 0.0007	-3.06e-03 -3.15 0.043	1.33e-03 1.28 0.94	-6.14e-04 -0.53 1.0	3.94e-04 0.4 1.0	-1.27e-03 -2.57 0.20	163 ± 14.48
	C x C	**C x M**	**M x C**	**M x M**	**M x T**	**T x M**	**T x T**	**T x C**	**C x T**

	Likelihood Ratio χ^2	*df*	*p*
Maternal Species	21.80	2	1.84e-05
Paternal Species	0.10	2	0.95
Maternal*Paternal	2.81	4	0.59

C N_{cross} =77 N_{total} = 198	167.13 ± 10.12		
M N_{cross} = 24 N_{total} = 46	2.30e-03 4.12 <0.0001	271.34 ± 31.18	
T N_{cross} = 46 N_{total} = 127	7.42e-04 1.34 0.373	1.56e-03 -2.61 0.024	190.78 ± 15.24
	C	**M**	**T**

Table S2.11. Pairwise differences in seed viability (morphological assessment per fruit) assessed using a post-hoc Tukey method. Cross types involved *M. caespitosa* (C), *M. minor* (M), and *M. tilingii* (T), with the maternal parent in each cross listed first. N_{cross} = number of unique maternal family combinations per cross type, and N_{total} = total number of fruits scored per cross type. Values on diagonal are lsmeans +/- standard error. In each box below the diagonal, the uppermost value is the model estimate, the middle value is the z-ration, and the bottom value is the *P*-value. Upper right: GLMM type III ANOVA results of intra- and interspecific morphological seed viability with Wald $\chi 2$ values for "Maternal Species" and "Paternal Species" (fixed effects) and "Maternal*Paternal" species interaction effect. Below ANOVA table: pairwise differences drive by maternal species. Shades of light gray denotes a $P<0.05$, medium gray denotes $P<0.01$, and dark gray denotes a $P<0.001$.

C x C N_{cross} = 43 N_{total} = 115	0.95 ± 0.02								
C x M N_{cross} = 10 N_{total} = 22	0.79 -0.68 1.0	0.96±0.02							
M x C N_{cross} = 12 N_{total} = 25	3.95 1.77 0.70	0.2 -1.90 0.62	0.84±0.09						
M x M N_{cross} = 4 N_{total} =7	1.71 0.64 1.0	2.16 0.98 0.99	0.43 -2.46 0.25	0.92±0.05					
M x T N_{cross} = 8 N_{total} = 14	1.86e03 9.02 <0.0001	2.35e03 8.89 <0.0001	471.87 19.86 <0.0001	1.09e03 17.41 <0.0001	0.01±0.01				
T x M N_{cross} = 7 N_{total} = 14	6.67 2.74 0.13	8.40 3.48 0.015	1.69 0.58 1.0	3.90 1.61 0.80	279.47 6.08 <0.0001	0.76 ±0.10			
T x T N_{cross} = 14 N_{total} = 36	2.04 1.08 0.98	2.57 1.33 0.92	0.52 -0.75 1.0	1.19 0.19 1.0	1.1e-03 -7.97 <0.0001	0.31 -3.27 0.03	0.91±0.04		
T x C N_{cross} = 25 N_{total} = 75	2.15 1.31 0.94	0.37 -1.44 0.88	0.55 -0.72 1.0	0.79 -0.25 1.0	865.37 7.58 <0.0001	3.10 3.37 0.022	0.95 -0.21 1.0	0.91±0.04	
C x T N_{cross} = 24 N_{total} = 60	85.65 16.99 <0.0001	107.91 12.82 <0.0001	21.68 3.76 0.005	50.03 4.57 0.0002	21.76 3.88 0.003	12.84 3.62 0.009	0.02 -6.15 <0.0001	39.77 5.58 <0.0001	0.20±0.07
	C x C	**C x M**	**M x C**	**M x M**	**M x T**	**T x M**	**T x T**	**T x C**	**C x T**

	Wald χ^2	*df*	*p*
Maternal Species	3.76	2	0.15
Paternal Species	321.12	2	< 2.2e-16
Maternal*Paternal	5848.23	4	< 2.2e-16

Table S2.12. Pairwise differences in seed viability (germination rate per fruit) assessed using a post-hoc Tukey method. Cross types involved *M. caespitosa* (C), *M. minor* (M), and *M. tilingii* (T), with the maternal parent in each cross listed first. N_{cross} = number of unique maternal family combinations per cross type, and N_{total} = total number of fruits scored per cross type. Values on diagonal are lsmeans +/- standard error. In each box below the diagonal, the uppermost value is the model estimate, the middle value is the z-ration, and the bottom value is the *P*-value. Upper right: GLMM type III ANOVA results of intra- and interspecific germination rate with Wald $\chi 2$ values for "Maternal Species" and "Paternal Species" (fixed effects) and "Maternal*Paternal" species interaction effect. Below ANOVA table: pairwise differences drive by maternal species. Shades of light gray denotes a $P<0.05$, medium gray denotes $P<0.01$, and dark gray denotes a $P<0.001$.

C x C N_{cross} = 36 N_{total} = 54	0.59 ± 0.06								
C x M N_{cross} = 8 N_{total} = 13	3.06 3.53 0.012	0.32±0.07							
M x C N_{cross} = 7 N_{total} =13	1.70 1.46 0.88	1.80 1.22 0.95	0.46±0.09						
M x M N_{cross} = 3 N_{total} =3	1.97 1.4 0.9	0.64 -1.20 0.96	1.16 0.45 1.0	0.42±0.1					
M x T N_{cross} = 7 N_{total} = 9	707.24 9.87 <0.0001	230.8 7.71 <0.0001	415.65 10.8 <0.0001	359.88 9.7 <0.0001	0±0				
T x M N_{cross} = 7 N_{total} = 11	0.94 -0.15 1.0	0.031 -4.06 0.0016	0.55 -1.178 0.96	0.47 -1.85 0.65	752.73 9.18 <0.0001	0.6±0.09			
T x T N_{cross} = 10 N_{total} = 19	0.53 -1.70 0.75	0.17 -3.96 0.0025	0.31 -2.53 0.22	0.27 -2.5 0.22	7.0e-04 -11.31 <0.0001	0.56 -1.68 0.76	0.73±0.06		
T x C N_{cross} = 20 N_T = 40	0.46 -2.75 0.13	6.72 4.48 0.0003	0.27 -3.35 0.023	4.31 2.89 0.09	1.5e04 10.78 <0.0001	2.06 2.28 0.36	1.16 0.58 1.0	0.76±0.05	
C x T N_{cross} = 23 N_{total} = 47	4.21 5.82 <0.0001	1.37 0.93 0.99	2.47 2.06 0.5	2.14 1.52 0.85	168.06 8.28 <0.0001	4.48 3.38 0.021	0.13 -7.23 <0.0001	9.23 5.9 <0.0001	0.25 ±0.05
	C x C	**C x M**	**M x C**	**M x M**	**M x T**	**T x M**	**T x T**	**T x C**	**C x T**

	Wald χ^2	*df*	*p*
Maternal Species	13.07	2	1.46e-3
Paternal Species	37.75	2	6.36e-09
Maternal*Paternal	680.30	4	< 2.2e-16

Table S2.13. Pairwise differences in days to flower (from seedling) assessed using a post-hoc Tukey method. Cross types involved *M. caespitosa* (C), *M. minor* (M), and *M. tilingii* (T), with the maternal parent in each cross listed first. N_{cross} = number of unique maternal family combinations per cross type, and N_{total} = total number of individuals scored to flowering per cross type. Values on diagonal are lsmeans +/- standard error. In each box below the diagonal, the uppermost value is the model estimate, the middle value is the z-ration, and the bottom value is the *P*-value. Upper right: GLMM type III ANOVA results of intra- and interspecific days to first flower with Wald $\chi 2$ values for "Maternal Species" and "Paternal Species" (fixed effects) and "Maternal*Paternal" species interaction effect. Below ANOVA table: pairwise differences drive by maternal species. Shades of light gray denotes a $P<0.05$, medium gray denotes $P<0.01$, and dark gray denotes a $P<0.001$.

	C x C	C x M	M x C	M x M	M x T	T x M	T x T	T x C	C x T
C x C N_{cross} =17 N_{total} =199	49.15 ± 2.04								
C x M N_{cross} = 5 N_{total} = 57	1.36 4.51 0.0002	36.11 ± 2.41							
M x C N_{cross} = 4 N_{total} = 56	1.14 1.97 0.56	1.20 1.96 0.57	43.25 ± 2.76						
M x M N_{cross} = 2 N_{total}= 23	1.16 1.60 0.81	0.85 -2.22 0.39	1.02 0.29 1.0	42.31± 3.56					
M x T									
T x M N_{cross} = 4 N_{total}= 54	1.11 1.29 0.94	0.82 -3.57 0.011	0.98 -0.22 1.0	0.96 -0.59 1.0		44.19 ± 3.16			
T x T N_{cross} = 8 N_{total}= 93	1.01 0.17 1.0	0.74 -3.35 0.023	0.89 -1.35 1.0	0.87 -1.35 0.92		0.91 -1.23 0.95	48.56± 2.79		
T x C N_{cross} = 43 N_{total} = 93	1.18 3.2 0.037	1.16 1.76 0.71	1.03 0.48 1.0	0.99 -0.12 1.0		0.95 -0.79 1.0	0.86 -2.66 0.16	41.82 ± 2.09	
C x T N_{cross} = 4 N_{total} = 44	0.96 -0.76 1.0	0.70 -4.55 0.0002	084 -2.02 0.53	0.82 -1.93 0.59		0.86 -1.67 0.77	1.06 0.92 0.99	0.82 -2.79 0.12	51.29 ± 2.76

	Wald χ^2	*df*	*p*
Maternal Species	11.63	2	2.99e-03
Paternal Species	24.02	2	6.1e-06
Maternal*Paternal	93.40	3	< 2.2e-16

Table S2.14. Pairwise differences in F1 pollen viability assessed using a post-hoc Tukey method. Cross types involved *M. caespitosa* (C), *M. minor* (M), and *M. tilingii* (T), with the maternal parent in each cross listed first. N_{cross} = number of unique maternal family combinations per cross type, and N_{total} = total number of flowers scored for viable pollen per cross type. Values on diagonal are lsmeans +/- standard error. In each box below the diagonal, the uppermost value is the model estimate, the middle value is the z-ration, and the bottom value is the *P*-value. Upper right: GLMM type III ANOVA results of F1 pollen viability with Wald $\chi 2$ values for "Maternal Species" and "Paternal Species" (fixed effects) and "Maternal*Paternal" species interaction effect. Below ANOVA table: pairwise differences drive by maternal species. Shades of light gray denotes a $P<0.05$, medium gray denotes $P<0.01$, and dark gray denotes a $P<0.001$.

	Wald χ^2	*df*	*p*
Maternal Species	376.71	2	< 2.2e-16
Paternal Species	293.33	2	< 2.2e-16
Maternal*Paternal	10162.86	3	< 2.2e-16

C x C N_{cross} = 17 N_{total} = 136	0.90 ± 0.02								
C x M N_{cross} = 5 N_{total} = 38	177.91 16.0 <0.0001	0.05 ± 0.01							
M x C N_{cross} = 4 N_{total} = 34	176.49 17.85 <0.0001	1.01 0.02 1.0	0.05 ± 0.01						
M x M N_{cross} = 2 N_{total} = 13	0.55 -1.39 0.90	3.1e-03 -20.16 <0.0001	3.1e-03 -16.92 <0.0001	0.94± 0.02					
M x T									
T x M N_{cross} = 4 N_{total} = 26	757.55 15.68 <0.0001	4.26 5.07 <0.0001	4.29 3.06 0.057	1.38e03 20.24 <0.0001		0.01 ± 0			
T x T N_{cross} = 8 N_{total} = 57	2.35 2.45 0.25	0.01 -10.16 <0.0001	0.01 -10.47 <0.0001	4.29 3.04 0.06		3.1e-03 -14.35 <0.0001	0.79 ± 0.05		
T x C N_{cross} = 9 N_{total} = 65	14.69 12.26 <0.0001	12.11 6.40 <0.0001	0.08 -7.98 <0.0001	0.04 -7.35 <0.0001		51.55 10.86 <0.0001	0.16 -6.68 <0.0001	0.38± 0.05	
C x T N_{cross} = 5 N_{total} = 29	15.77 9.98 <0.0001	0.09 -6.57 <0.0001	0.09 -6.06 <0.0001	28.80 7.20 <0.001		0.02 -8.46 <0.0001	0.15 -8.53 <0.0001	1.07 0.20 1.0	0.36 ± 0.06
	C x C	**C x M**	**M x C**	**M x M**	**M x T**	**T x M**	**T x T**	**T x C**	**C x T**

Table S2.15. Pairwise differences in F1 seed production assessed using a post-hoc Tukey method. Cross types involved *M. caespitosa* (C), *M. minor* (M), and *M. tilingii* (T), with the maternal parent in each cross listed first. N_{cross} = number of unique maternal family combinations per cross type, and N_{total} = total number of fruits scored per cross type. Values on diagonal are lsmeans +/- standard error. In each box below the diagonal, the uppermost value is the model estimate, the middle value is the z-ration, and the bottom value is the *P*-value. Upper right: GLMM type III ANOVA results of F1 seed set Wald $\chi 2$ values for "Maternal Species" and "Paternal Species" (fixed effects) and "Maternal*Paternal" species interaction effect. Below ANOVA table: pairwise differences drive by maternal species. Shades of light gray denotes a $P<0.05$, medium gray denotes $P<0.01$, and dark gray denotes a $P<0.001$.

C x C N_{cross} = 17 N_{total} = 76	206.03 ± 45.63								
C x M N_{cross} = 5 N_{total} = 22	39 8.5 <0.0001	5.28 ± 2.09							
M x C N_{cross} = 4 N_{total} = 17	65.01 16.42 <0.0001	0.60 -1.02 0.98	3.17 ± 0.97						
M x M N_{cross} = 2 N_{total} = 9	0.41 -1.89 0.62	0.01 -18.77 <0.0001	6.25e-03 -11.36 <0.0001	507.06± 214.34					
M x T									
T x M N_{cross} = 4 N_{total} = 11	42.3 7.97 <0.0001	1.08 0.34 1.0	0.65 -0.84 1.0	104.11 16.58 <0.0001		4.87 ± 2.02			
T x T N_{cross} = 8 N_{total} = 34	1.23 0.57 1.0	0.03 -6.97 <0.0001	0.02 -9.32 <0.0001	3.04 2.15 0.44		0.03 -7.46 <0.0001	167± 49.58		
T x C N_{cross} = 9 N_{total} = 43	4.47 8.80 <0.0001	8.72 4.68 0.0001	0.07 -9.92 <0.0001	0.09 -4.94 <0.0001		9.46 5.12 <0.0001	0.28 -3.89 0.0032	46.09 ± 11.02	
C x T N_{cross} = 4 N_{total} = 19	8.34 6.39 <0.0001	0.21 -3.30 0.027	0.13 -4.91 <0.0001	20.53 5.92 <0.0001		0.2 -3.22 0.034	0.15 -10.66 <0.0001	1.87 1.68 0.76	24.70 ± 7.06
	C x C	**C x M**	**M x C**	**M x M**	**M x T**	**T x M**	**T x T**	**T x C**	**C x T**

	Wald χ^2	*df*	*p*
Maternal Species	294.77	2	< 2.2e-16
Paternal Species	90.35	2	< 2.2e-16
Maternal*Paternal	4896.76	3	< 2.2e-16

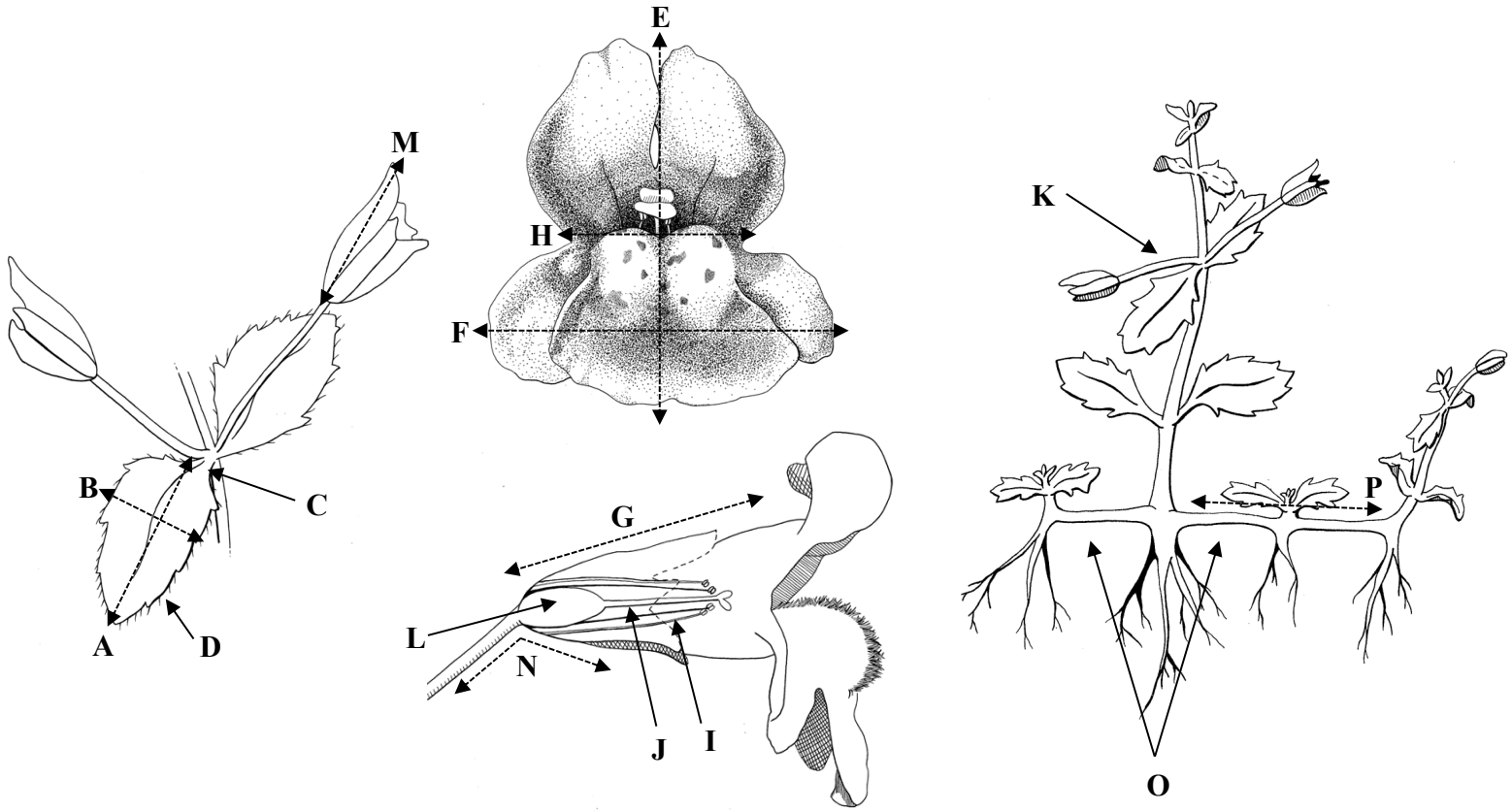

Figure S2.1. Morphological traits measured in a common garden experiment. Vegetative leaf traits measured on second leaf pair: **A.** Leaf length. **B.** Leaf width. **C.** Petiole length. **D.** Trichomes exerted past edge of leaf. **E.** Corolla height. **F.** Corolla width. **G.** Corolla tube length. **H.** Corolla tube width. **I.** Stamen length. **J.** Pistil length. **K.** Pedicel length. **L.** Capsule length. **M.** Calyx length. **N.** Degree of flower nodding. **O.** Number of stolons. **P.** Stolon length.

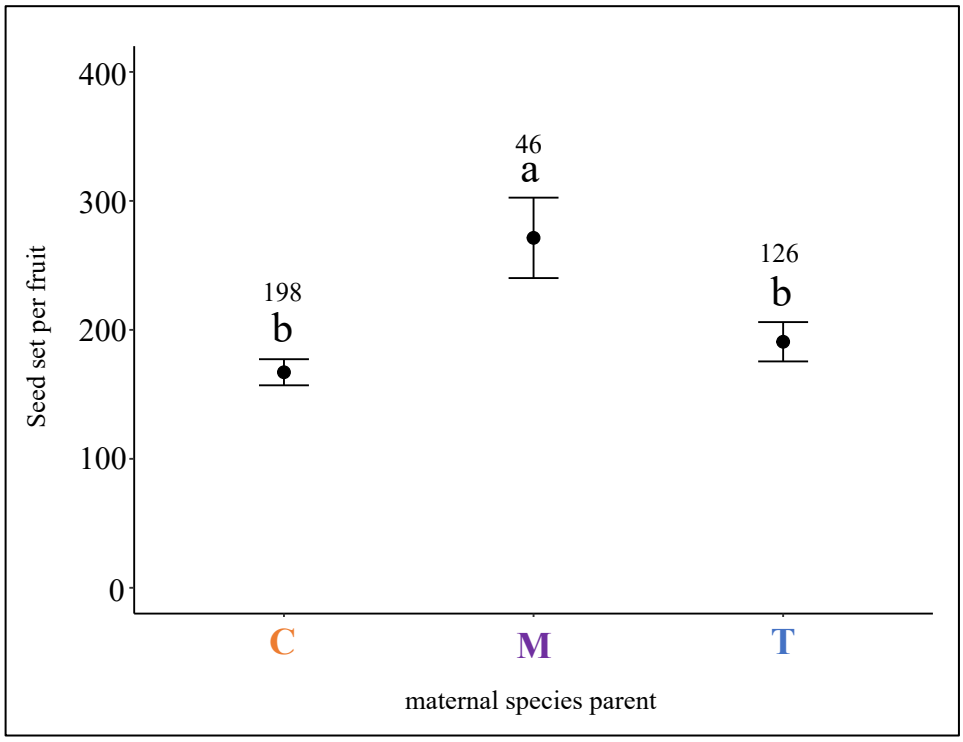

Figure S2.2. Total seed produced by maternal species parent of intra- and interspecific crosses when *M. caespitosa* (C), *M. minor* (M), and *M. tilingii* (T) act as the maternal parent. Least square means for each cross type are given with standard error bars. Least square means denoted by a different letter indicate significant differences among cross types (P <0.05) determined by post-hoc Tukey method. Sample sizes assessed for each cross type are listed above letters

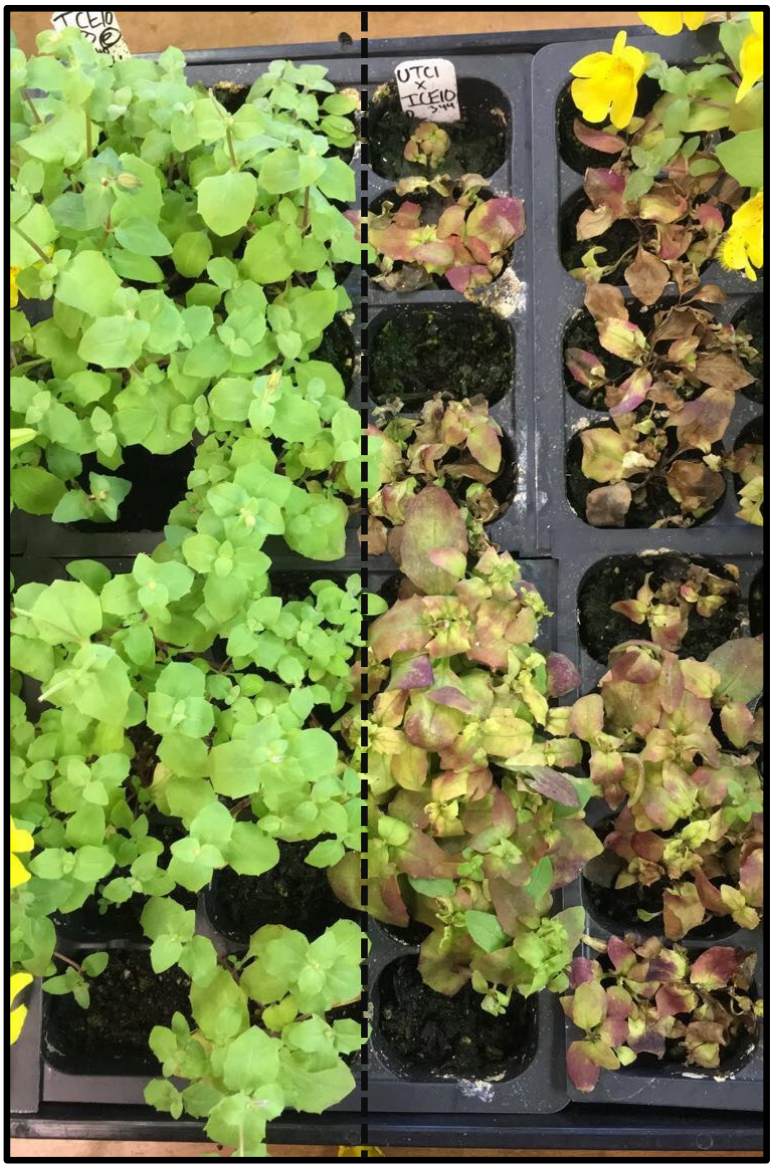

Figure S2.3. Hybrid inviability phenotype. Left: Intraspecific *M. tilingii* cross (TxT: ICE10xICE10). Right: interspecific *M. caespitosa* x *M. tilingii* cross (CxT: UTC1xICE 10).

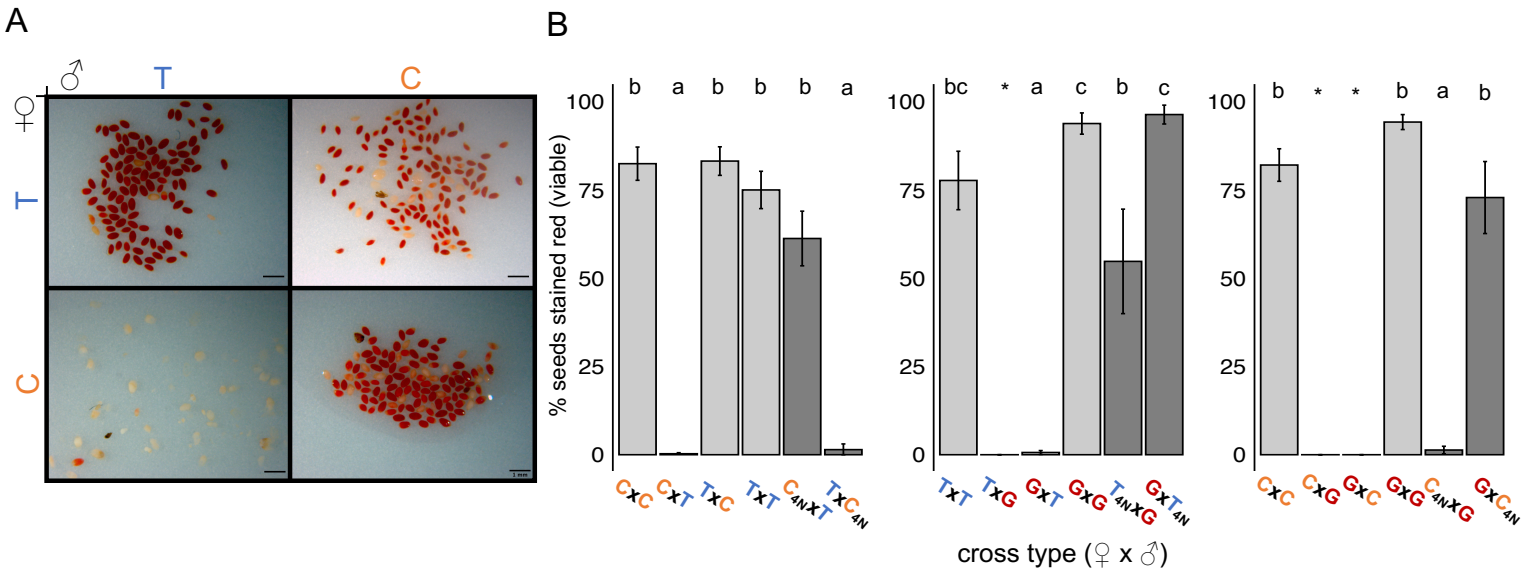

Figure S3.1: Tetrazolium assay for seed viability of intra-, interspecific, and interploidy crosses among *M. caespitosa* (C), *M. tilingii* (T), and *M. guttatus* (G). **A.** Example of tetrazolium test on seeds from intra and interspecific crosses of *M. tilingii* and *M. caespitosa.* Intraspecific crosses: TxT (top left) and CxC (bottom right). Interspecific crosses, maternal parent is always listed first: CxT (bottom left), TxC (top right). Dark red seeds are viable, and pink or white seeds are inviable. Scale bar is 1 mm. **B.** Percentage of seeds stained red from intra- and interspecific crosses. Least square means given with +/- SE. Light gray bars represent cross types between diploid parents, and dark gray bars represent crosses where one parent is a synthetic tetraploid, as denoted by the "4N" subscript in the cross. Different letters indicate significant differences in lsmeans among crosses ($P<0.05$) determined by a post hoc Tukey method. Analyses were performed separately, only comparing reciprocal interspecific and interploidy crosses and their corresponding intraspecific crosses. Asterisk denotes lack of variation in response variable to determine statistical differences. Note that for some interploidy crosses, 5-10 fully-developed seeds were planted to test for ploidy prior to tetrazolium assay.

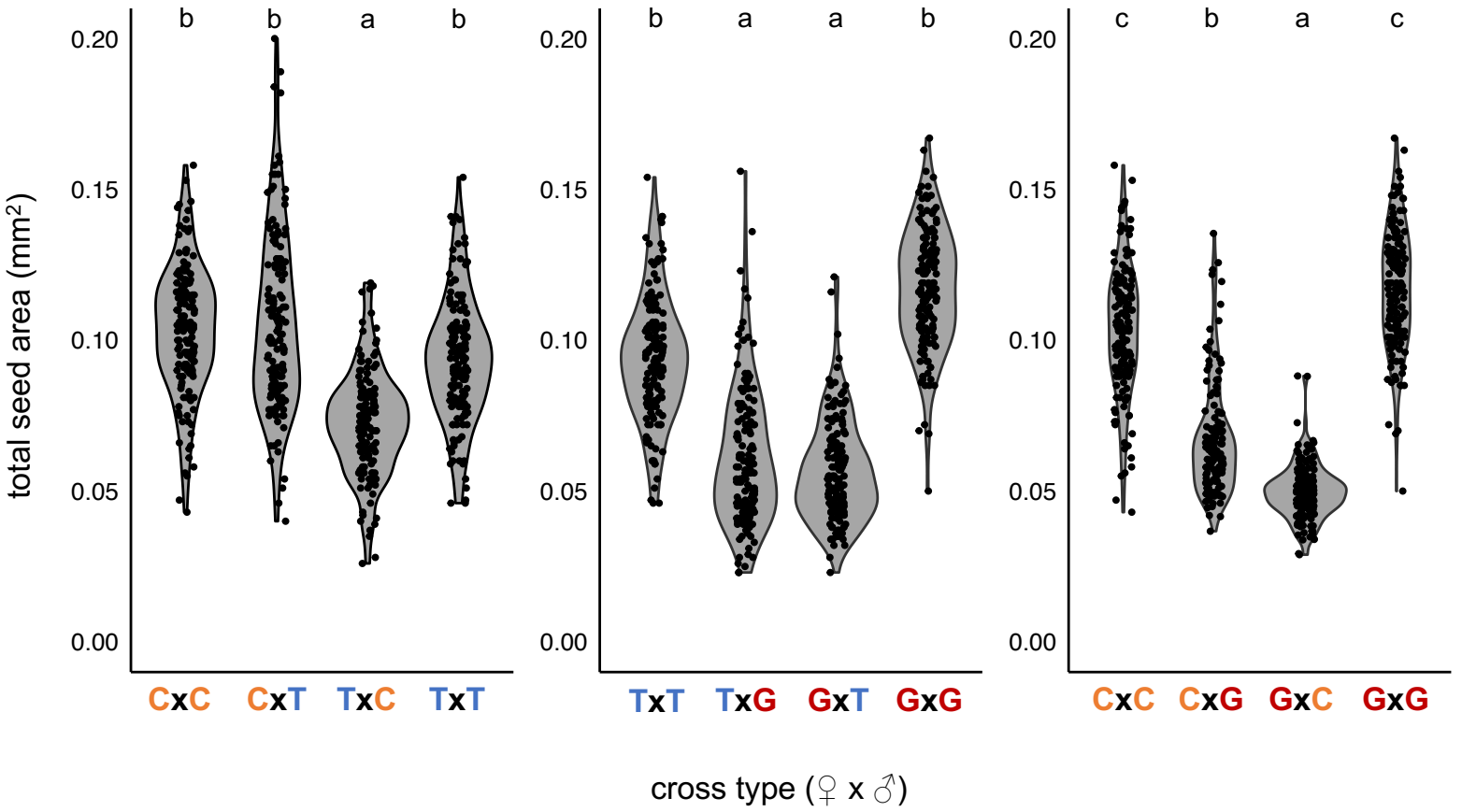

Figure S3.2: Total seed area from crosses within and between *M. caespitosa* (C), *M. tilingii* (T), and *M. guttatus* (G). The first letter of each cross indicates the maternal species. Different letters indicate significant differences in lsmeans among crosses ($P<0.05$) determined by a post hoc Tukey method. Analyses were performed separately, only comparing reciprocal interspecific crosses and their corresponding parents.

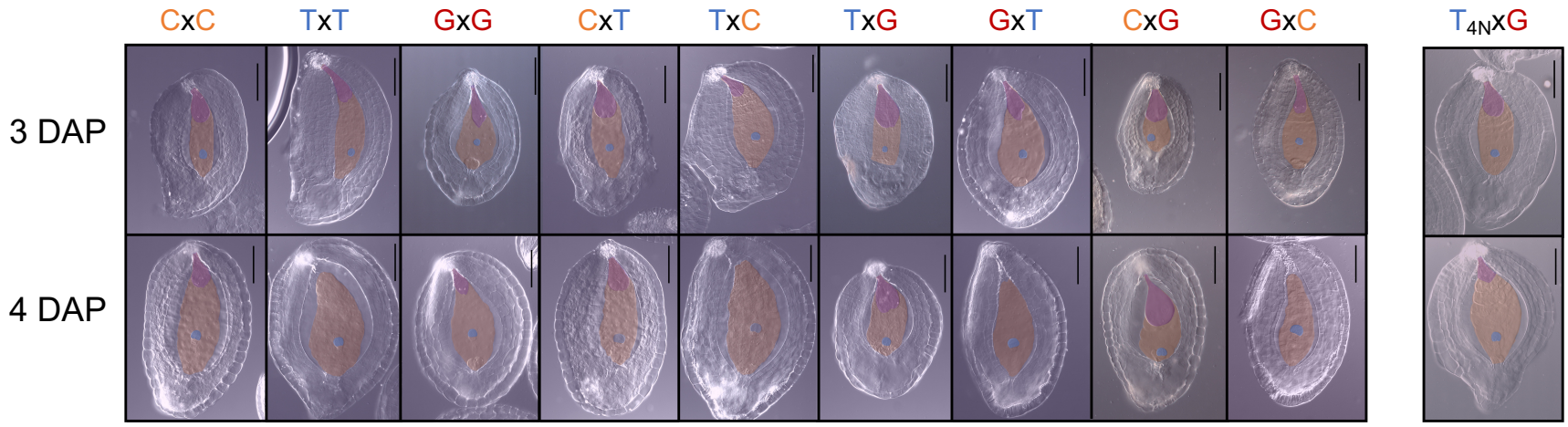

Figure S3.3: Developing seeds 3 and 4 days after pollination (DAP) in crosses among *M. caespitosa* (C), *M. tilingii* (T), and *M. guttatus* (G). We also included one interploidy cross (T_{4N}xG). Maternal parent is listed first in interspecific crosses. Seeds were cleared with Hoyer's solution. Blue shading represents embryo, orange shading represents endosperm region, and purple shading represents chalazal haustoria. Scale bar is 0.1mm. At 3 DAP, chalazal and micropylar haustoria domains are fully established. The micropylar domain is composed of two cells (arrow points to two nuclei in micropylar region of the TxT seed) at the anterior end of the seed, and this region invades nearby seed integuments. We also sometimes observe micropylar haustoria extending towards the chalazal domain (see GxG, GxT, and GxC). The chalazal haustoria is composed of two cells that occupy the posterior end of the seed. The chalazal haustoria extends from the maternal-filial boundary towards the anterior end of the seed. At 4 DAP, the chalazal haustoria has largely degenerated in TxT, TxC, GxT, GxC, and T_{4N}xG crosses, as the central endosperm proliferates. The area of the endosperm that is filled by the chalazal haustoria decreases from 3 to 4 DAP in almost all crosses, except for CxG.

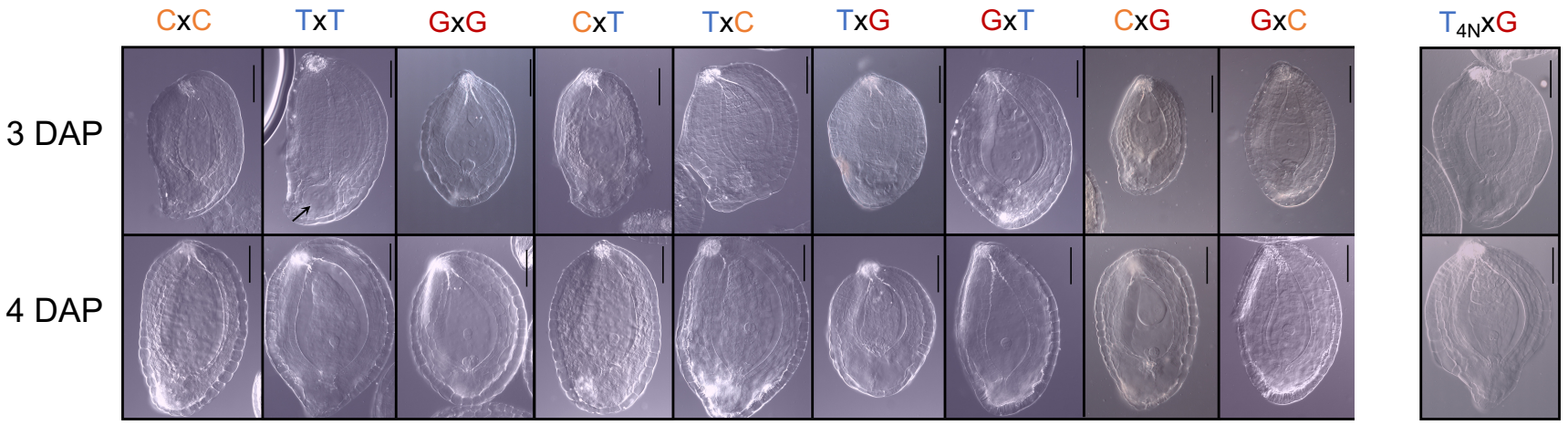

Figure S3.4. Replicate of Figure S3.3 without artificial shading. Developing seeds 3 and 4 days after pollination (DAP) in crosses among *M. caespitosa* (C), *M. tilingii* (T), and *M. guttatus* (G). We also included one interploidy cross (T_{4N}xG). Maternal parent is listed first in interspecific crosses. Seeds were cleared with Hoyer's solution. Blue shading represents embryo, orange shading represents endosperm region, and purple shading represents chalazal haustoria. Scale bar is 0.1mm. At 3 DAP, chalazal and micropylar haustoria domains are fully established. The micropylar domain is composed of two cells (arrow points to two nuclei in micropylar region of the TxT seed) at the anterior end of the seed, and this region invades nearby seed integuments. We also sometimes observe micropylar haustoria extending towards the chalazal domain (see GxG, GxT, and GxC). The chalazal haustoria is composed of two cells that occupy the posterior end of the seed. The chalazal haustoria extends from the maternal-filial boundary towards the anterior end of the seed. At 4 DAP, the chalazal haustoria has largely degenerated in TxT, TxC, GxT, GxC, and T_{4N}xG crosses, as the central endosperm proliferates. The area of the endosperm that is filled by the chalazal haustoria decreases from 3 to 4 DAP in almost all crosses, except for CxG.

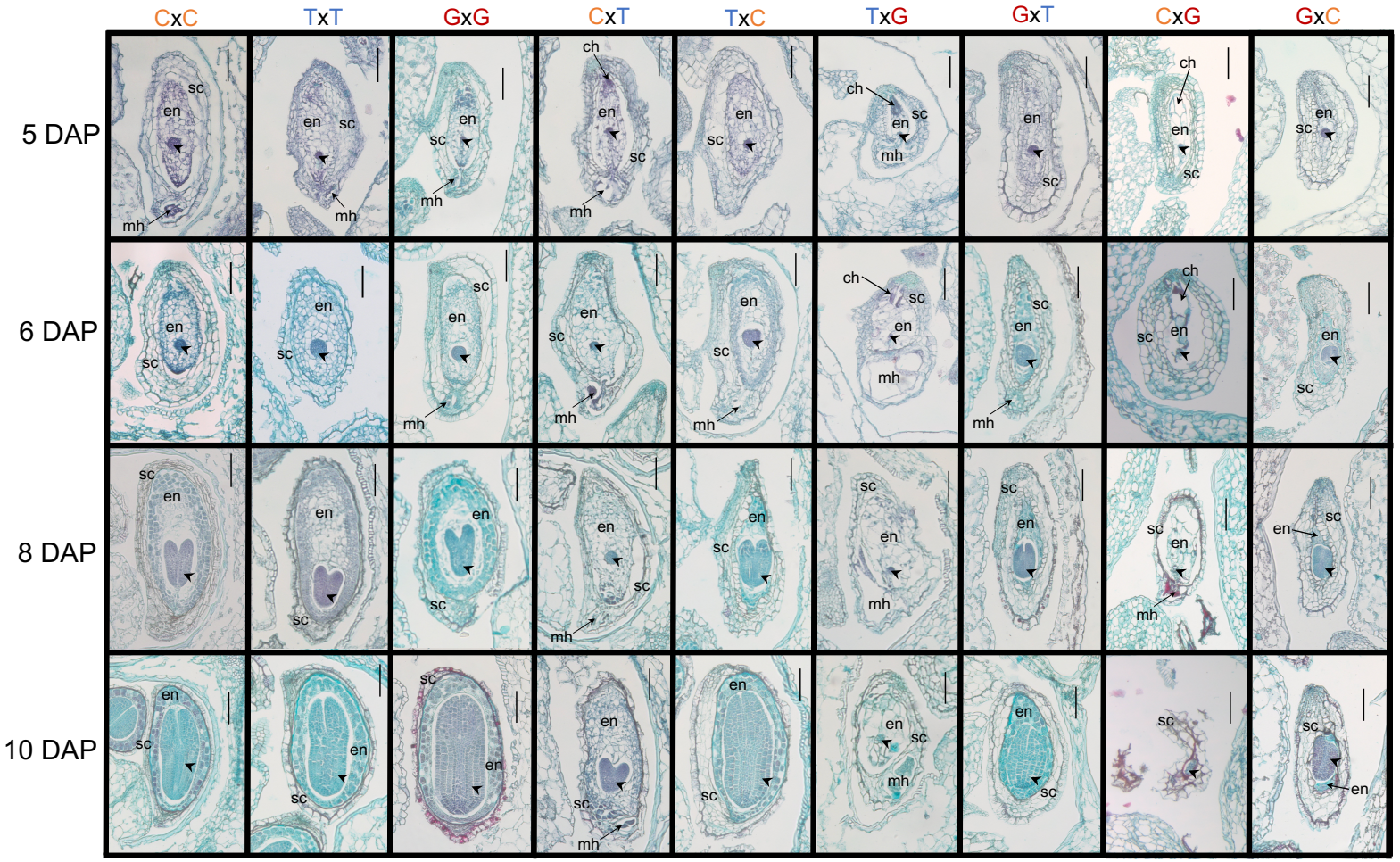

Figure S3.5: Histological sections of whole fruits from intra- and interspecific crosses among *M. caespitosa* (C), *M. tilingii* (T), and *M. guttatus* (G) at 5, 6, 8, and 10 days after pollination (DAP). Maternal parent is listed first in all interspecific crosses. Arrowhead = embryo, en = endosperm, sc = seed coat, ch = chalazal haustoria, mh = micropylar haustoria. Note that ch and mh are only labeled when the haustoria are visible in the image. Scale bar is 0.1mm. At **5**

and 6 DAP, intraspecific crosses have reached a globular embryo stage, where the embryo is surrounded by 'empty' cells, and the chalazal haustoria has degenerated. Embryos of GxT and GxC maternal excess crosses are surrounded by dense, starch-filled cells, again with no chalazal haustoria present. In paternal excess crosses (CxT, TxG, and CxG), the embryo has not yet reached a full globular stage, and the chalazal haustoria is still intact in some seeds of paternal excess crosses at 5 DAP and in TxG and CxG at 6 DAP. We also note here that the chalazal haustoria of CxT and TxG is deeply stained, likely with sugars, while the CxG haustoria is large and unstained. At **8DAP**, intraspecific and maternal excess crosses have reached the heart shaped embryo stage, though heart embryos of maternal excess crosses GxT and GxC appear abnormal. While in the intraspecific crosses, the central endosperm cells begin to break down and the peripheral endosperm near the seed coat starts to differentiate into starch-filled cells, the maternal excess crosses appear fully differentiated and the endosperm area appears reduced. In contrast, endosperm cells in paternal excess crosses remain empty and enlarged, and the embryo is underdeveloped. By **10 DAP**, all intraspecific crosses and TxC have developed torpedo shaped embryos surrounded by a few layers of dense, starch-filled cells, and the micropylar haustoria is completely degenerated. The maternal excess crosses, GxT and GxC, fail to develop into a torpedo shape and remain as an abnormal heart shaped embryo, with little to no endosperm and no apparent micropylar haustoria. In CxT, the embryo has finally reached a heart shape, but the endosperm cells remain undifferentiated and micropylar cells are evident in some seeds. While TxG seeds are severely underdeveloped, with a prominent micropylar haustoria in some seeds, the seeds of CxG crosses have already collapsed around the underdeveloped embryo.